DPF-PHENO 2024

Probing effective field theory operators in top quark pair events in the lepton+jets channel using charge asymmetry and angular variables

by
Ricardo Escobar Franco[1], Cecilia E. Gerber[1], Robert Schoefbeck[2], Beren Ozek Cetinok[1], and Titas Roy[1]

[1]University of Illinois, Chicago, IL, USA
[2]Institut fuer Hochenergiephysik, Vienna, Austria

rescob8@uic.edu

MAY 2024

Overview

- Top quark physics
- Charge Asymmetry measurement
- Angular Variables

Overview

- Top quark physics
- Charge Asymmetry measurement
- Angular Variables
- Standard Model Effective Field Theory
- Correlations in Constraints
- Complimentary Observables

Top Quark Physics

- Heaviest and most precisely[1] measured of all the Standard Model (SM) quarks.

extreme mass $\Longrightarrow$ extreme instability $\Longrightarrow$ extremely short lifetime, τ_{top}

<u>Top quark lifetime</u>

$$\tau_{top} \approx 10^{-25}s$$

<<

<u>Hadronization scale</u>

$$\frac{1}{\Lambda_{QCD}} \approx 10^{-24}s$$

<<

<u>Spin Decorrelation scale</u>

$$\frac{m_t}{\Lambda_{QCD}^2} \approx 10^{-21}s$$

[1] https://atlas.web.cern.ch/Atlas/GROUPS/PHYSICS/CONFNOTES/ATLAS-CONF-2023-066/

Top Quark Physics

- Heaviest and most precisely[1] measured of all the Standard Model (SM) quarks.

extreme mass $\Longrightarrow$ extreme instability $\Longrightarrow$ extremely short lifetime, τ_{top}

Top quark lifetime — Hadronization scale — Spin Decorrelation scale

$$\tau_{top} \approx 10^{-25}s \quad << \quad \frac{1}{\Lambda_{QCD}} \approx 10^{-24}s \quad << \quad \frac{m_t}{\Lambda^2_{QCD}} \approx 10^{-21}s$$

only quark whose properties can be studied directly

initial spin state information is fully inherited by decay products

[1] https://atlas.web.cern.ch/Atlas/GROUPS/PHYSICS/CONFNOTES/ATLAS-CONF-2023-066/

Top Quark Physics

- Top quarks primarily decay into a W boson and b quark so a $t\bar{t}$ pair can decay into one of the following channels:

all jets

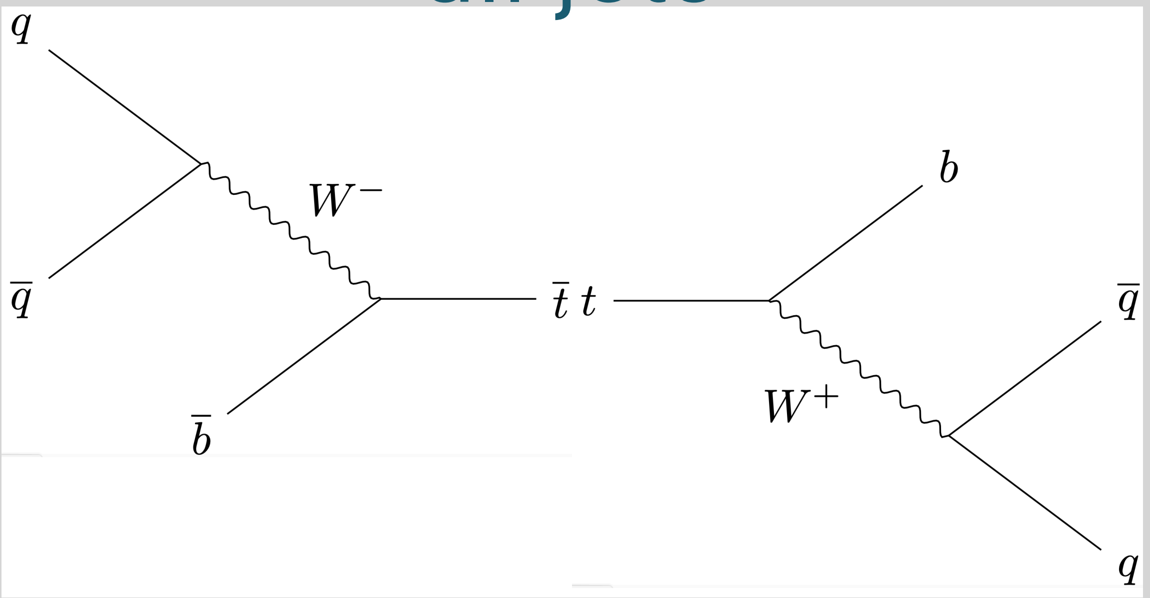

lepton+jets

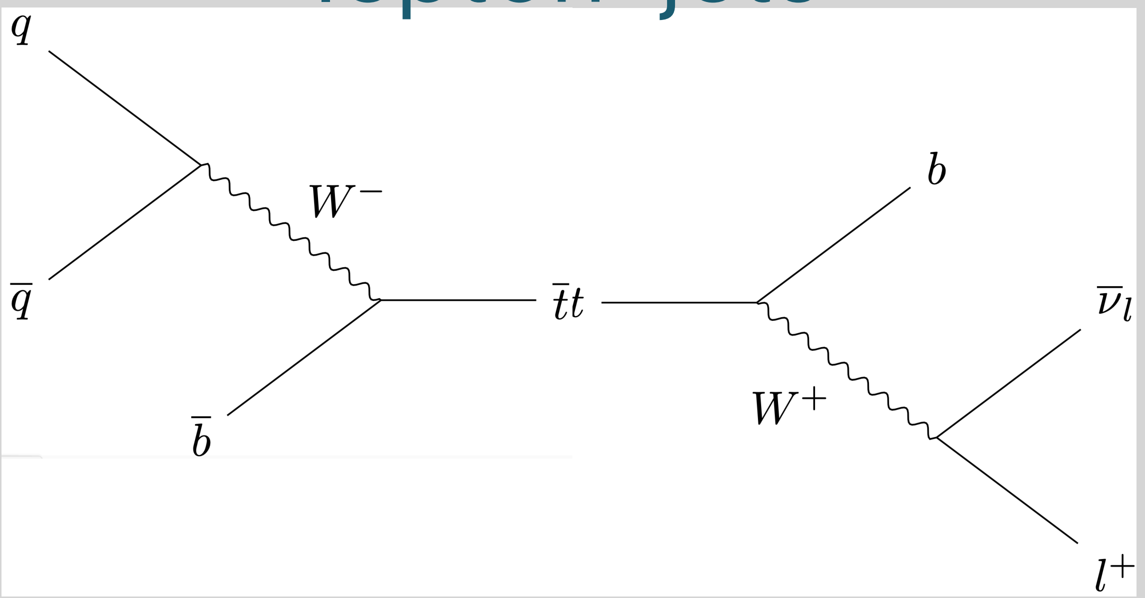

di-lepton

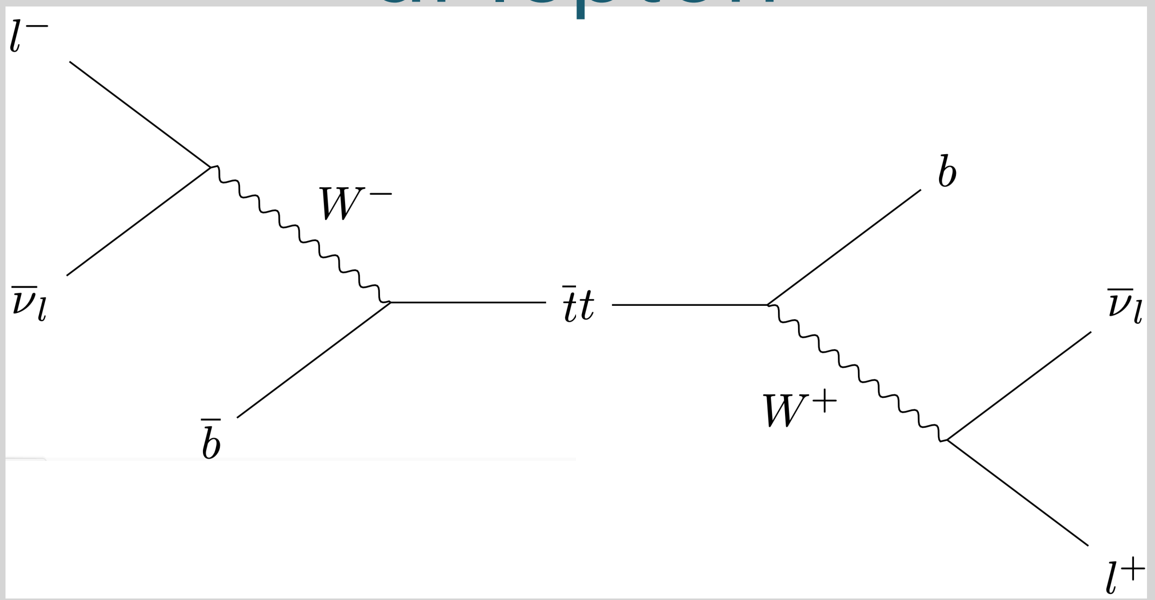

Top Quark Physics

- Top quarks primarily decay into a W boson and b quark so a $t\bar{t}$ pair can decay into one of the following channels:

all jets

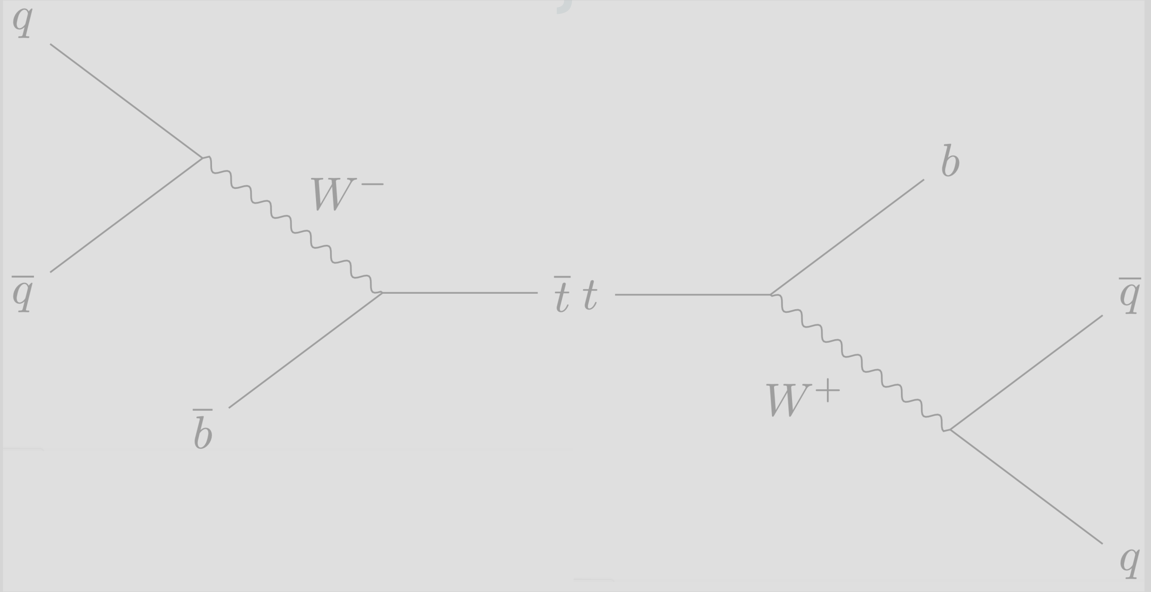

lepton+jets

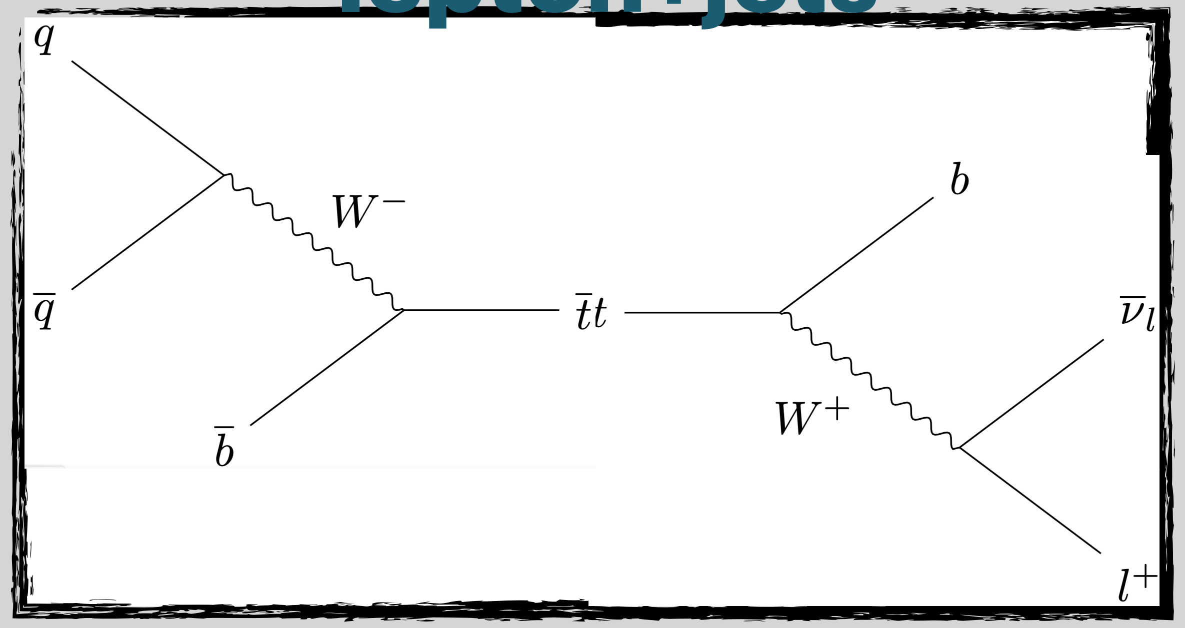

$l = e, \mu$

di-lepton

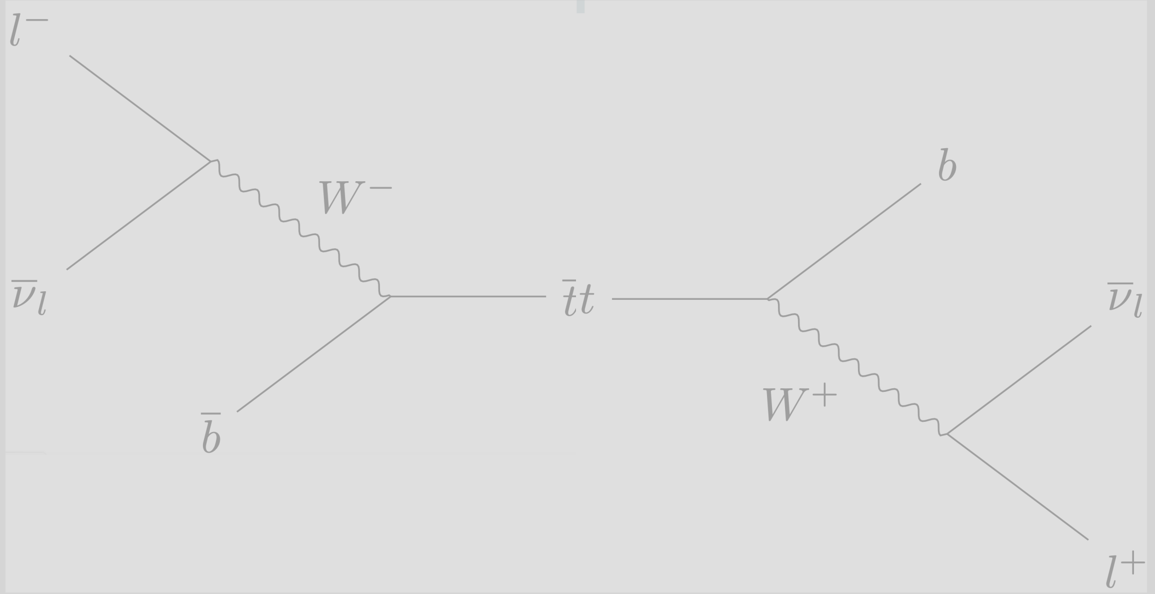

Top Quark Physics

- Top quarks primarily decay into a W boson and b quark so a $t\bar{t}$ pair can decay into one of the following channels:

all jets

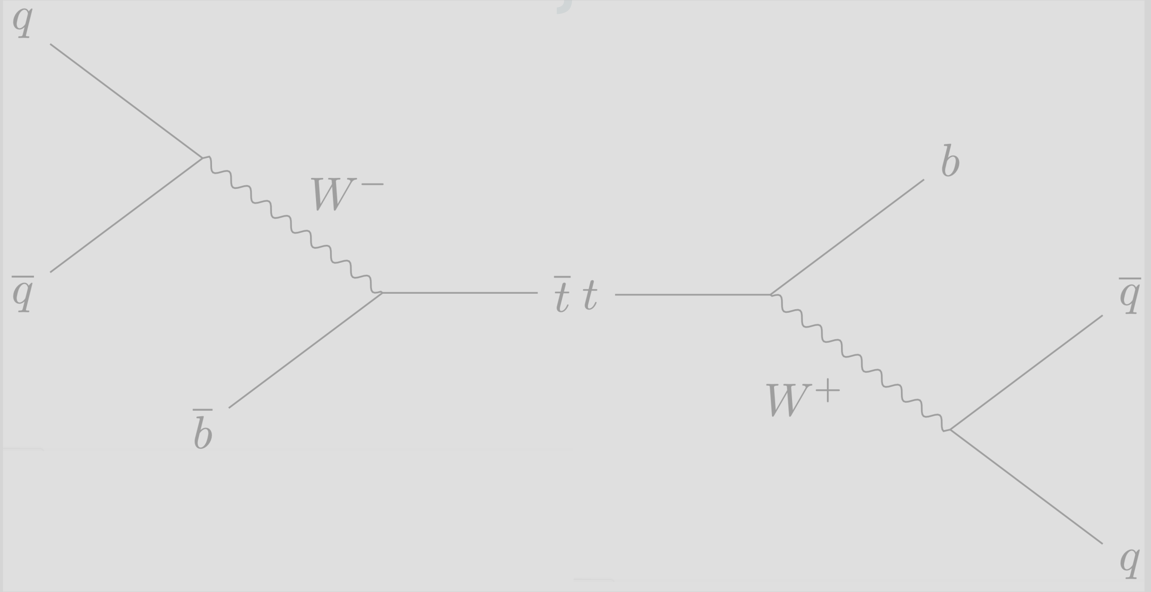

lepton+jets

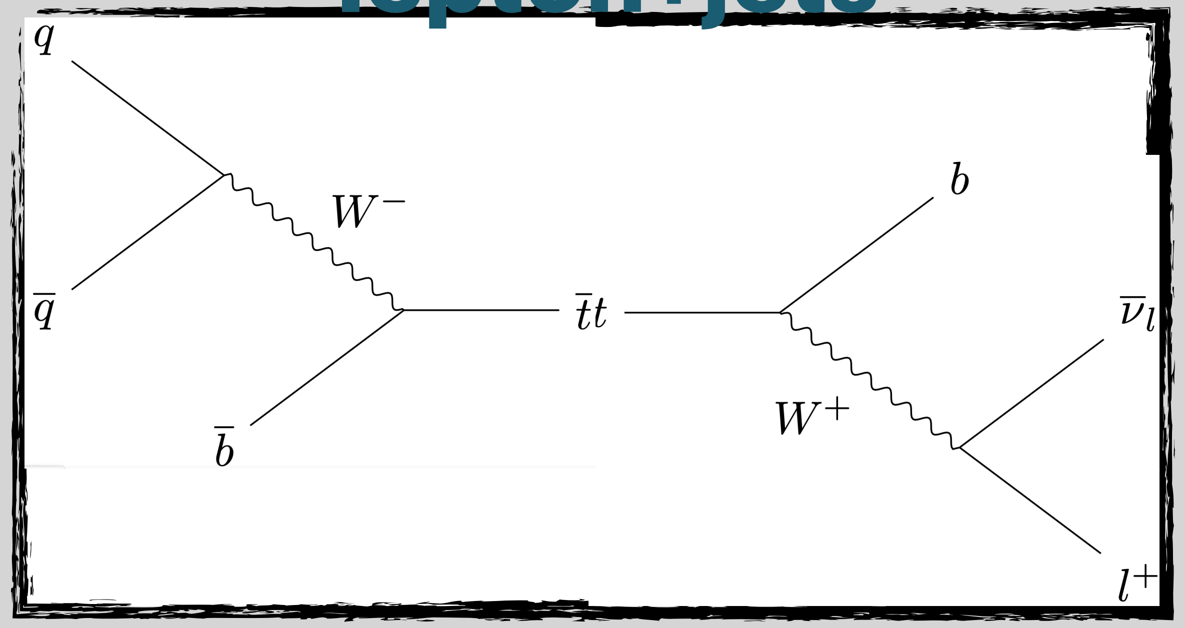

$l = e, \mu$

di-lepton

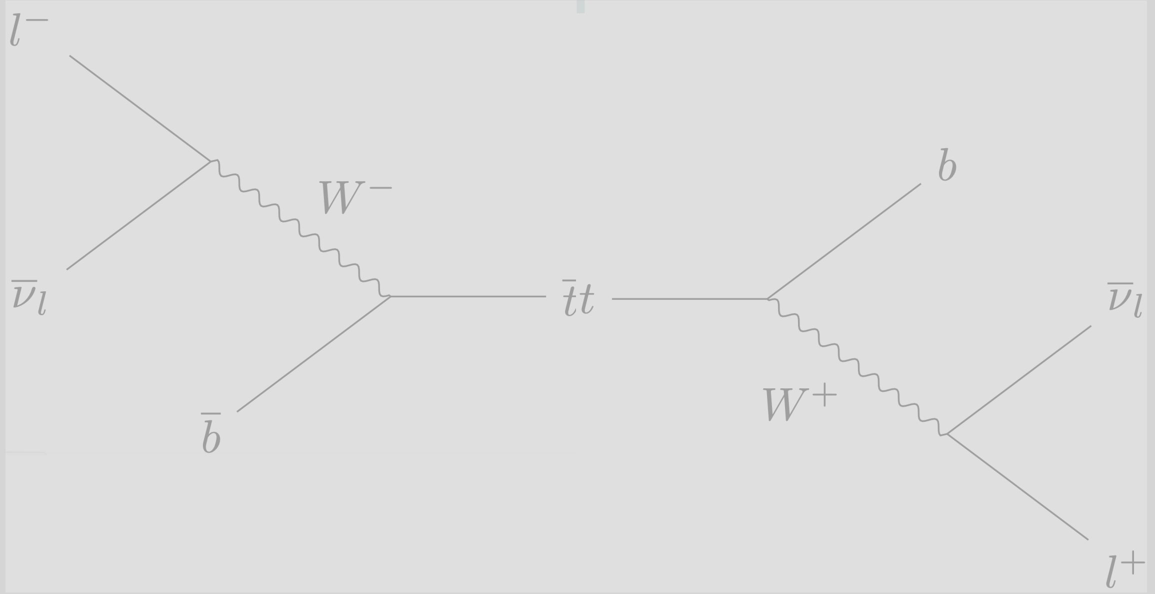

- $t\bar{t}$ pairs are produced with a small "forward-central" charge asymmetry

  $\Longrightarrow$ higher order corrections enhance this asymmetry

  - **this small charge asymmetry (A_C) has been measured**

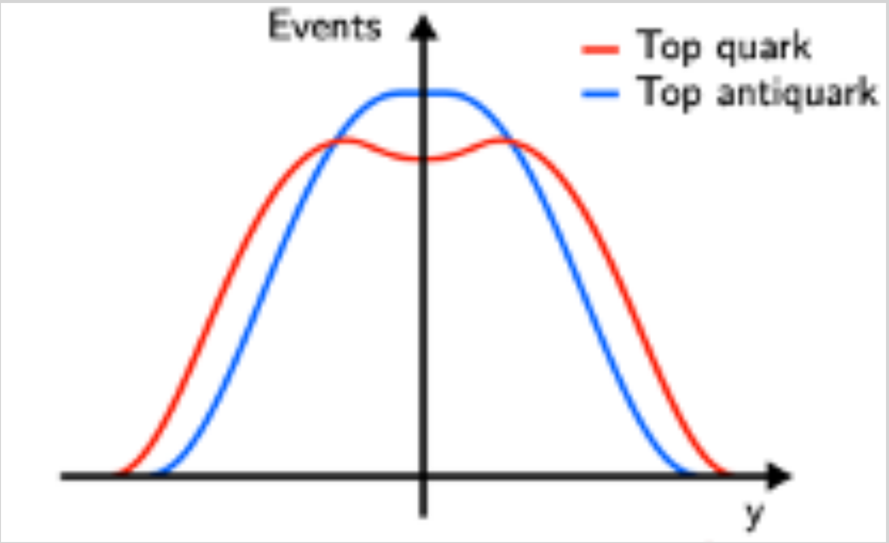

Top Quark Physics

- Top quarks primarily decay into a W boson and b quark so a $t\bar{t}$ pair can decay into one of the following channels:

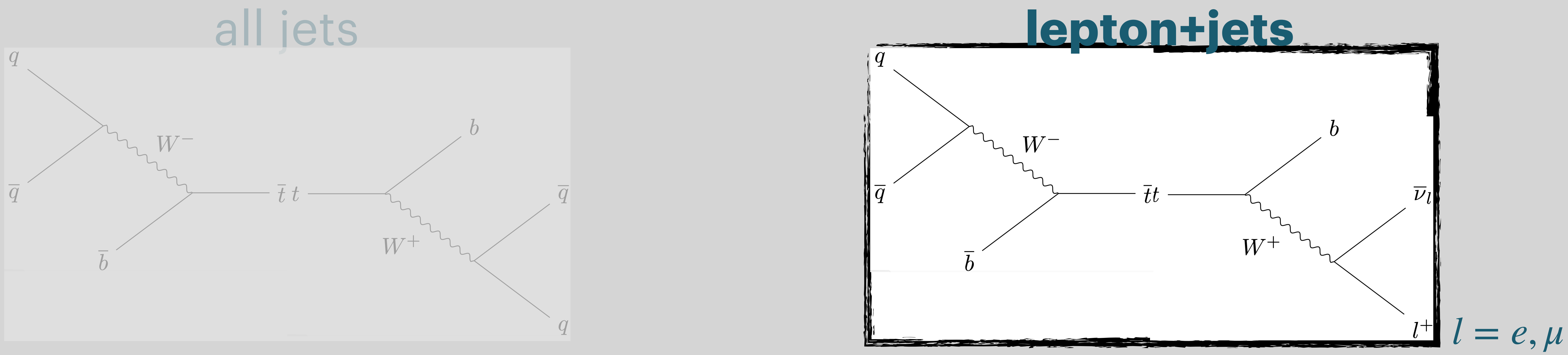

- $t\bar{t}$ pairs are produced with a small "forward-central" charge asymmetry

  $\Longrightarrow$ higher order corrections enhance this asymmetry

  - **this small charge asymmetry (A_C) has been measured**

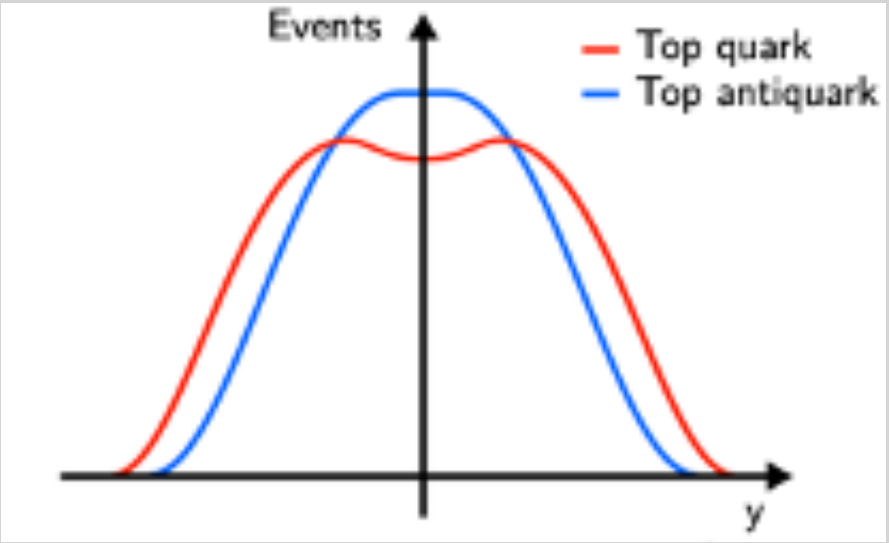

- individual top quark are produced unpolarised

  $\Longrightarrow$ spins of top quark pairs are still strongly correlated

  - **correlations observed in angular distributions of decay products**

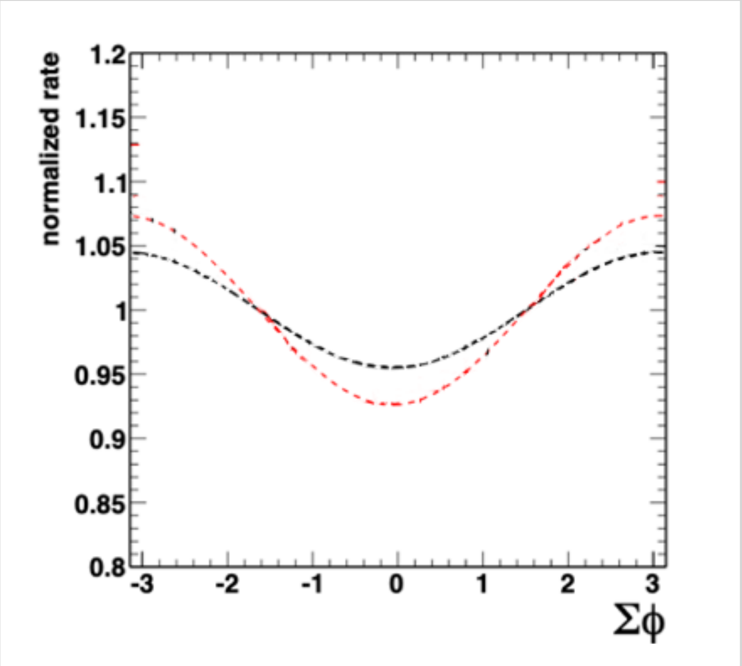

Charge Asymmetry[1] (Physics Letters B)

- Optimized for top quark pairs produced with large Lorentz boosts which have enhanced asymmetry due to valence quarks carrying larger fraction of proton's momentum

- Results corrected for detector and acceptance effects using a binned maximum likelihood fit

[1] https://doi.org/10.1016/j.physletb.2023.137703

Charge Asymmetry[1] (Physics Letters B)

- Optimized for top quark pairs produced with large Lorentz boosts which have enhanced asymmetry due to valence quarks carrying larger fraction of proton's momentum

- Results corrected for detector and acceptance effects using a binned maximum likelihood fit

$$A_C = \frac{N(\Delta|y| > 0) - N(\Delta|y| < 0)}{N(\Delta|y| > 0) + N(\Delta|y| < 0)}$$

- y = rapidity of the top quark (antiquark)
- $\Delta|y| = |y_t| - |y_{\bar{t}}|$

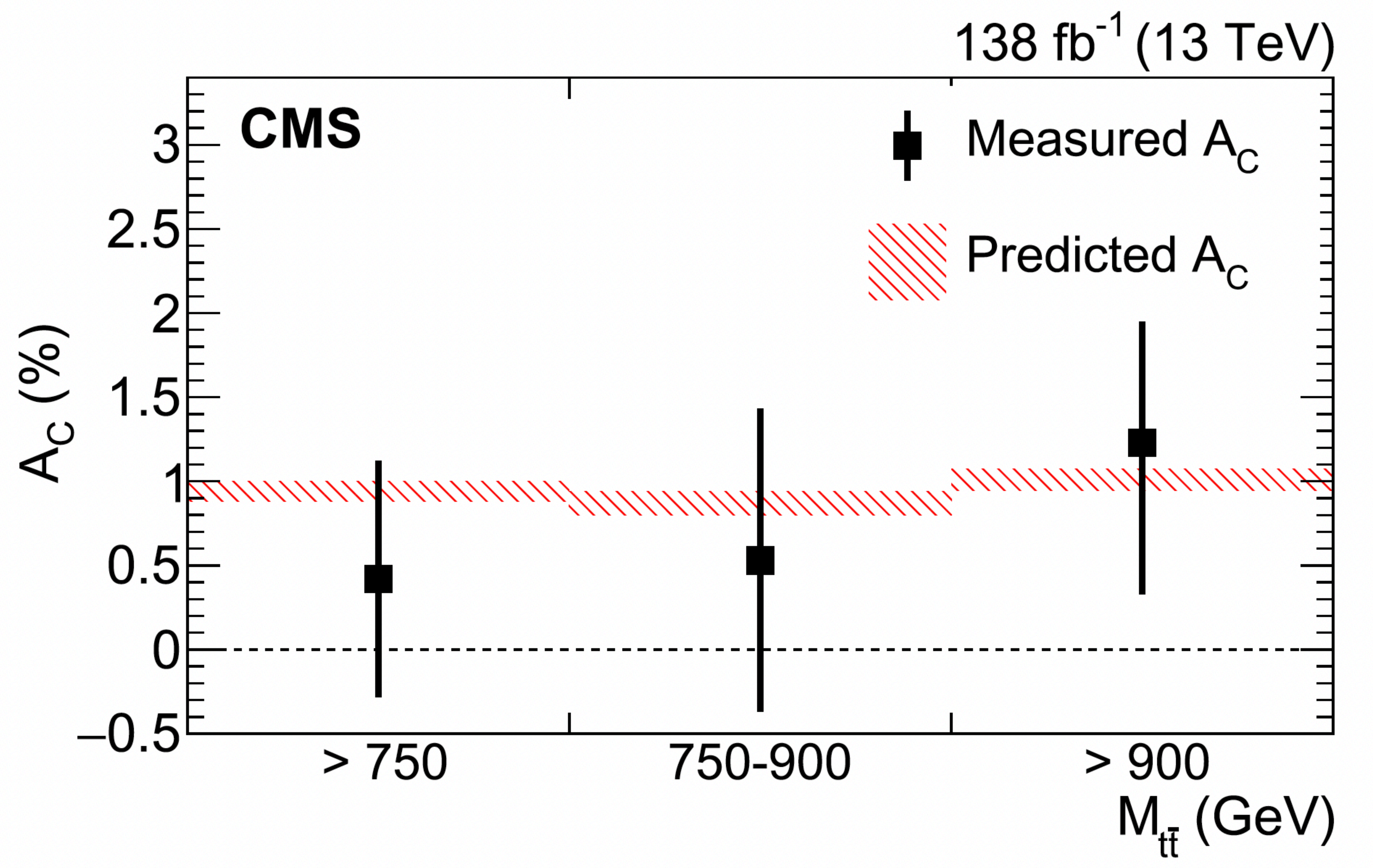

[1] https://doi.org/10.1016/j.physletb.2023.137703

Charge Asymmetry[1] (Physics Letters B)

- Looking forward, the analysis will be improved in the following ways:

	Published A_C	Optimized A_C
Invariant Mass of top quarks	$M_{t\bar{t}} > 750\ GeV$	$M_{t\bar{t}} > 0\ GeV$
Object selection	only high-p_T leptons	includes low-p_T *isolated* leptons
Background Suppression	event selection	Deep Neural Network

- Measurement will be at reconstruction level to maintain handle of systematic uncertainties

[1] https://doi.org/10.1016/j.physletb.2023.137703

Charge Asymmetry[1] (Physics Letters B)

- Looking forward, the analysis will be improved in the following ways:

	Published A_C	Optimized A_C
Invariant Mass of top quarks	$M_{t\bar{t}} > 750\ GeV$	$M_{t\bar{t}} > 0\ GeV$
Object selection	only high-p_T leptons	includes low-p_T *isolated* leptons
Background Suppression	event selection	Deep Neural Network

- Measurement will be at reconstruction level to maintain handle of systematic uncertainties
- Idea is to combine precise SM measurement of:
  - **charge asymmetry**
  - **invariant mass**
  - **angular variables**
- To be input for an **EFT interpretation**

[1] https://doi.org/10.1016/j.physletb.2023.137703

Angular Varibables

- For l+jets channel one can choose the following decay products of the top quarks:
  - **lepton** for leptonically decaying top quark
  - **b-quark** for hadronically decaying top quark

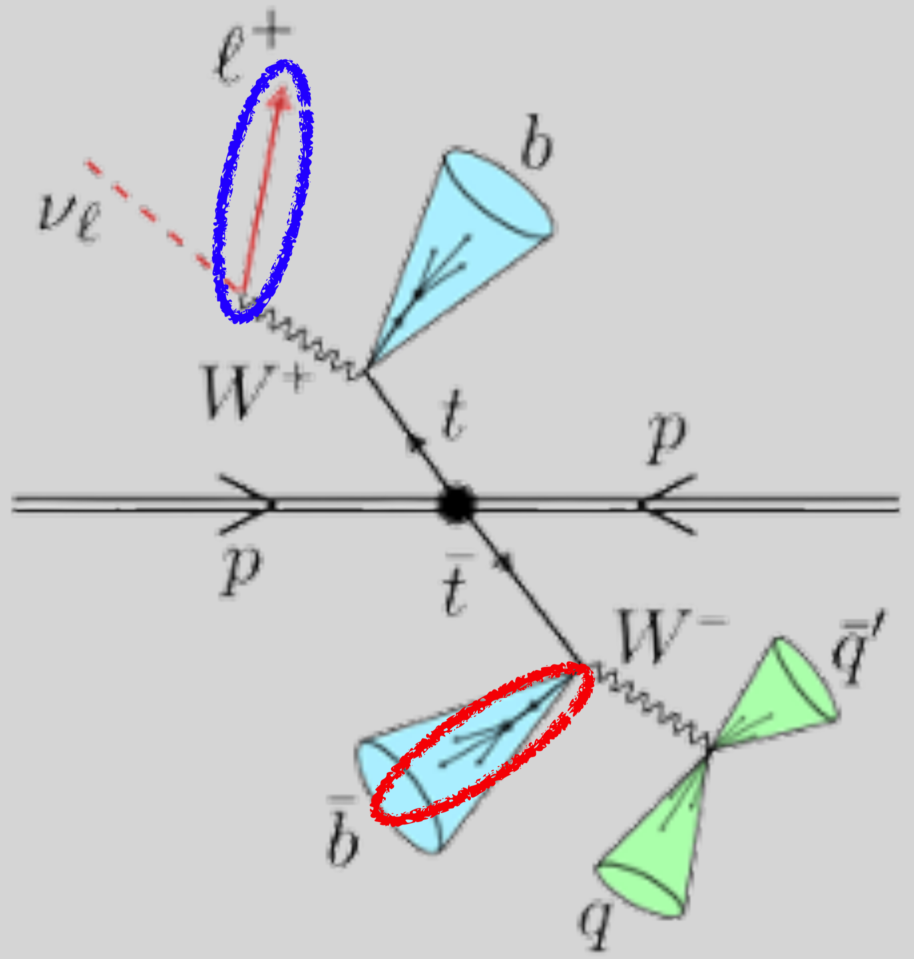

Angular Varibables

- For l+jets channel one can choose the following decay products of the top quarks:
  - **lepton** for leptonically decaying top quark
  - **b-quark** for hadronically decaying top quark

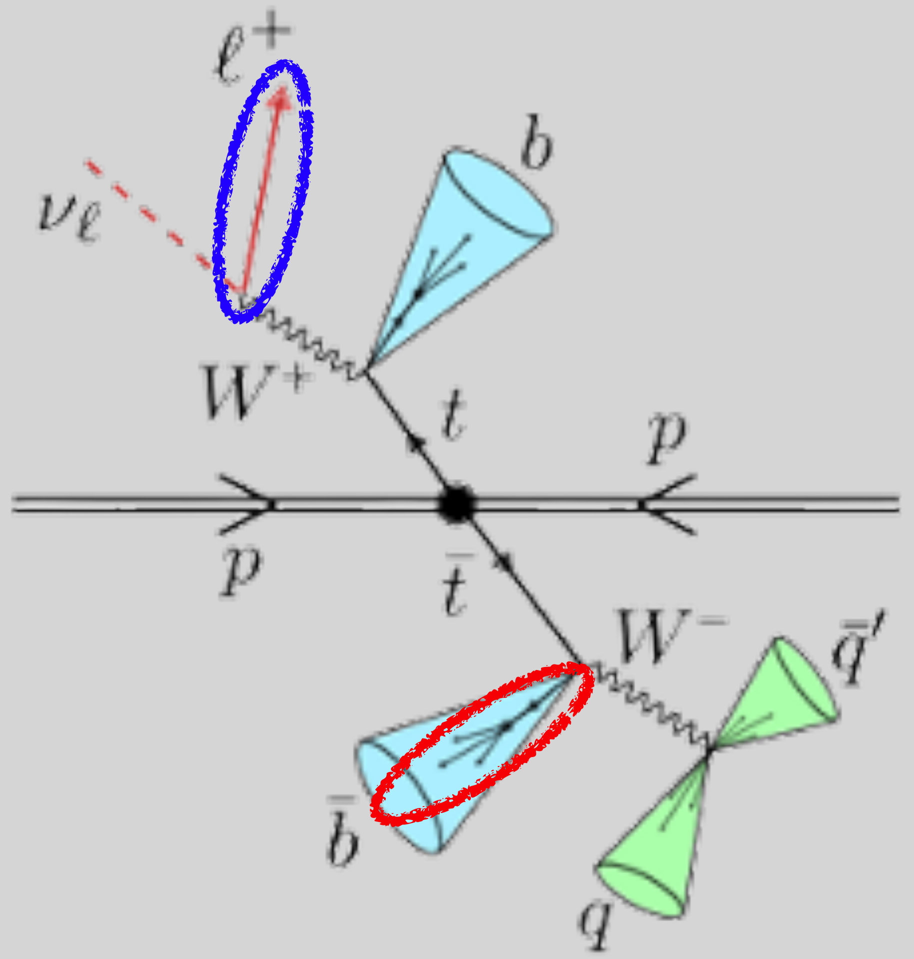

- The following angular distributions[1] involve the **azimuthal angles** of the chosen decay products:

$$\frac{d\sigma}{d(\phi-\bar{\phi})} \propto 1+\left(\frac{\pi}{4}\right)^2 \kappa\bar{\kappa}\left[\left(\frac{C^{11}+C^{22}}{2}\right)\cos(\phi-\bar{\phi})+\left(\frac{C^{21}-C^{12}}{2}\right)\sin(\phi-\bar{\phi})\right]$$

$$\frac{d\sigma}{d(\phi+\bar{\phi})} \propto 1+\left(\frac{\pi}{4}\right)^2 \kappa\bar{\kappa}\left[\left(\frac{C^{11}-C^{22}}{2}\right)\cos(\phi+\bar{\phi})+\left(\frac{C^{21}+C^{12}}{2}\right)\sin(\phi+\bar{\phi})\right]$$

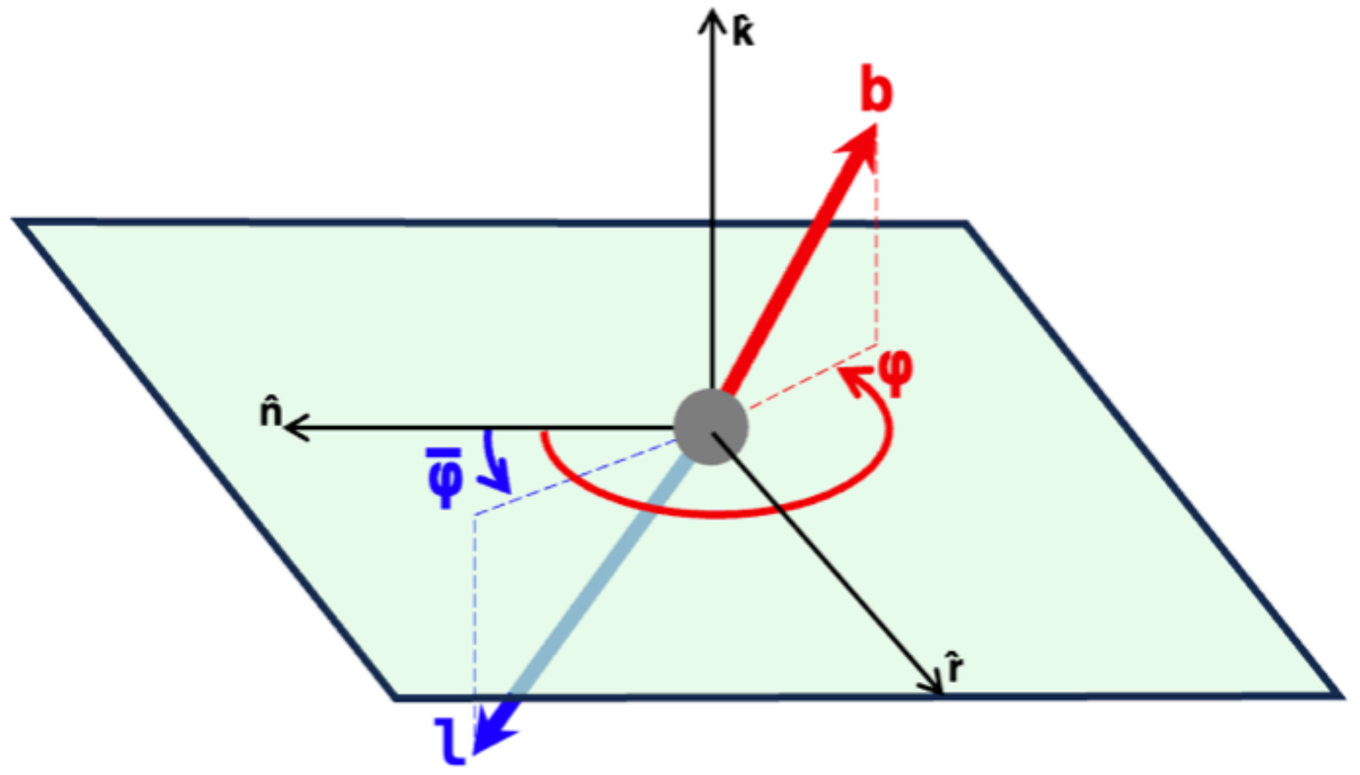

[1] https://doi.org/10.48550/arXiv.1212.4888

SM Effective Field Theory Framework

- The SM Effective Field Theory (SMEFT) Framework parameterizes new physics (NP) in terms of higher-dimension gauge-invariant operators, $\mathcal{O}_i$:

$$\mathscr{L}_{EFT} = \mathscr{L}_{SM} + \sum_{\forall i, n \geq 5} \frac{c_i^{(n)}}{\Lambda^{n-4}} \mathcal{O}_i^{(n)} + \ldots$$

  - Λ = NP mass scale
  - $\mathcal{O}_i$ = products of SM fields that describe new interactions
  - c_i = Wilson coefficients (WCs) that describe **the strength of the corresponding interaction**

SM Effective Field Theory Framework

- The SM Effective Field Theory (SMEFT) Framework parameterizes new physics (NP) in terms of higher-dimension gauge-invariant operators, $\mathcal{O}_i$:

$$\mathcal{L}_{EFT} = \mathcal{L}_{SM} + \sum_{\forall i, n \geq 5} \frac{c_i^{(n)}}{\Lambda^{n-4}} \mathcal{O}_i^{(n)} + \ldots$$

  - Λ = NP mass scale
  - $\mathcal{O}_i$ = products of SM fields that describe new interactions
  - c_i = Wilson coefficients (WCs) that describe **the strength of the corresponding interaction**
- All odd-dimension operators violate lepton and/or baryon number conservation, so we don't consider them.
- **Dim-6 operators** are least supressed by NP mass scale thus we focus on those.
- Collection of operators that affect $t\bar{t}$ production:

$$\mathcal{O}_{Qq}^{1,1}, \mathcal{O}_{Qq}^{3,1}, \mathcal{O}_{Qq}^{1,8}, \mathcal{O}_{Qq}^{3,8}, \mathcal{O}_{Qu}^{1}, \mathcal{O}_{Qu}^{8}, \mathcal{O}_{Qd}^{1}, \mathcal{O}_{Qd}^{8}, \mathcal{O}_{tq}^{1}, \mathcal{O}_{tq}^{8}, \mathcal{O}_{tu}^{1}, \mathcal{O}_{tu}^{8}, \mathcal{O}_{td}^{1}, \mathcal{O}_{td}^{8}, \text{ and } \mathcal{O}_{tG}^{I}$$

Correlations in Constraints

- Individual fits, one WC floats during fit
- Marginalised fits, multiple WC's float during fit
- Correlations between effects of certain operators can conspire to avoid constraints known as "blind directions" in WC space, as seen below[1]

Correlations in Constraints

- Individual fits, one WC floats during fit
- Marginalised fits, multiple WC's float during fit
- Correlations between effects of certain operators can conspire to avoid constraints known as "blind directions" in WC space, as seen below[1]

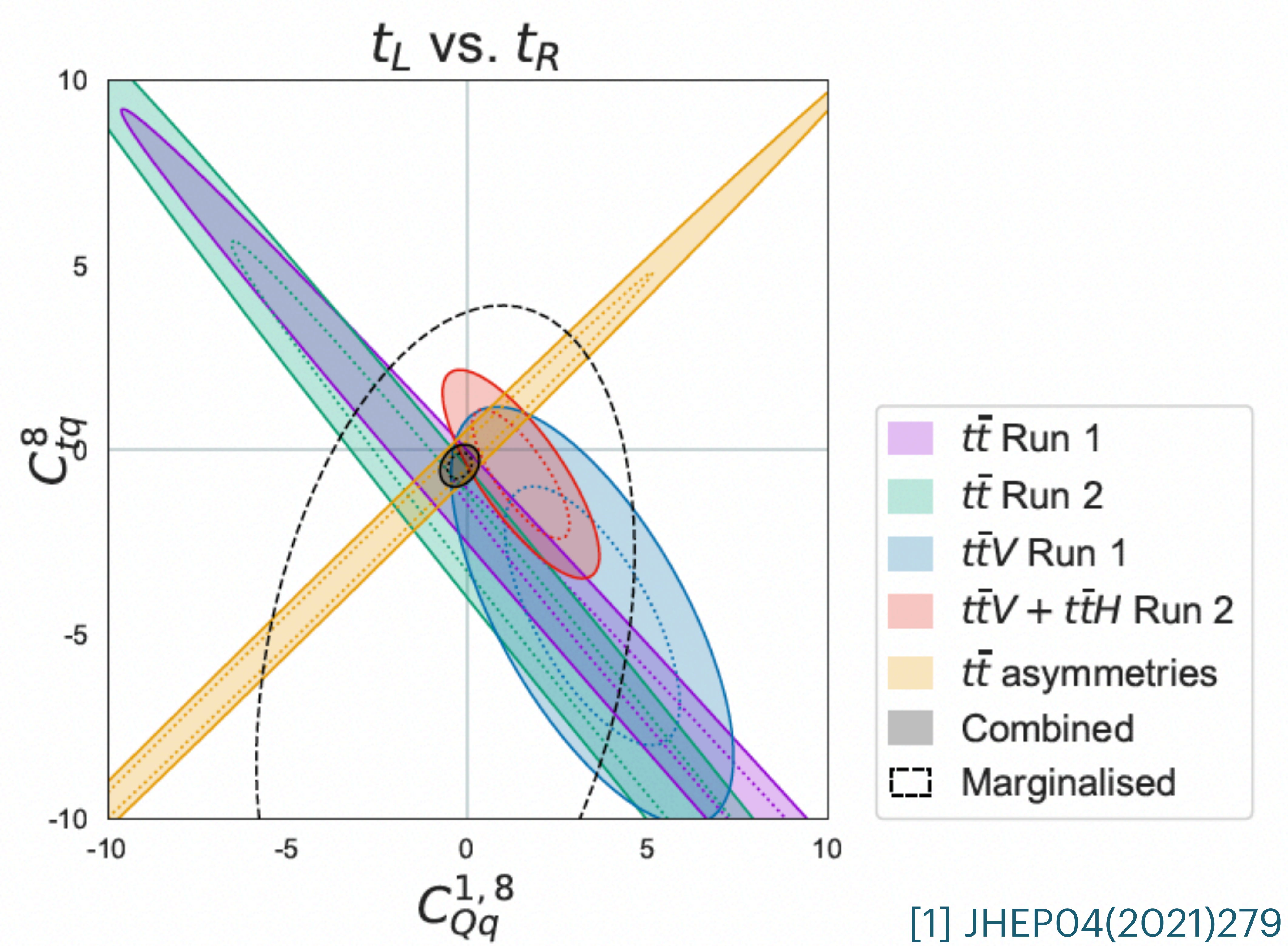

[1] JHEP04(2021)279

vertical axis:

$$c^8_{tq} \equiv C^{8(ii33)}_{qu},$$

$$O^{8(ijkl)}_{qu} = (\bar{q}_i \gamma^\mu T^A q_j)(\bar{u}_k \gamma_\mu T^A u_l)$$

horizontal axis:

$$c^{1,8}_{Qq} \equiv C^{1(i33i)}_{qq} + 3C^{3(i33i)}_{qq}$$

$$O^{1(ijkl)}_{qq} = (\bar{q}_i \gamma^\mu q_j)(\bar{q}_k \gamma_\mu q_l),$$

$$O^{3(ijkl)}_{qq} = (\bar{q}_i \gamma^\mu \tau^I q_j)(\bar{q}_k \gamma_\mu \tau^I q_l)$$

- **Different type of input data** with "orthogonal" blind direction **is complementary** in fit

Complimentary Observables

- Effects of operators on **angular** and **asymmetry** distributions, ξ_{kk} and $\Delta|\eta|$:

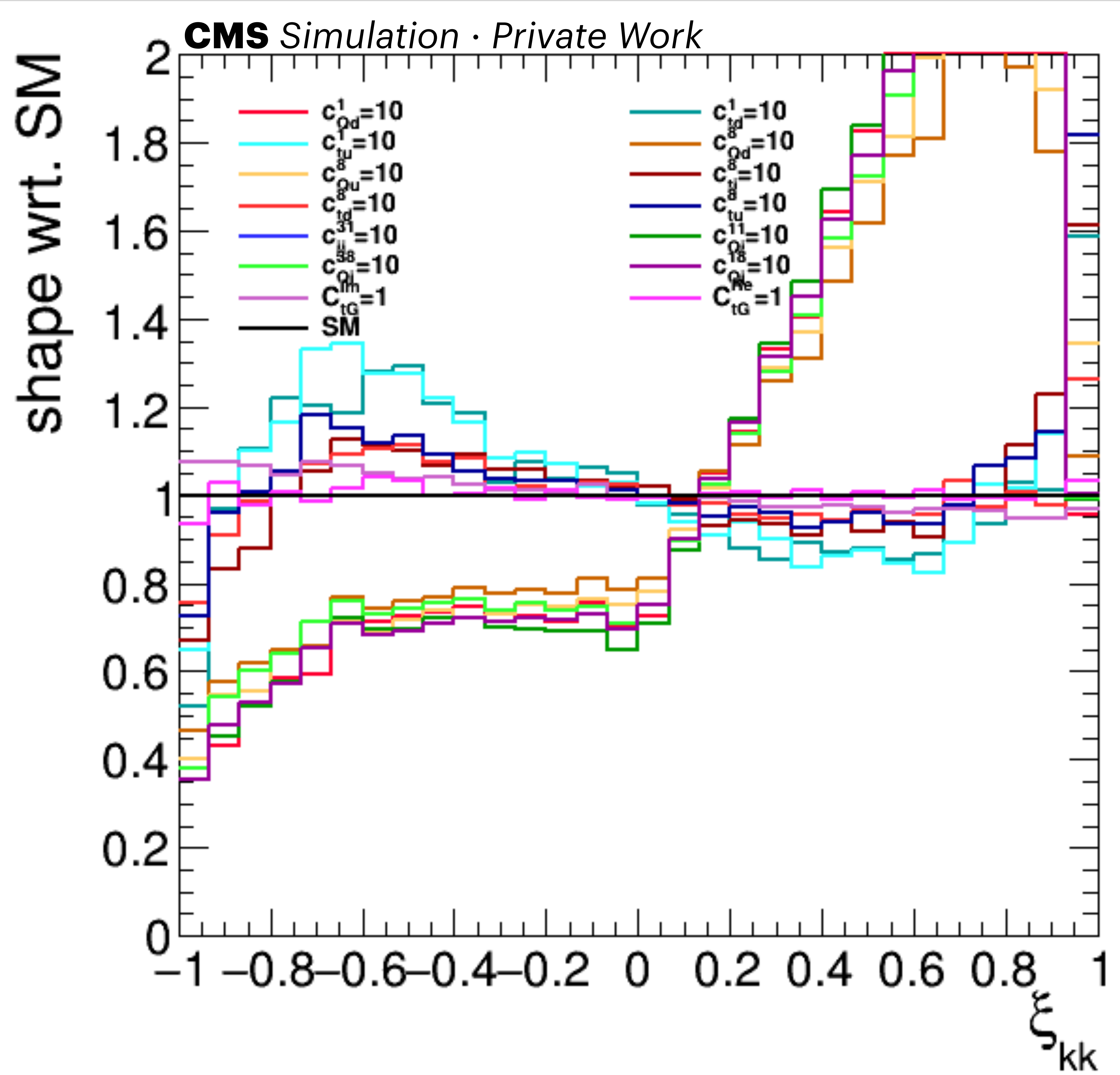

$$\xi_{kk} = \cos\theta * \cos\bar{\theta}$$

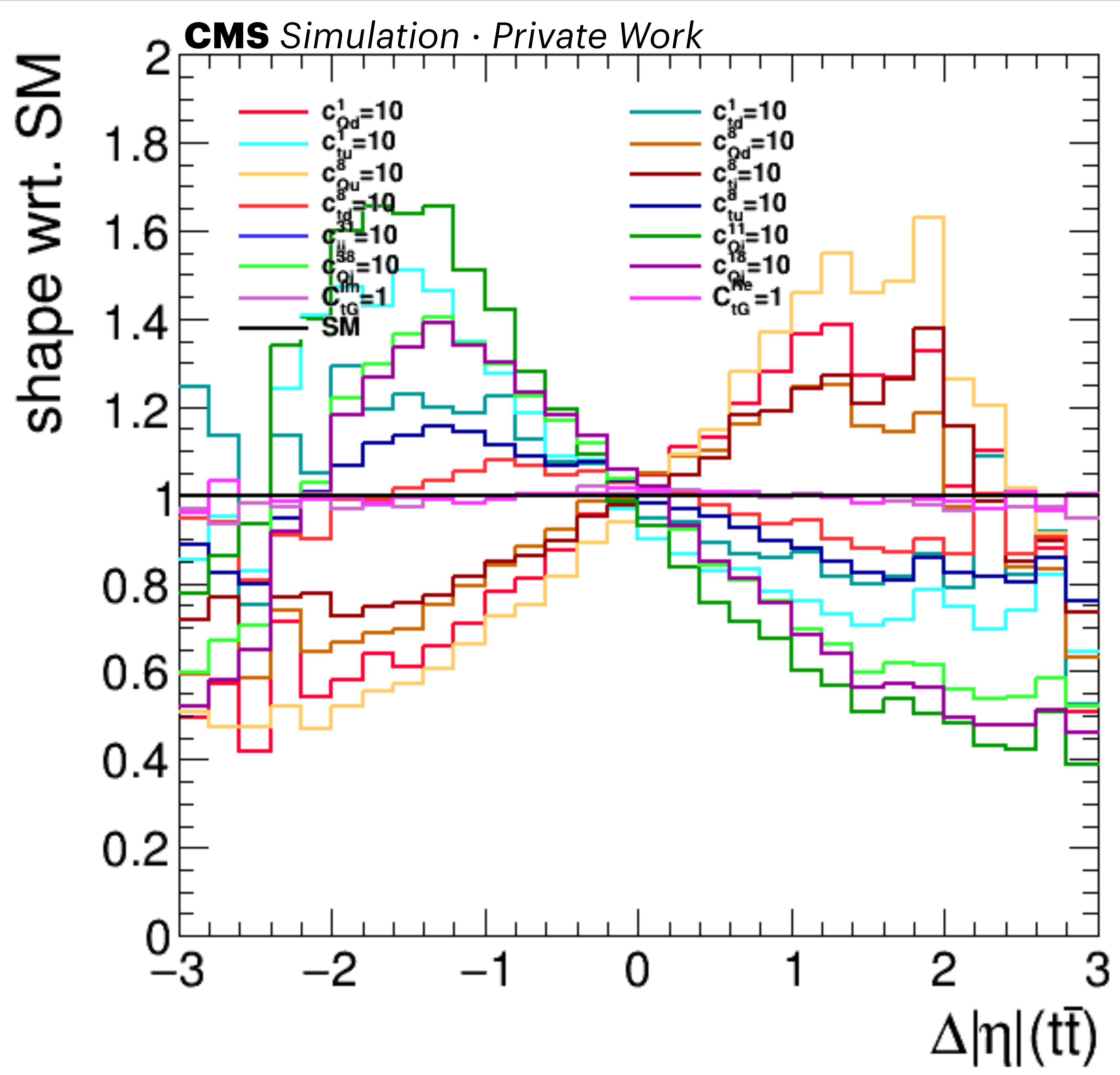

$$\Delta|\eta| = |\eta_t| - |\eta_{\bar{t}}|$$

Complimentary Observables

- Effects of operators on **angular** and **asymmetry** distributions, ξ_{kk} and $\Delta|\eta|$:

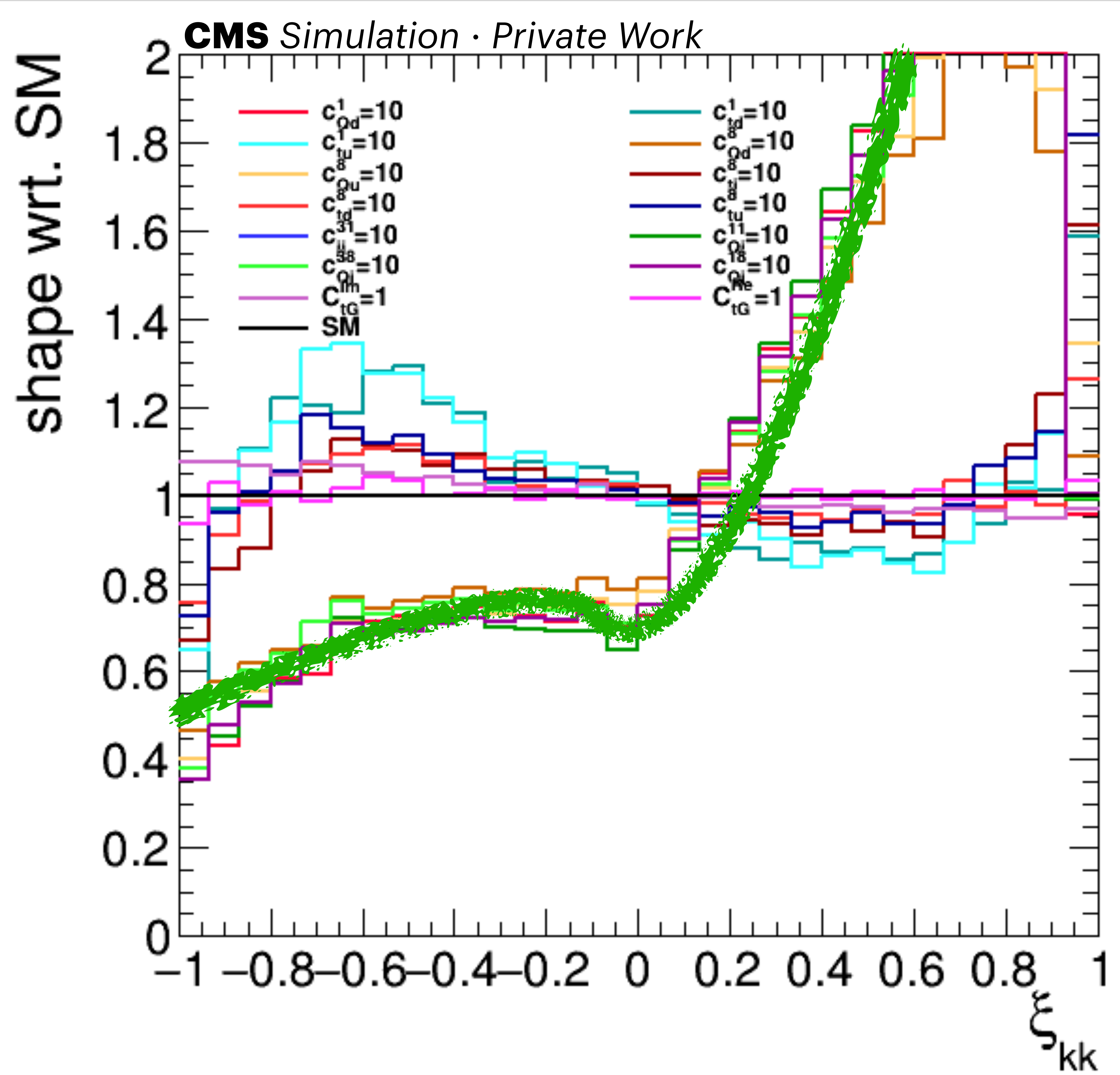

$\xi_{kk} = \cos\theta * \cos\bar{\theta}$

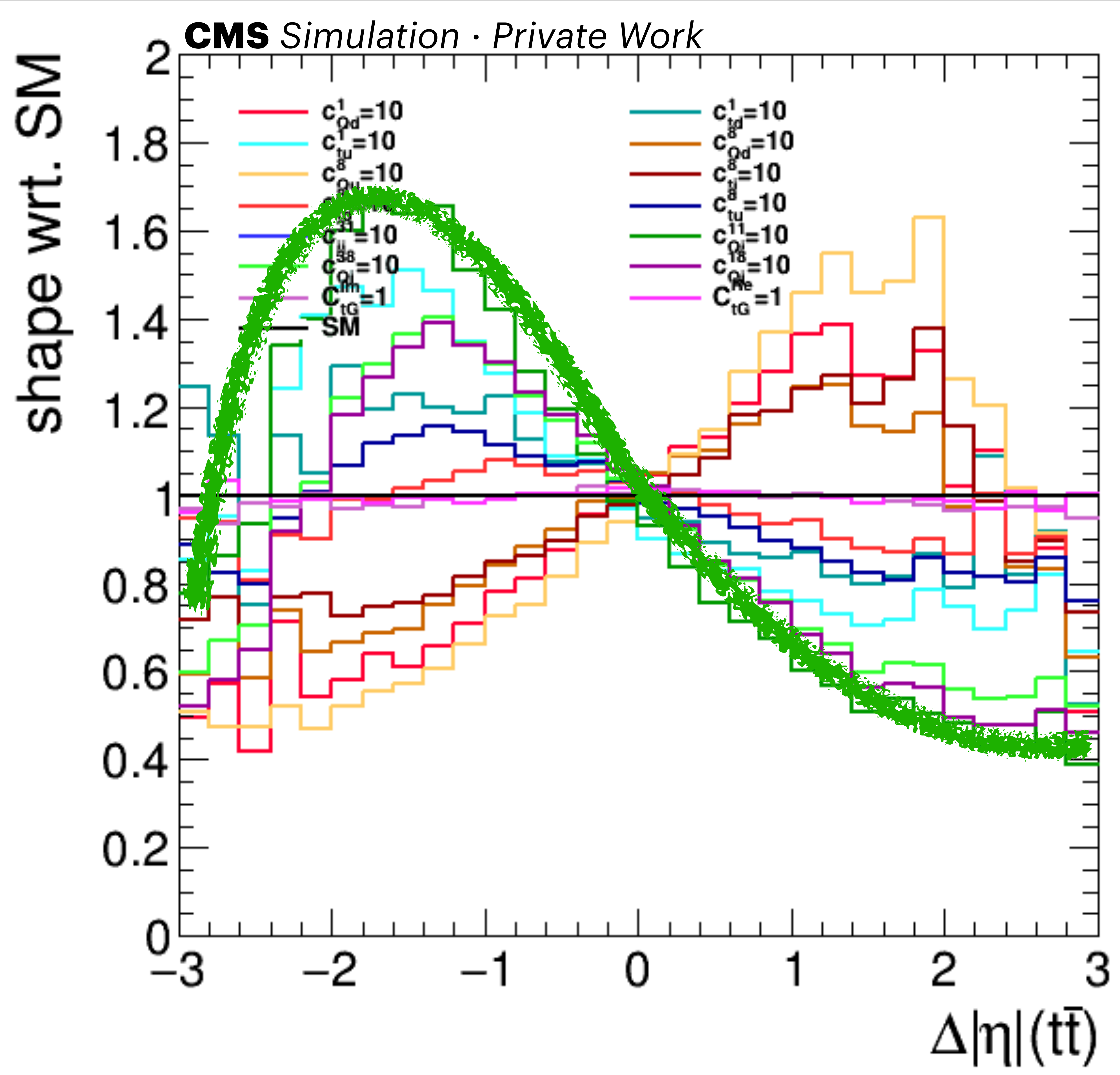

$\Delta|\eta| = |\eta_t| - |\eta_{\bar{t}}|$

Complimentary Observables

- Effects of operators on **angular** and **asymmetry** distributions, ξ_{kk} and $\Delta|\eta|$:

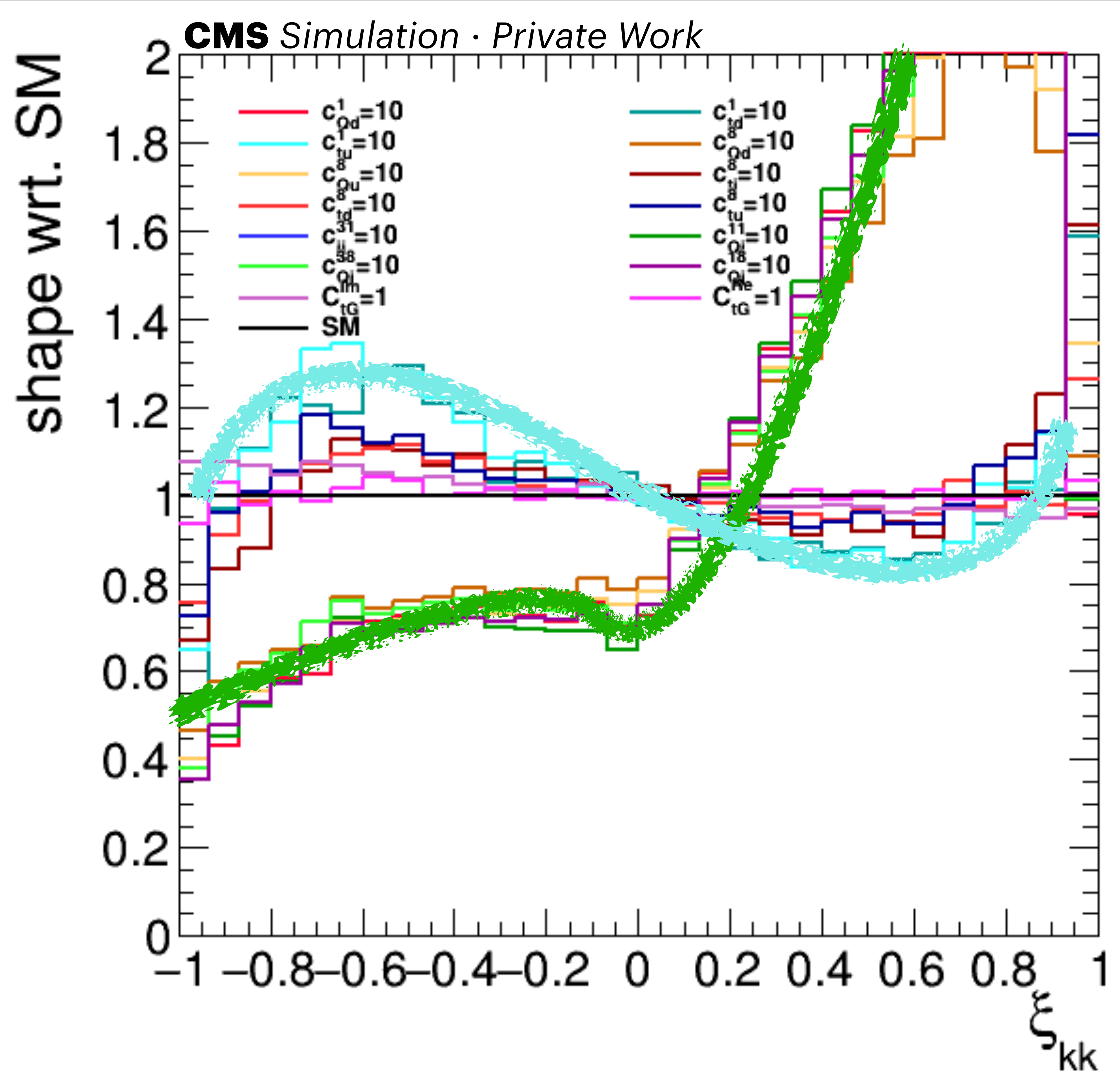

$$\xi_{kk} = \cos\theta * \cos\bar{\theta}$$

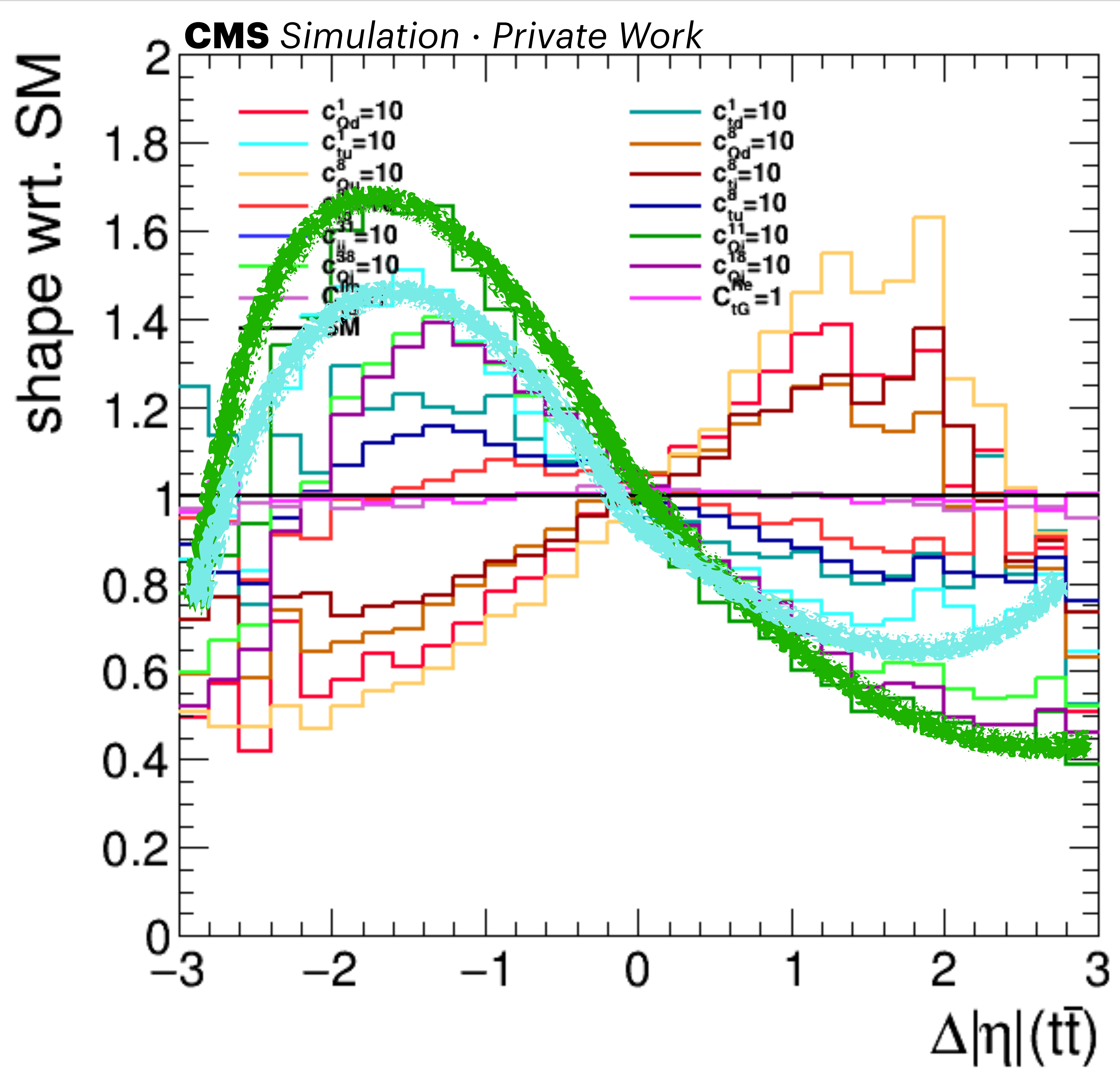

$$\Delta|\eta| = |\eta_t| - |\eta_{\bar{t}}|$$

Complimentary Observables

- Effects of operators on **angular** and **asymmetry** distributions, ξ_{kk} and $\Delta|\eta|$:

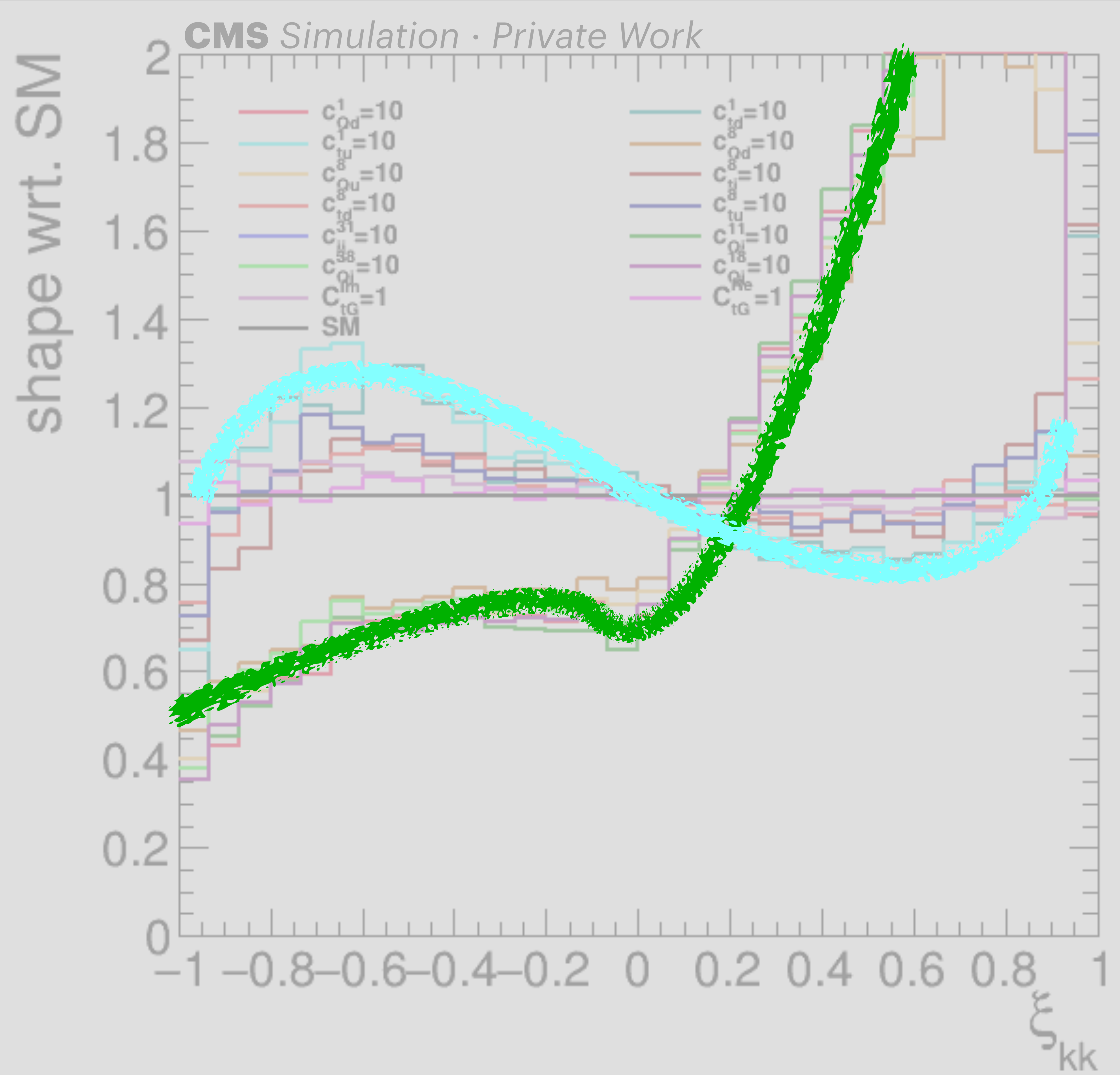

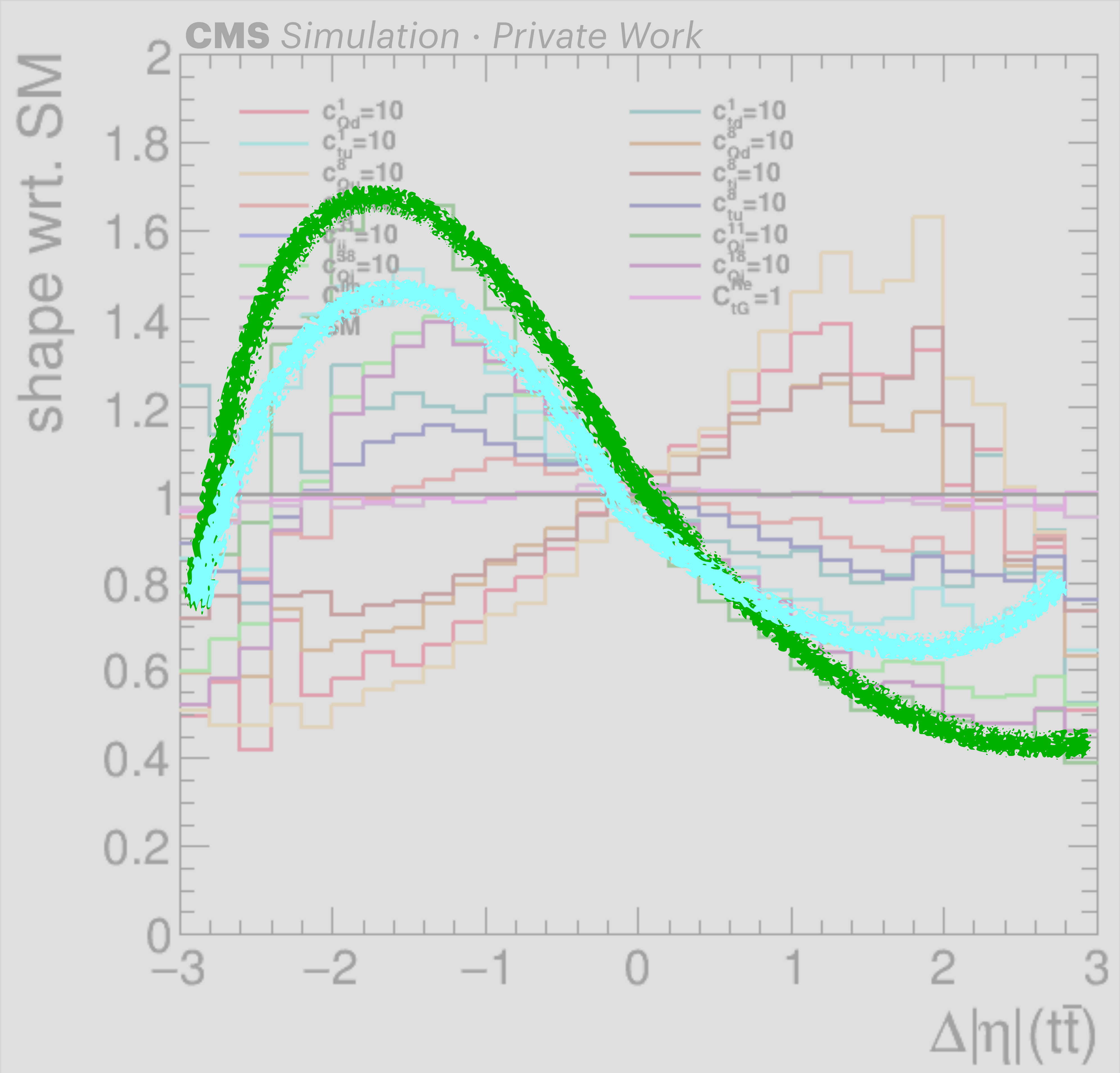

Observe **complimentary constraining power** in WC space

Summary/Outlook

- **Working to optimize our charge asymmetry measurement**
    - this time at reconstruction level to maintain handle on systematic uncertainties
- **Investigating new angular variables in our ttbar system**
- **Will use SMEFT to interpret any observed deviations from SM predictions**
    - interpretation is based on operators that affect ttbar production
- **Observed complimentary constraining power in different types of input data**
    - we hope to improve constraints of marginalised fits with this strategy

Summary/Outlook

- **Working to optimize our charge asymmetry measurement**
  - this time at reconstruction level to maintain handle on systematic uncertainties
- **Investigating new angular variables in our ttbar system**
- **Will use SMEFT to interpret any observed deviations from SM predictions**
  - interpretation is based on operators that affect ttbar production
- **Observed complimentary constraining power in different types of input data**
  - we hope to improve constraints of marginalised fits with this strategy
- **Optimization of ttbar system reconstruction** is also being investigated
  - Emphasis of getting **accurate directions** of angular variables
- Different methods to **extract constraints** for WCs are being investigated

Thank you

Time for questions and comments

BACKUP: Production Mechanisms

- A top quark antiquark pair (ttbar) can be produced, at leading order (LO), by the following:

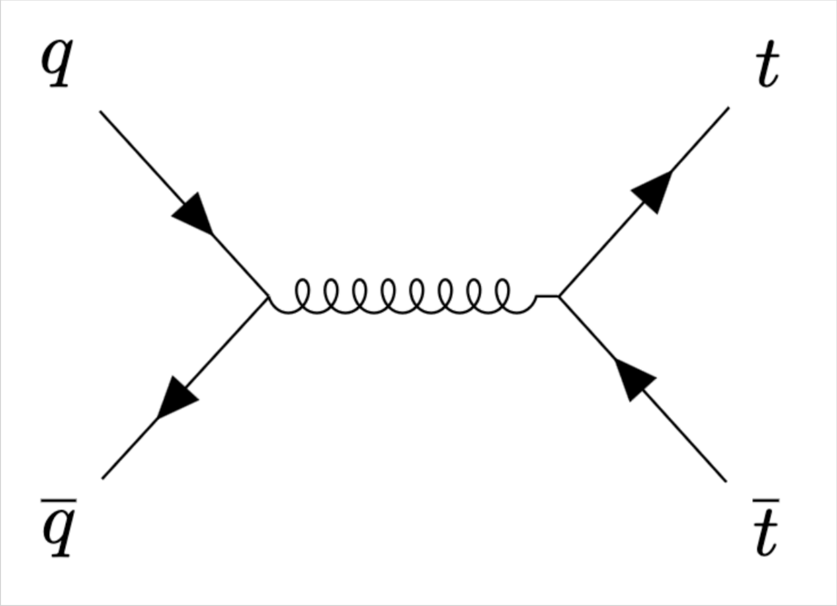

$q\bar{q}$ s-channel

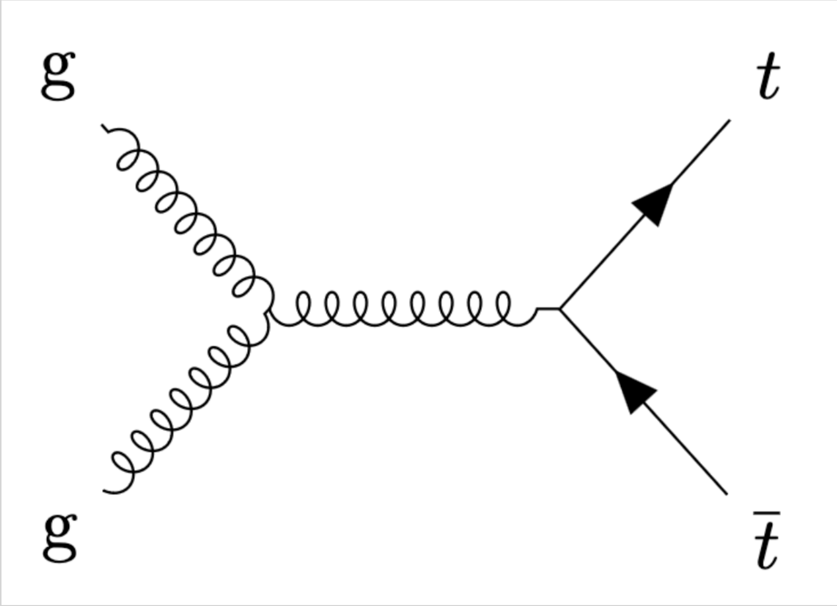

gg s-channel

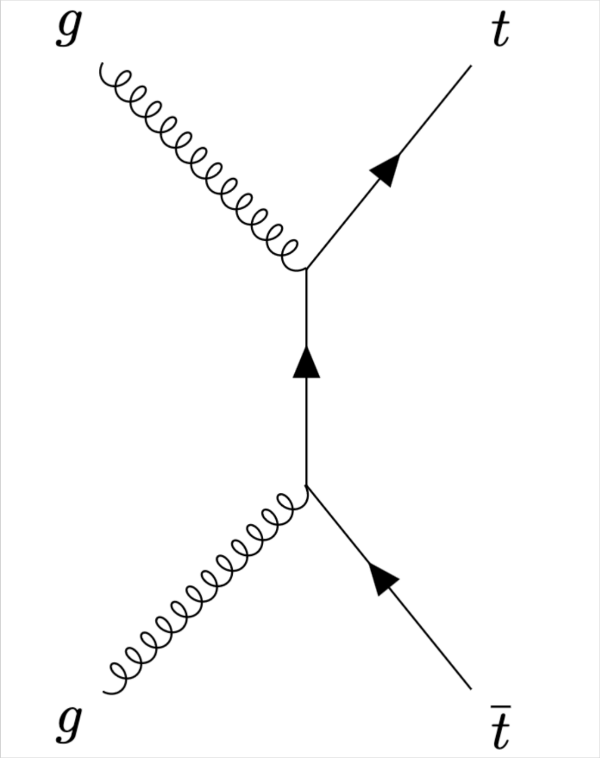

gg t-channel

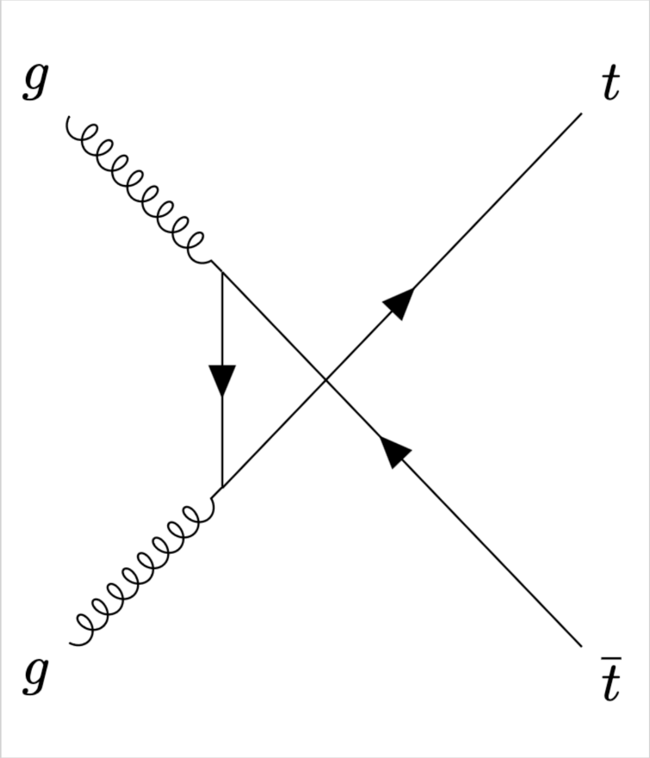

gg u-channel

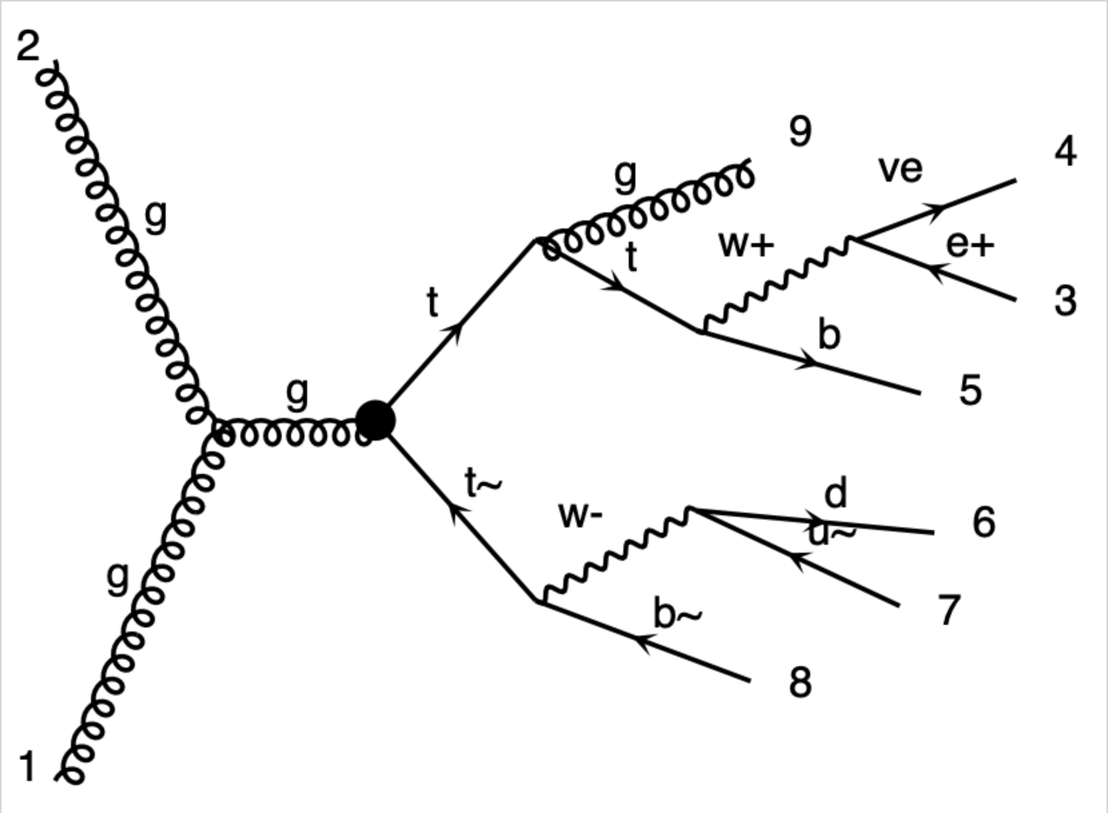

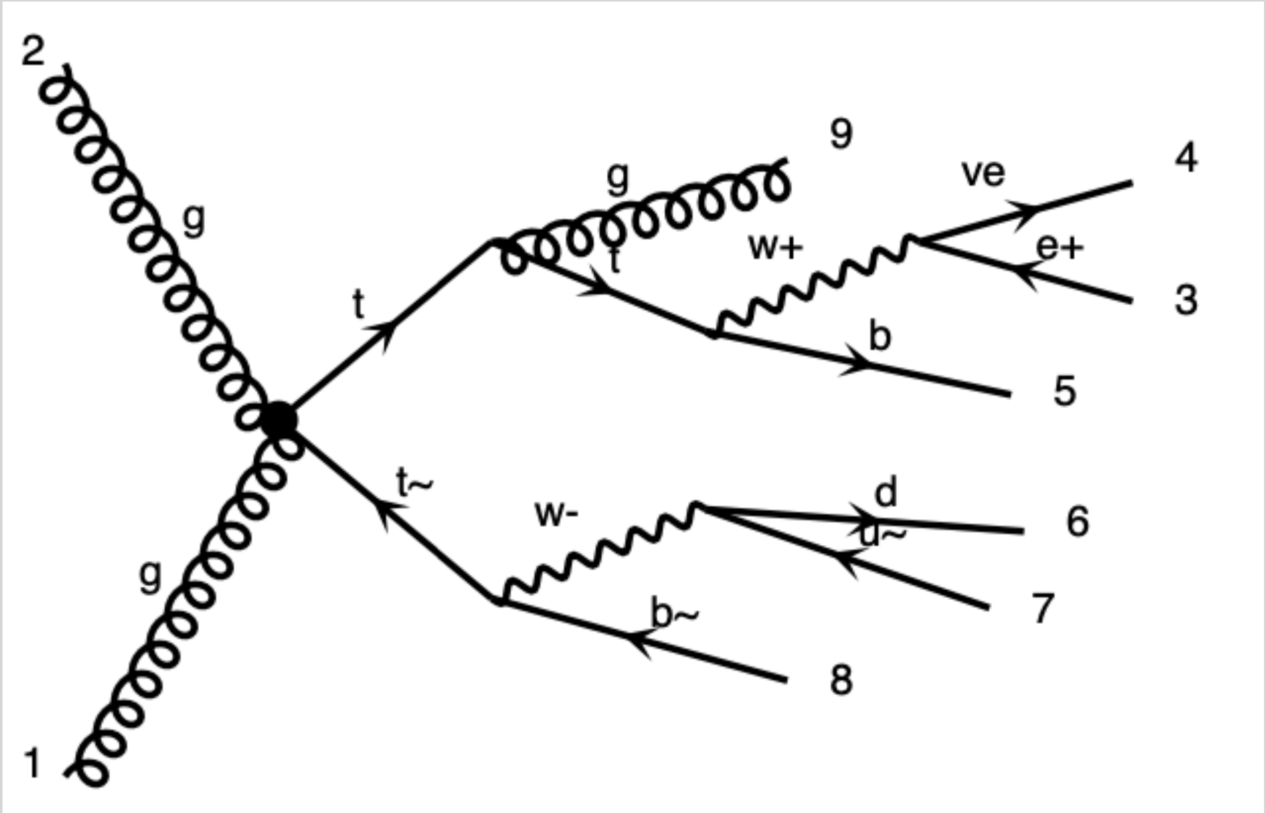

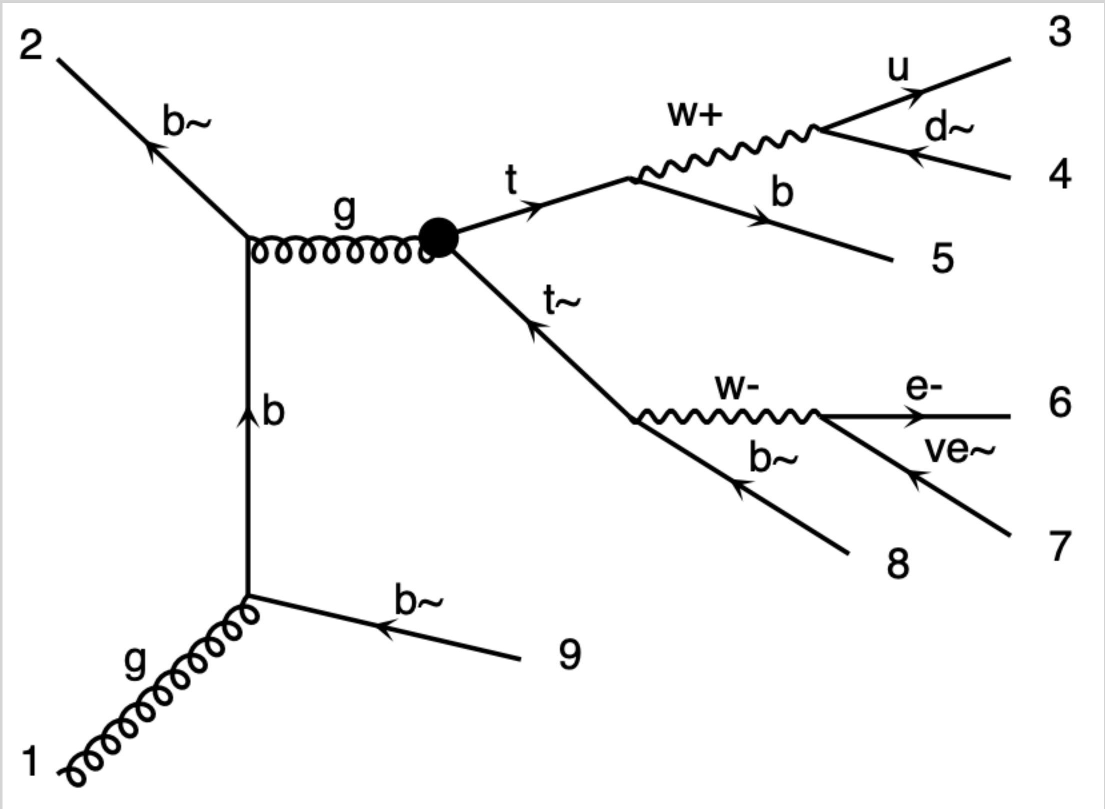

BACKUP: Object/Event Selection

- Triggers with isolation for low p_T leptons (e and μ) but not for high p_T leptons.
- AK4 and AK8 PUPPI jets are used.
- MET is negative vector sum of p_T of all PF candidates after being scaled by PUPPI algorithm.
- The DeepJet algorithm is used for b-tagging on AK4 jets.
- The DeepAK8-MD algorithm is used for t-tagging on AK8 jets.
- >2 AK4 jets are required and at least one has to be b-tagged.

Anti-Kt algorithm

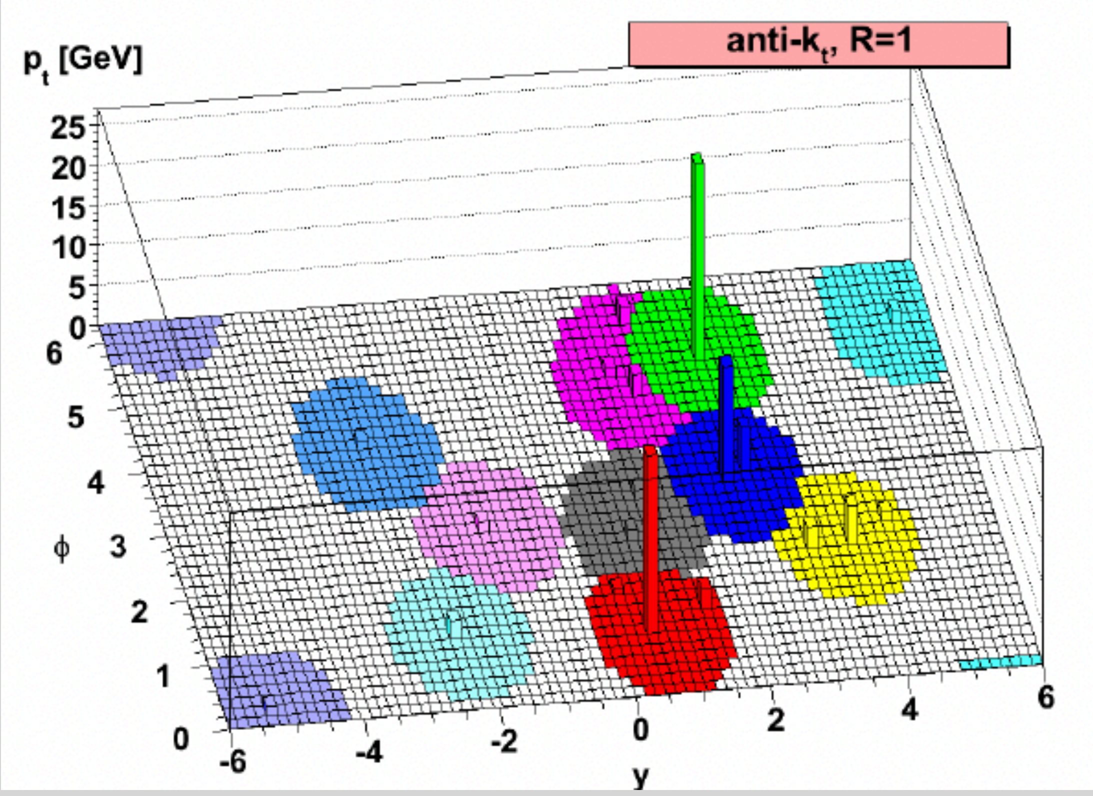

DeepJet ROC

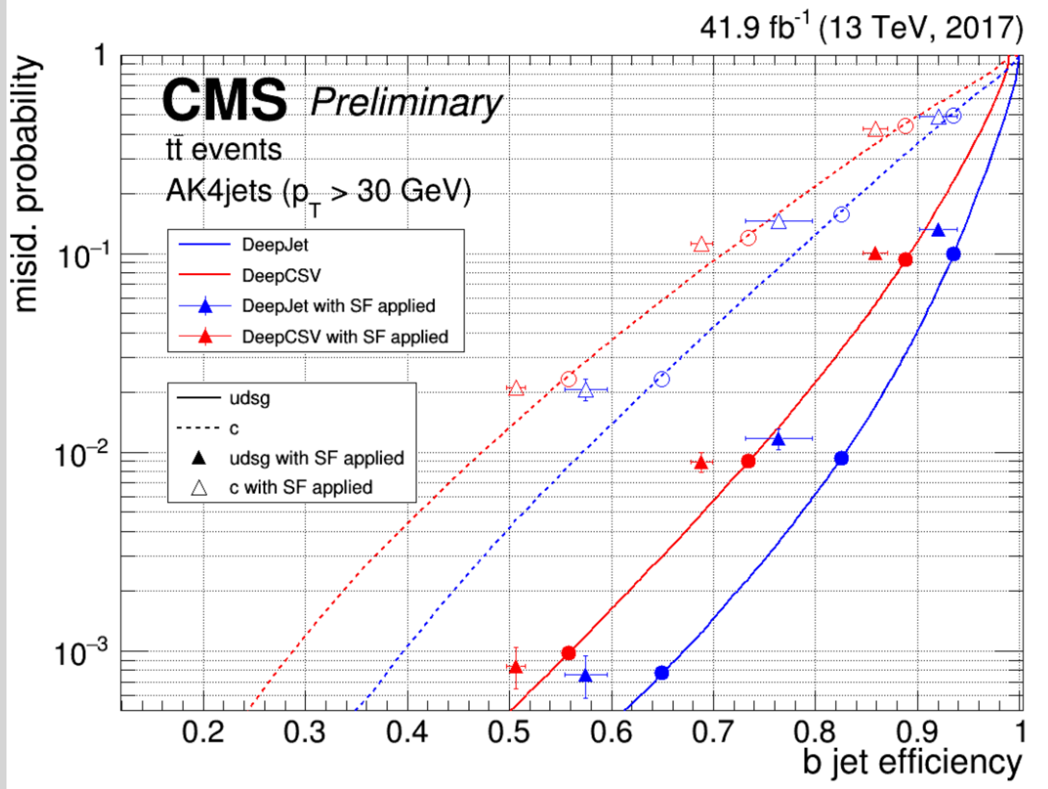

DeepAK8 performance

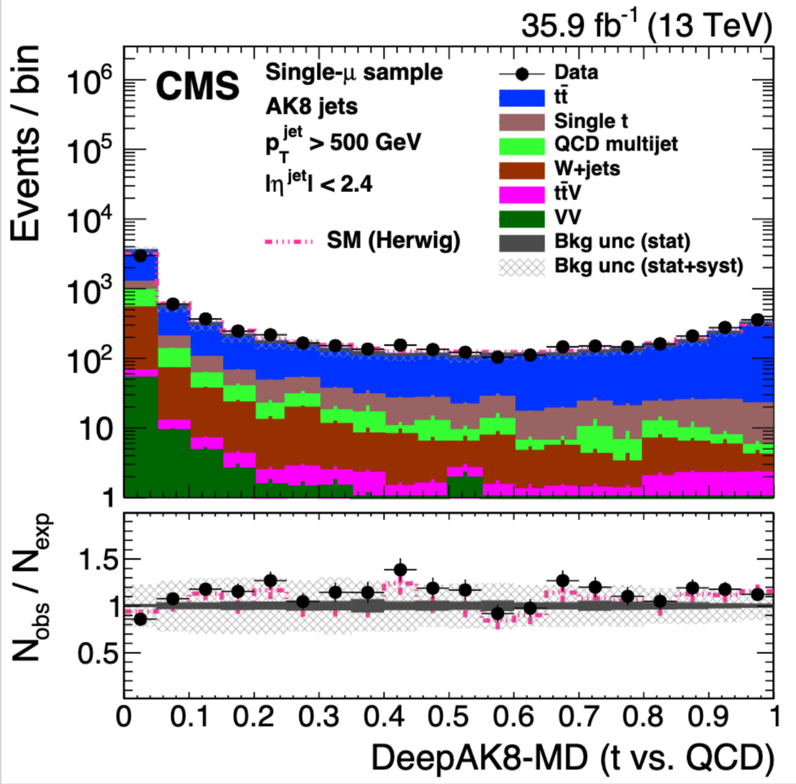

BACKUP: Backgrounds

Backgrounds

- The following 2D cut is incorporated into the event selection of high-p_T leptons to reduce the QCD multijet background events:

$$\Delta R_{min}\left(l, jet\right) > 0.4 \quad || \quad p_{T,rel}\left(l, jet\right) > 25\ GeV$$

- We use a Deep Neural Network (DNN) to classify events originating from the single-top, V+jets backgrounds and our ttbar signals.

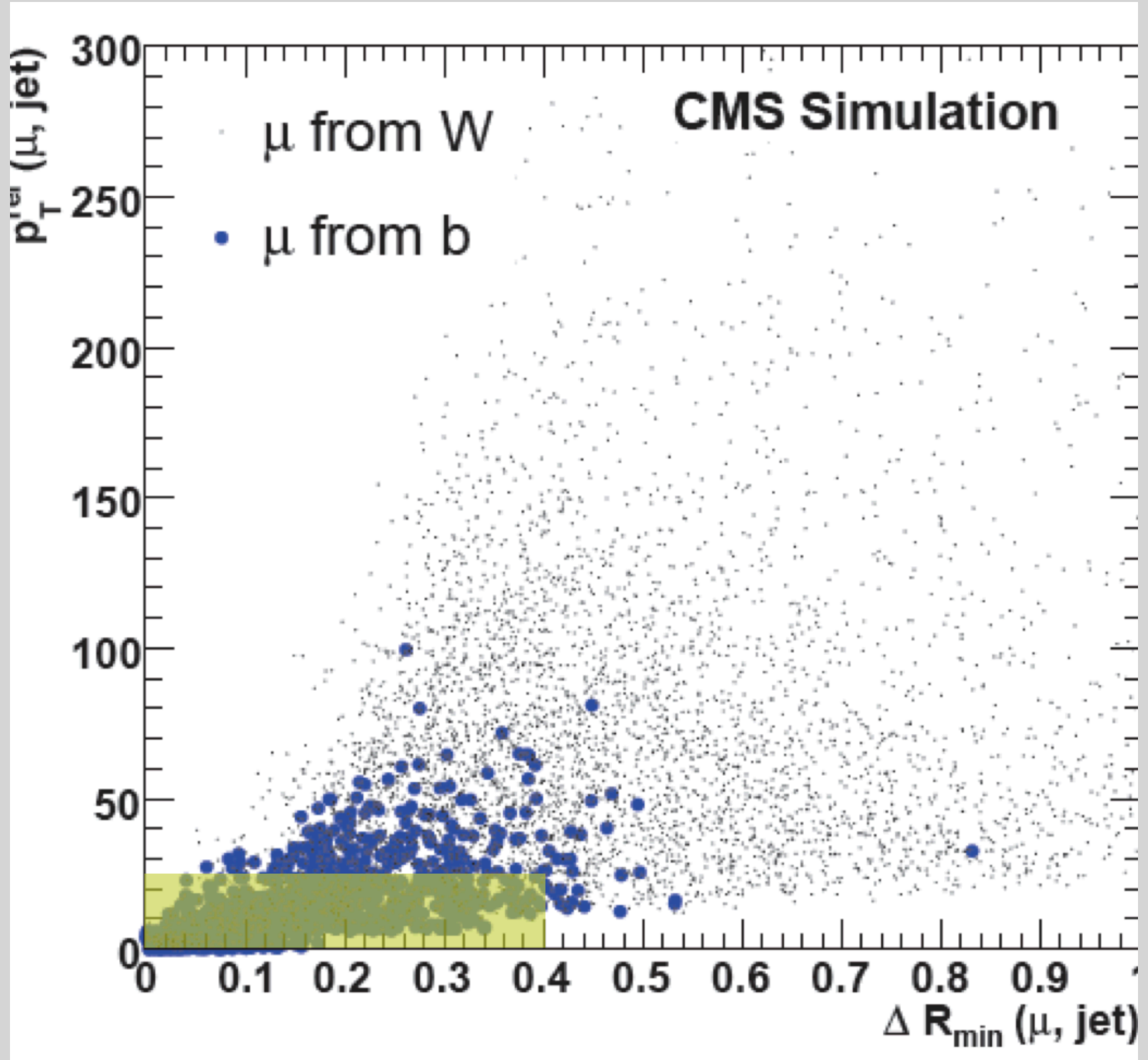

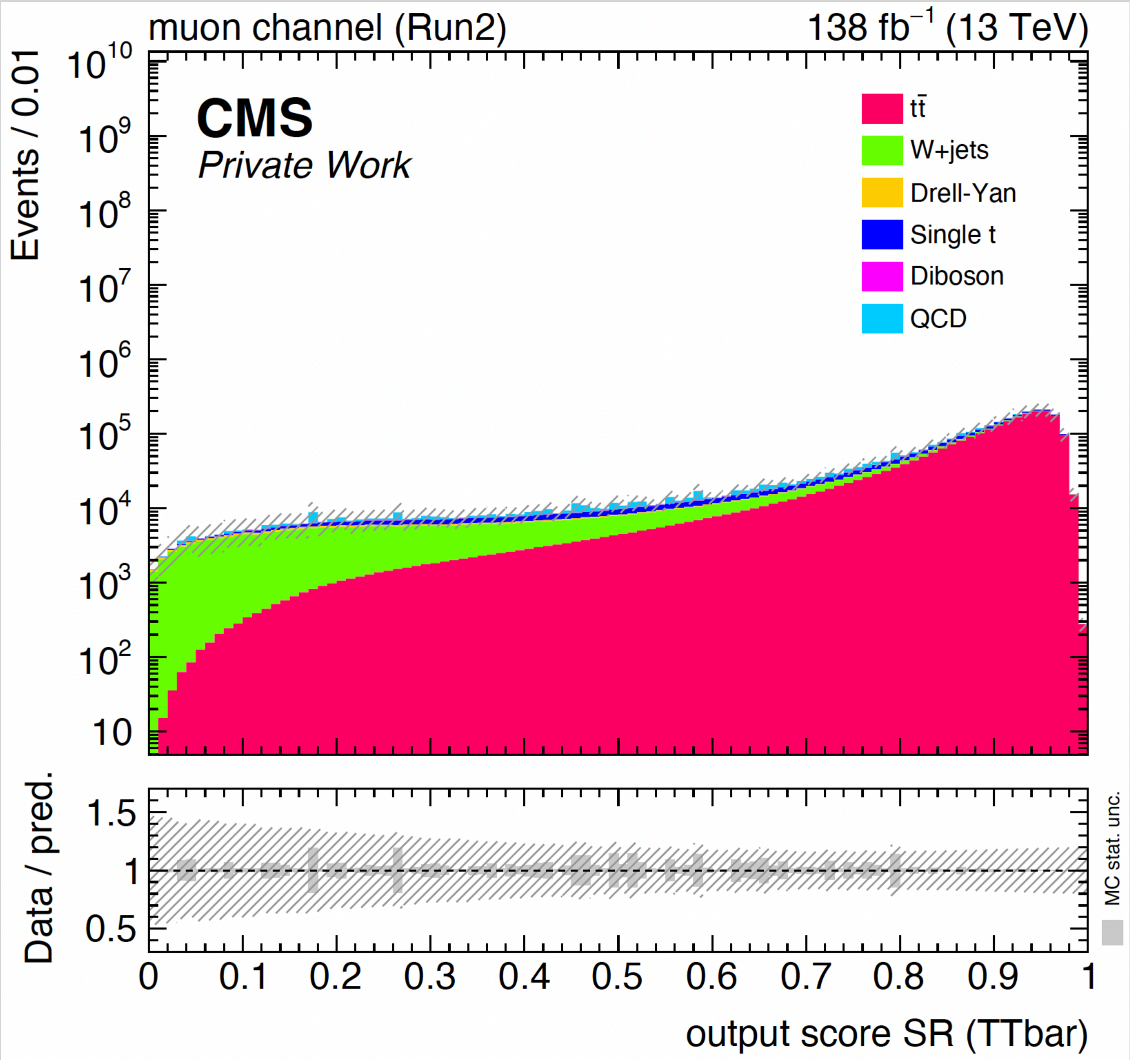

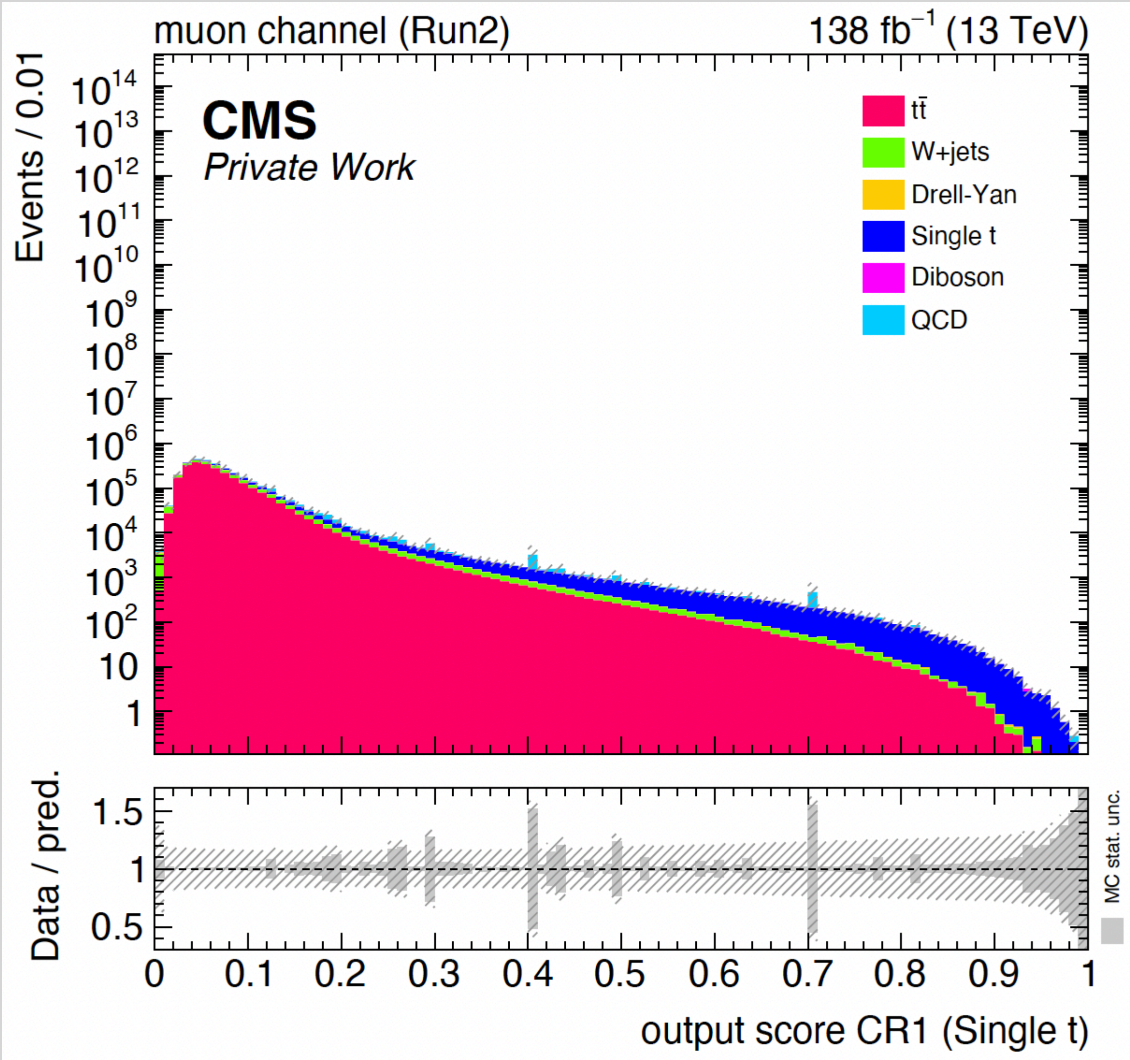

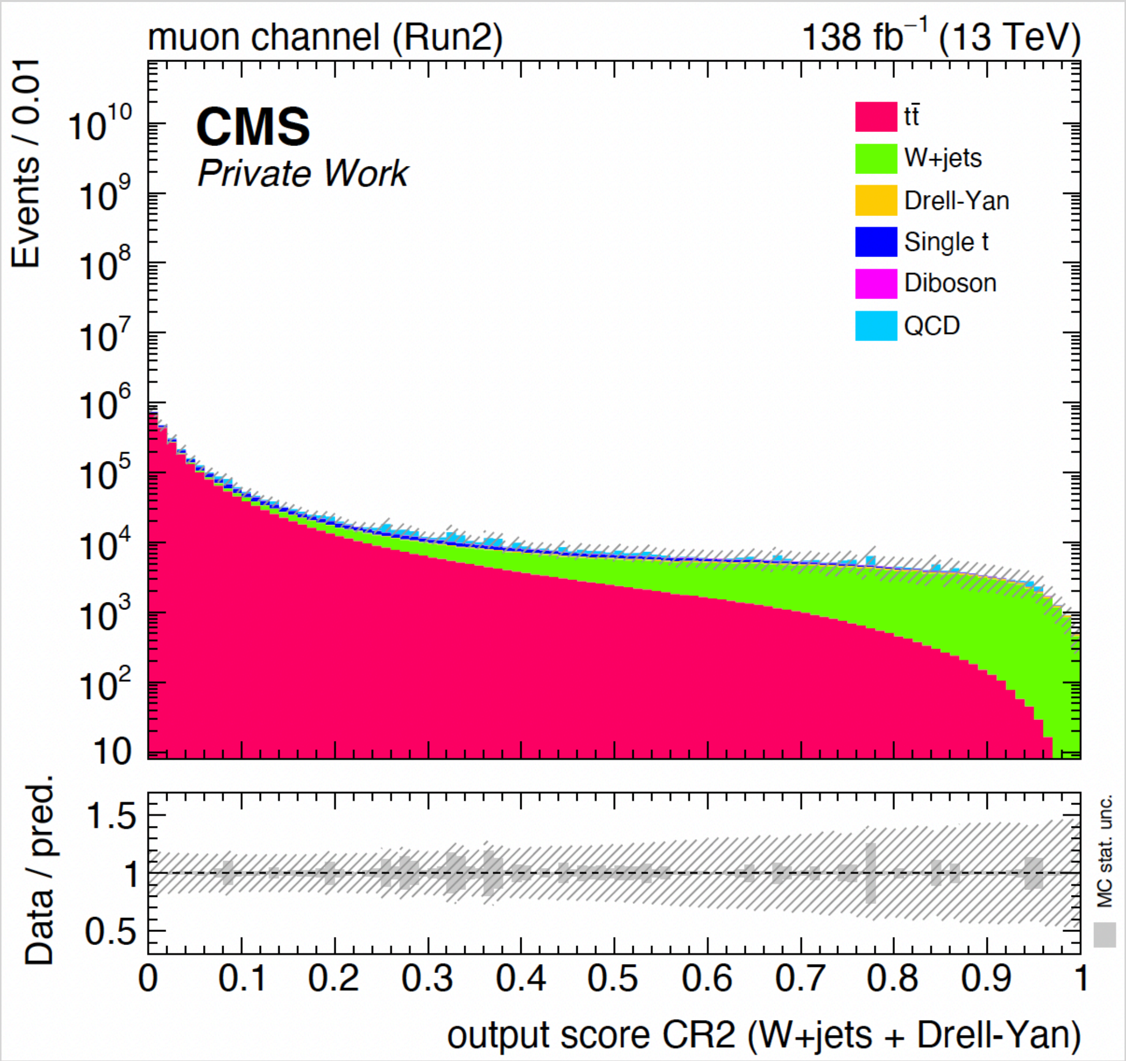

BACKUP: Event Reco

Event Reconstruction

- The ttbar system is reconstructed once the 4-vectors of the objects in the event selection are assigned to the leptonic or hadronic decaying top.

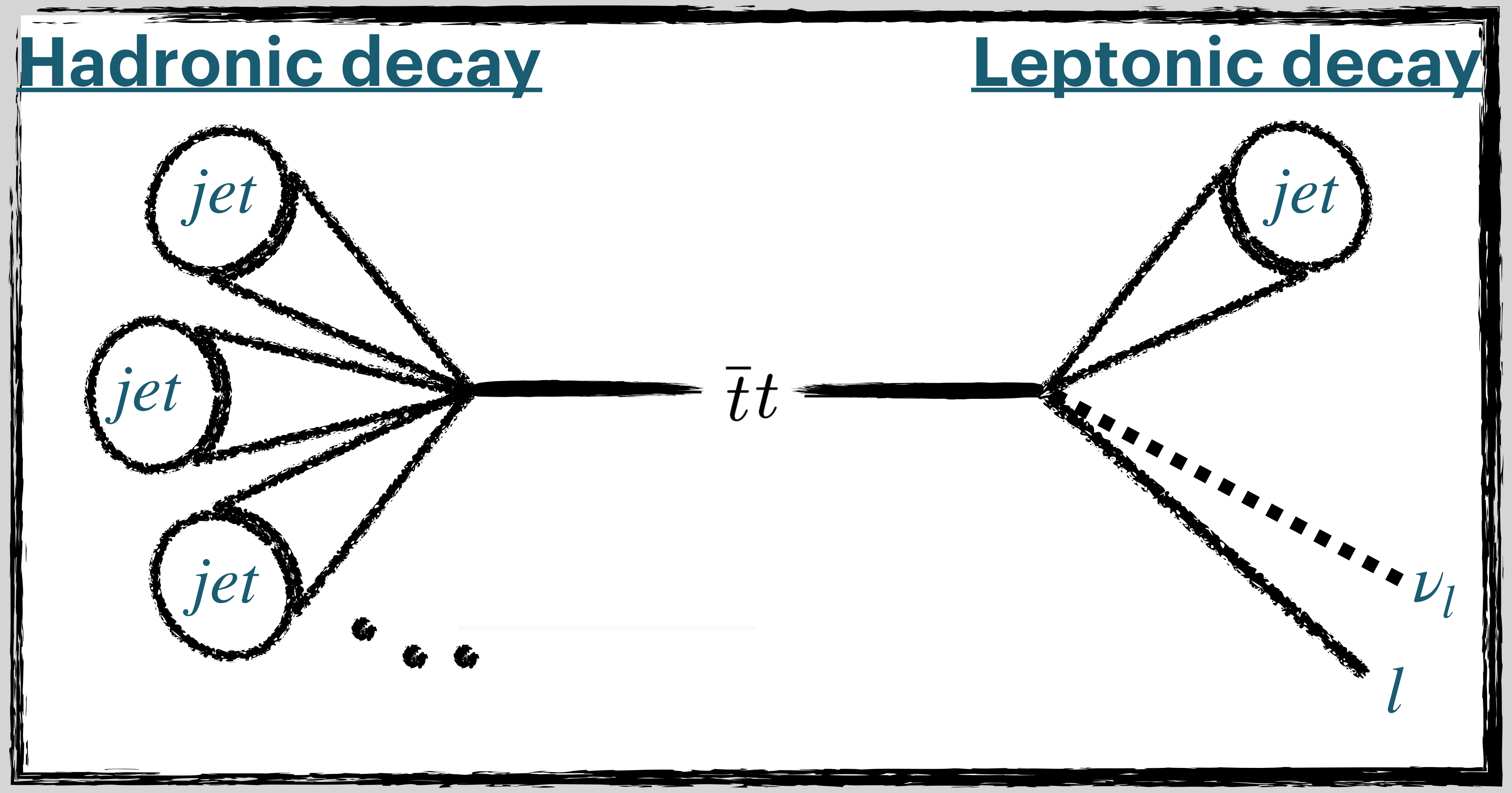

- The lepton and MET are always assigned to the leptonic decay.

- All the jets in event are considered in every possible permutation of jet assignments, each permutation is referred to as a candidate.

BACKUP: Event Reco

Event Reconstruction

- Events are sorted into two topologies based on the absence or presence of a top-tagged AK8 jet into the resolved and merged topology, respectively.

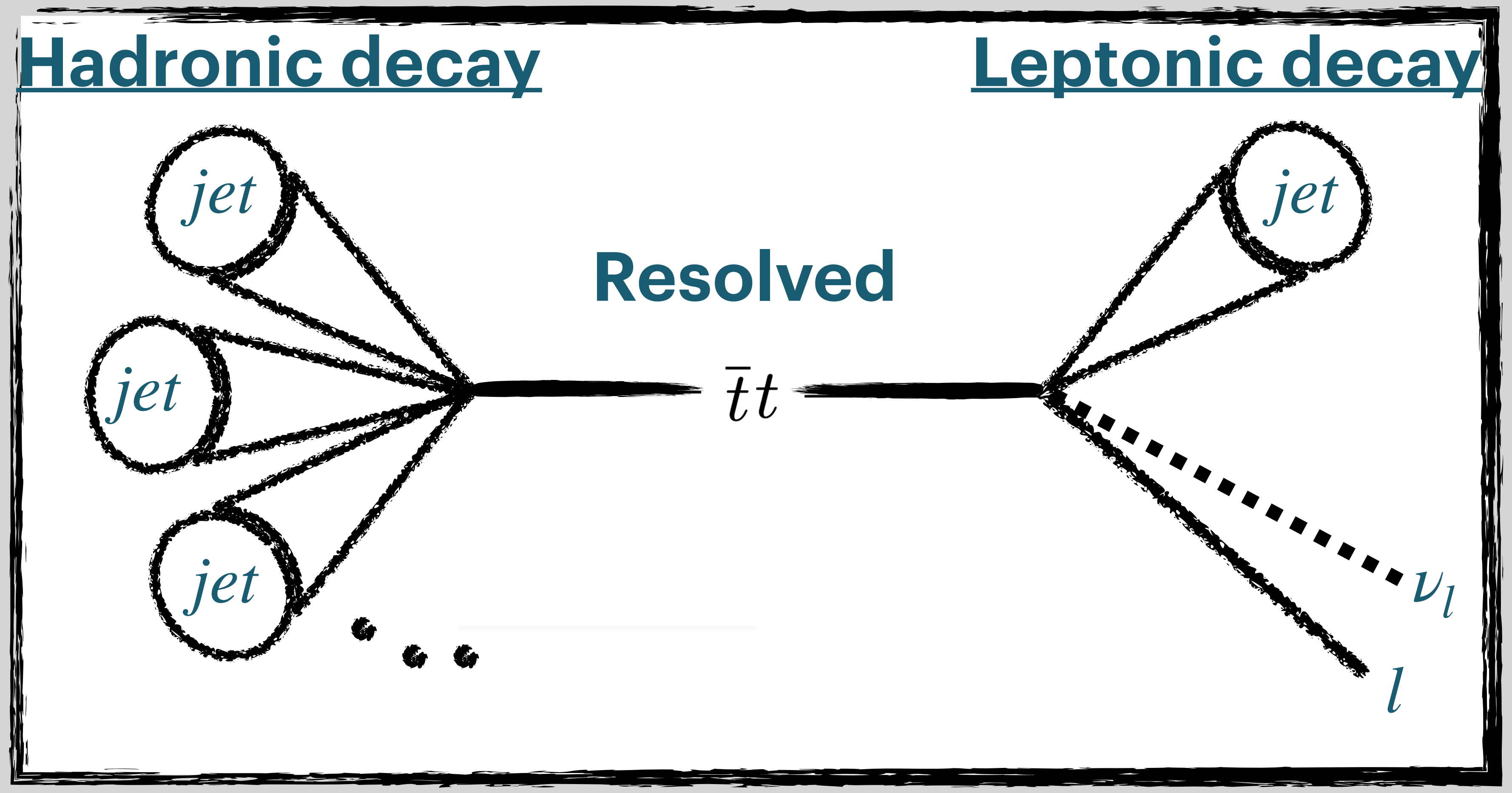

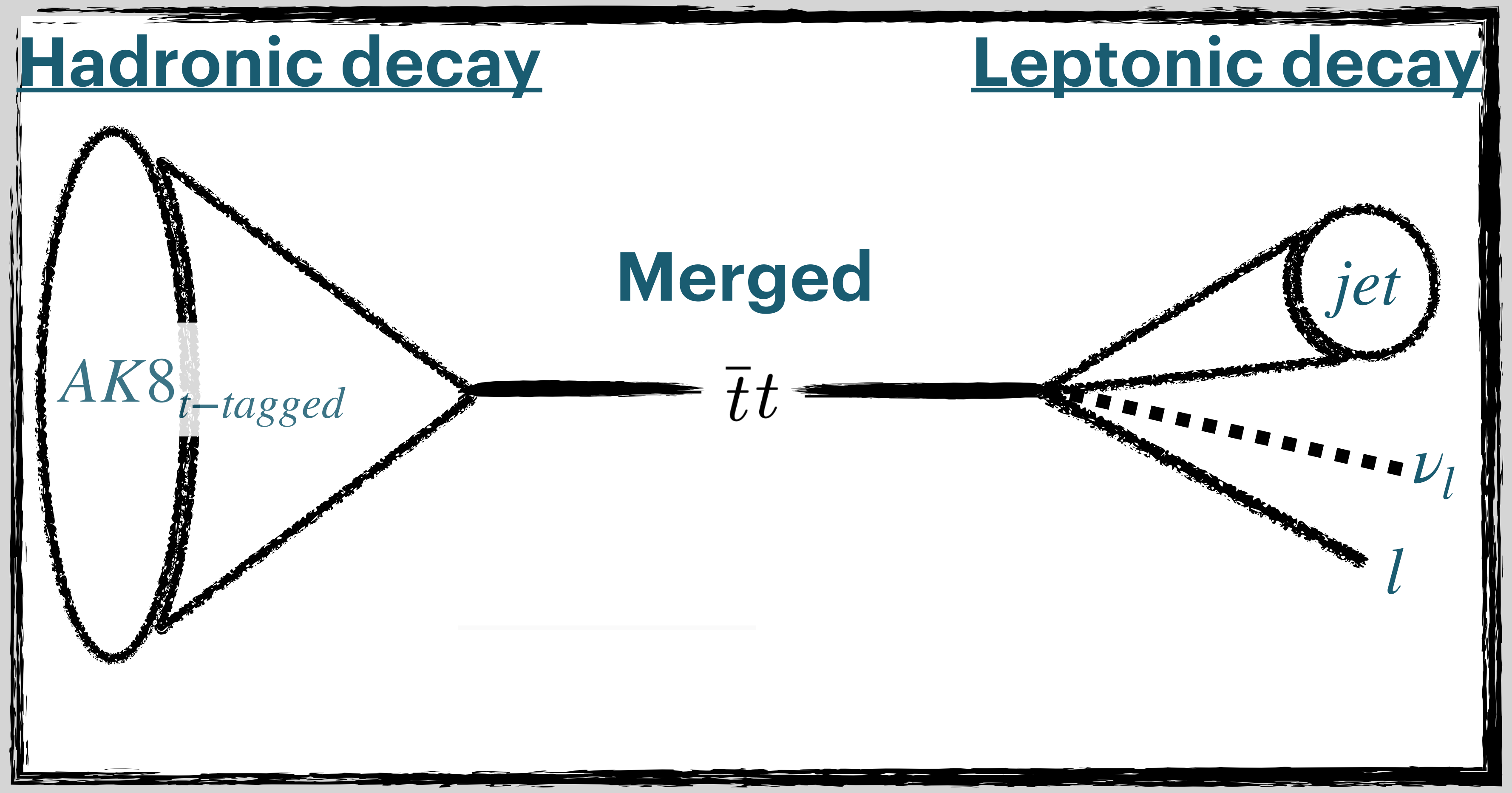

- Each event then has ~$3^{N_{jets}}$ or ~$2^{N_{jets}}$ candidates to consider in the resolved and merged topology.

- The best candidates is chosen by the one that minimizes a $\chi^2\left(M_{lep}^{cand}, M_{had}^{cand}\right)$ function.

$$\left[\frac{M_{\text{lep}} - \bar{M}_{\text{lep}}}{\sigma_{\bar{M}_{\text{lep}}}}\right]^2 + \left[\frac{M_{\text{had}} - \bar{M}_{\text{had}}}{\sigma_{\bar{M}_{\text{had}}}}\right]^2$$

BACKUP: DeepAK8 Tagger

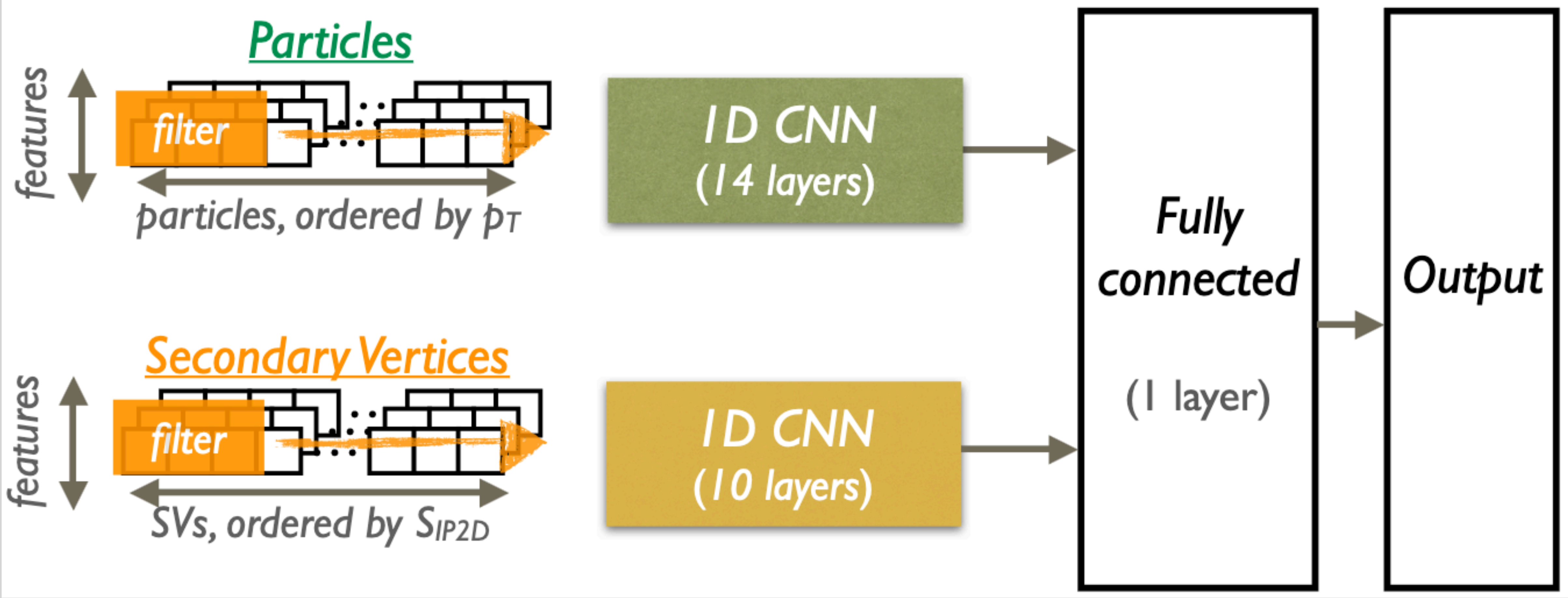

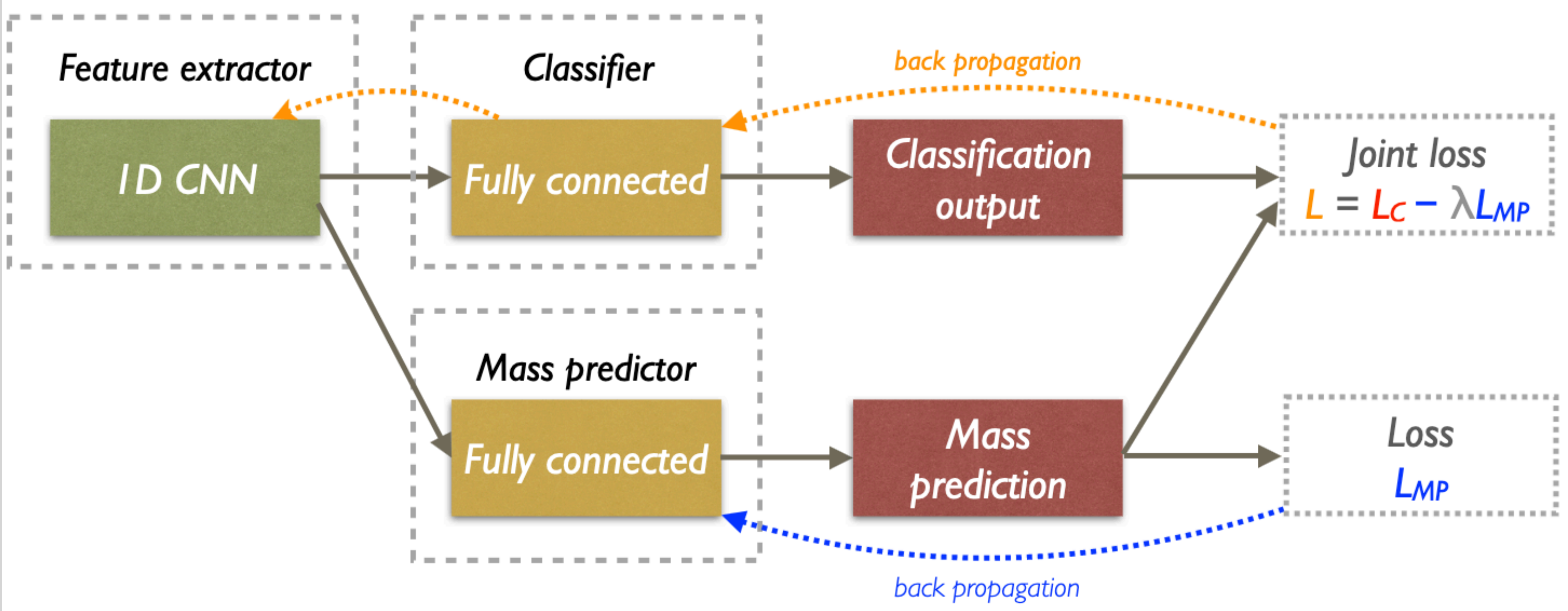

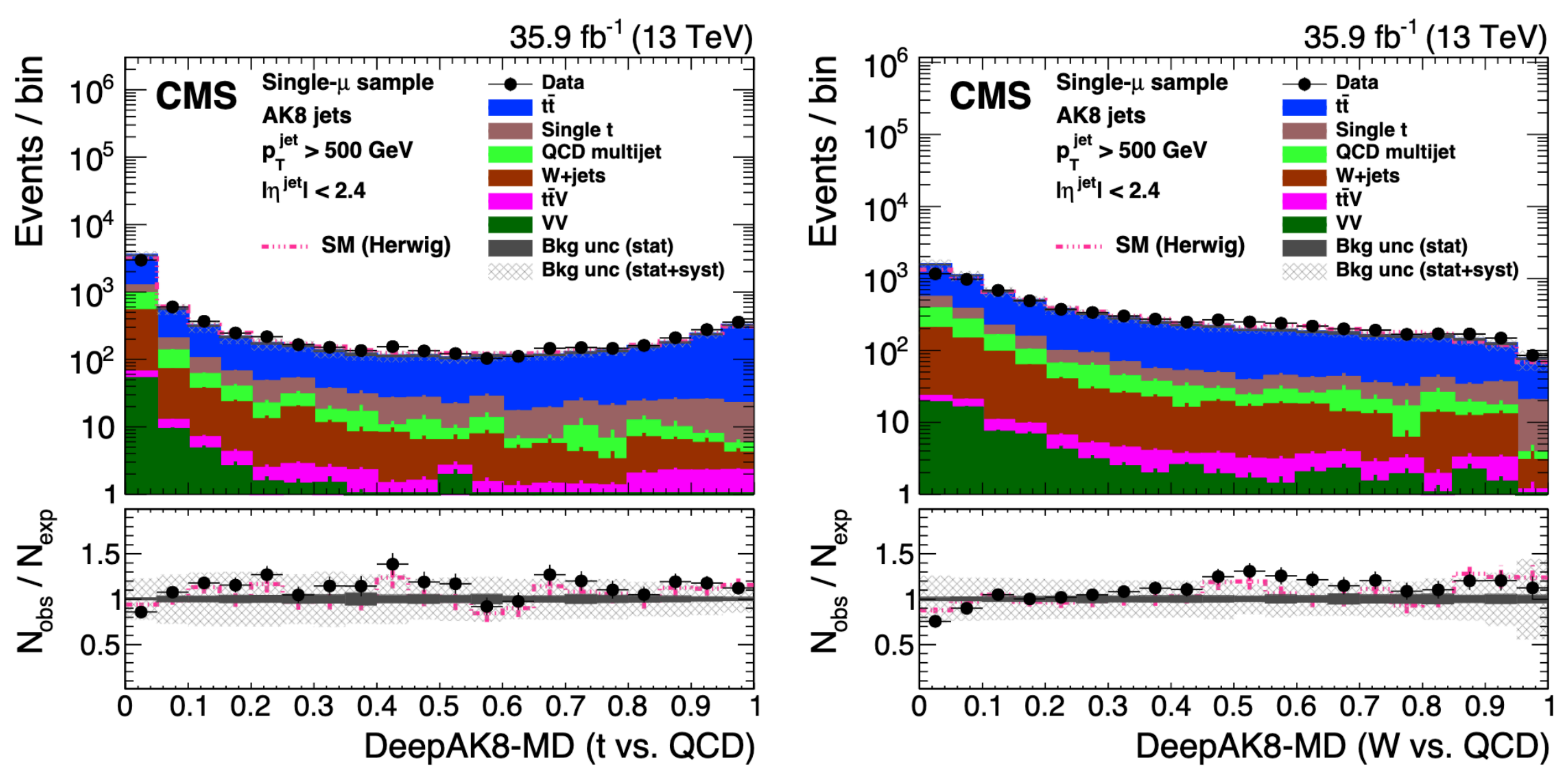

BACKUP: DeepAK8 Tagger

Currently using the UHH2 analysis framework[1].

Recent studies look at b-scores of AK4 jets in resolved topology and AK8 subjets in merged topology.

We see the expected distribution amongst our jet collections.

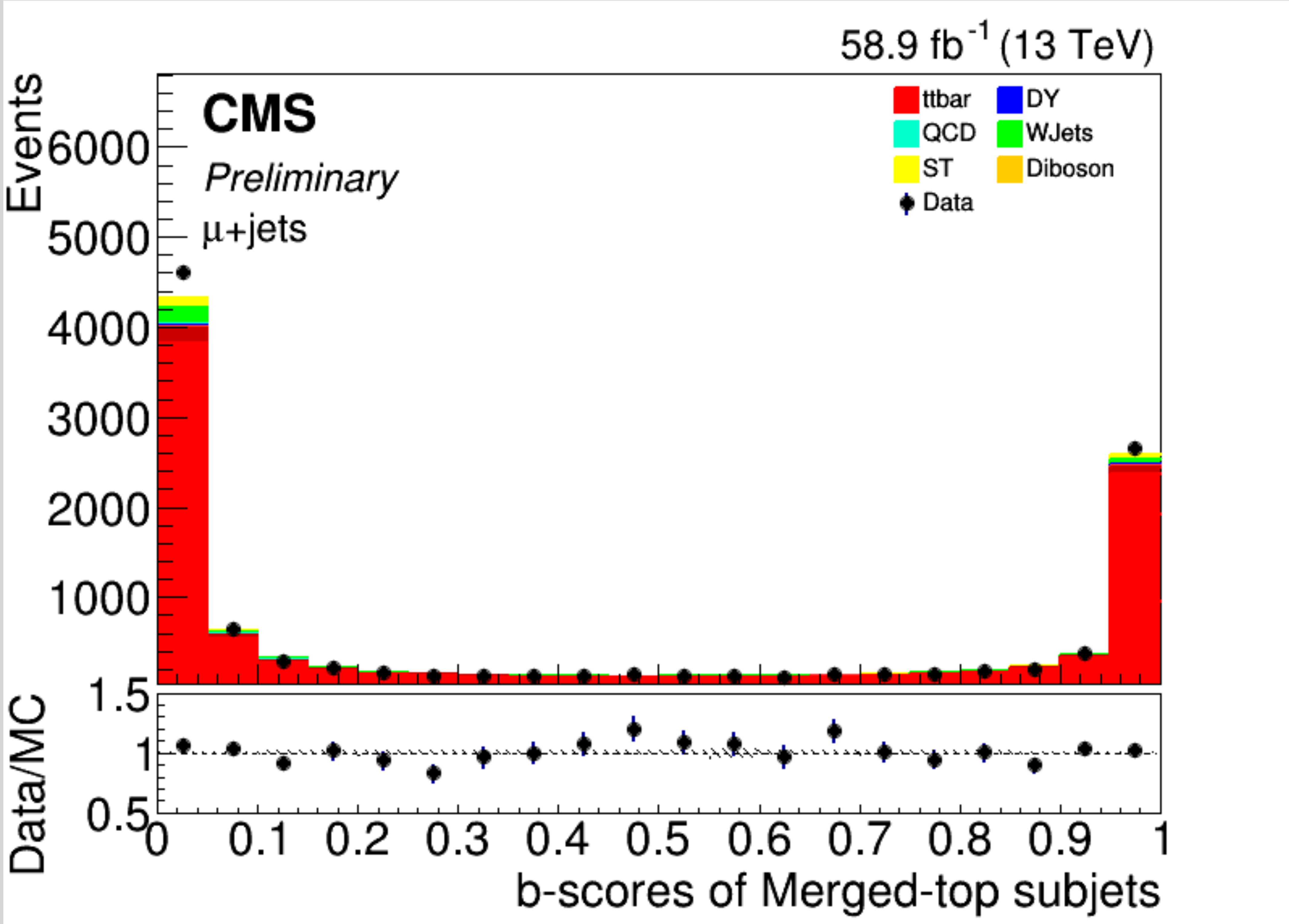

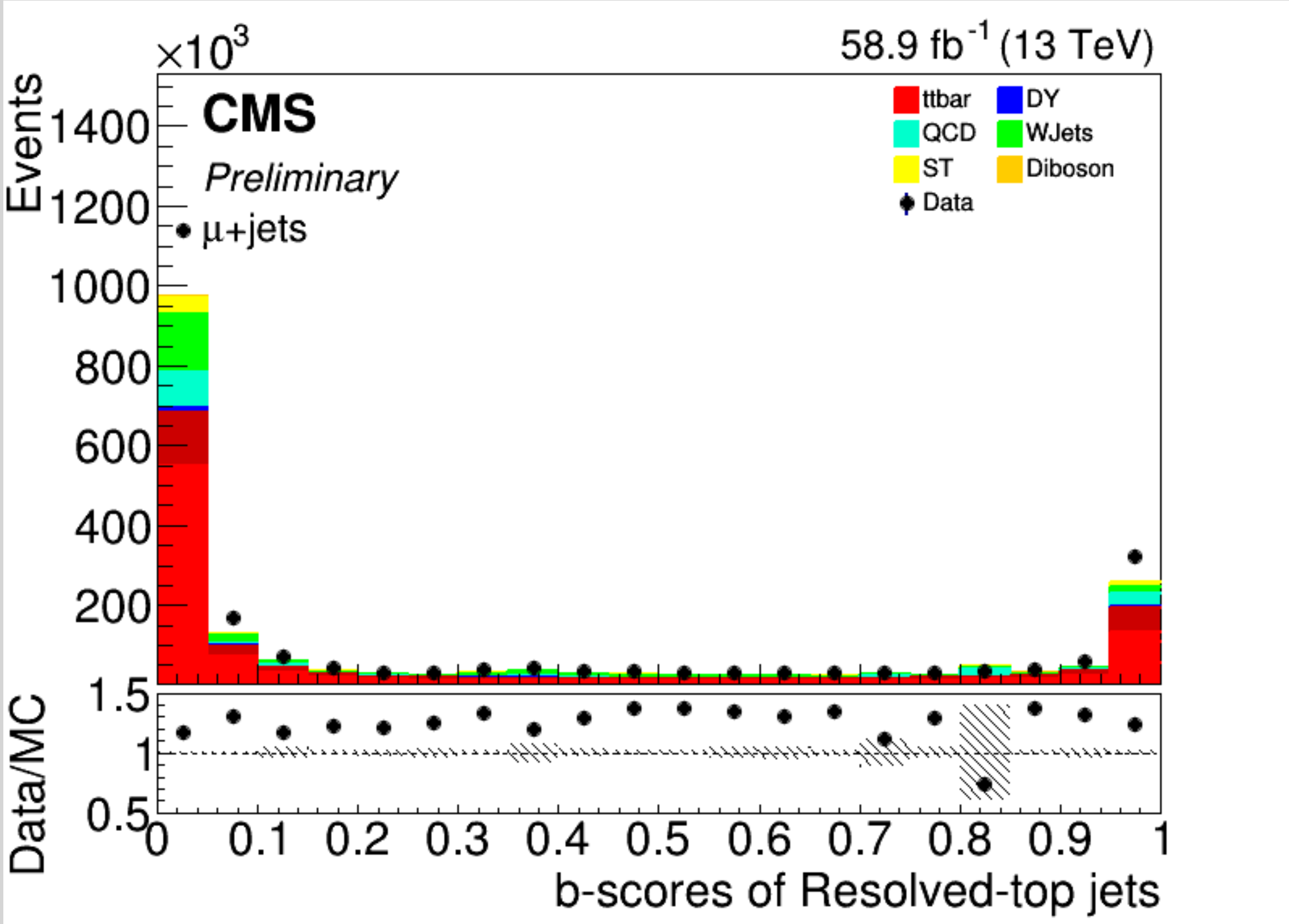

BACKUP: Candidate Kinematic Distributions

The distributions are shown after the likelihood normalization.

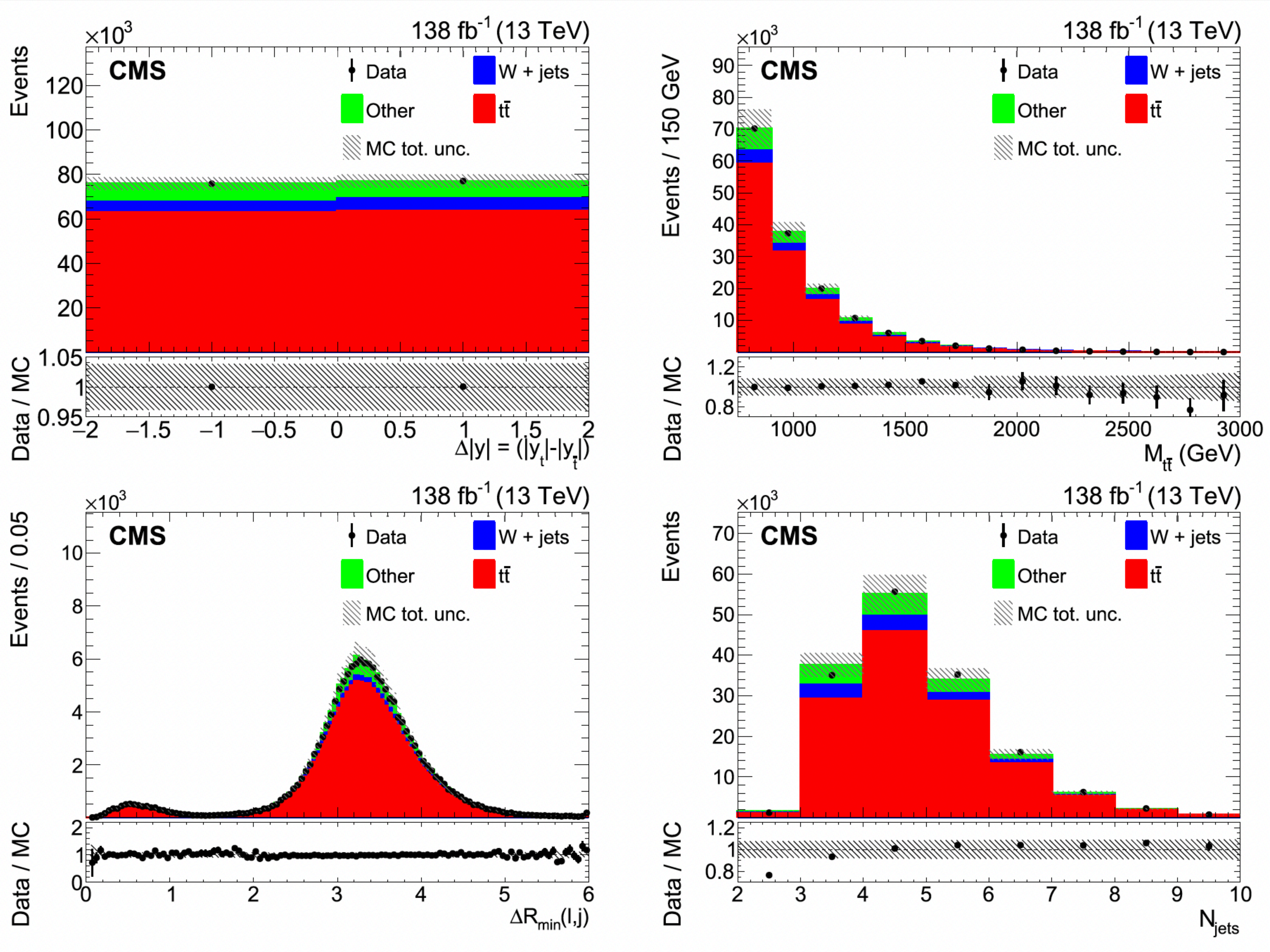

rescob8@uic.edu

BACKUP: Likelihood Function

- For each channel k (specific bin and category) the corresponding likelihood function is:

$$\mathscr{L}_k = \prod_{j=1}^{N_{reco}} P\left(n_j; \sum_{i=1}^{N_{gen}} A_{ji}(\vec{\delta}_u)\mu_i(\vec{\delta}_u) + b_j(\vec{\delta}_u)\right) N(\vec{\delta}_u)$$

- P (n; μ) represents the Poisson probability of observing n events when μ are ex- pected
- i, j are number of bins
- A_{ji} is the response matrix, which gives the probability for an event reconstructed in bin j to have been produced in bin i
- μ_i are signal events
- b_i are background events
- $N(d_u)$ are priors for nuisance parameters

BACKUP: Chi2 Effeciency

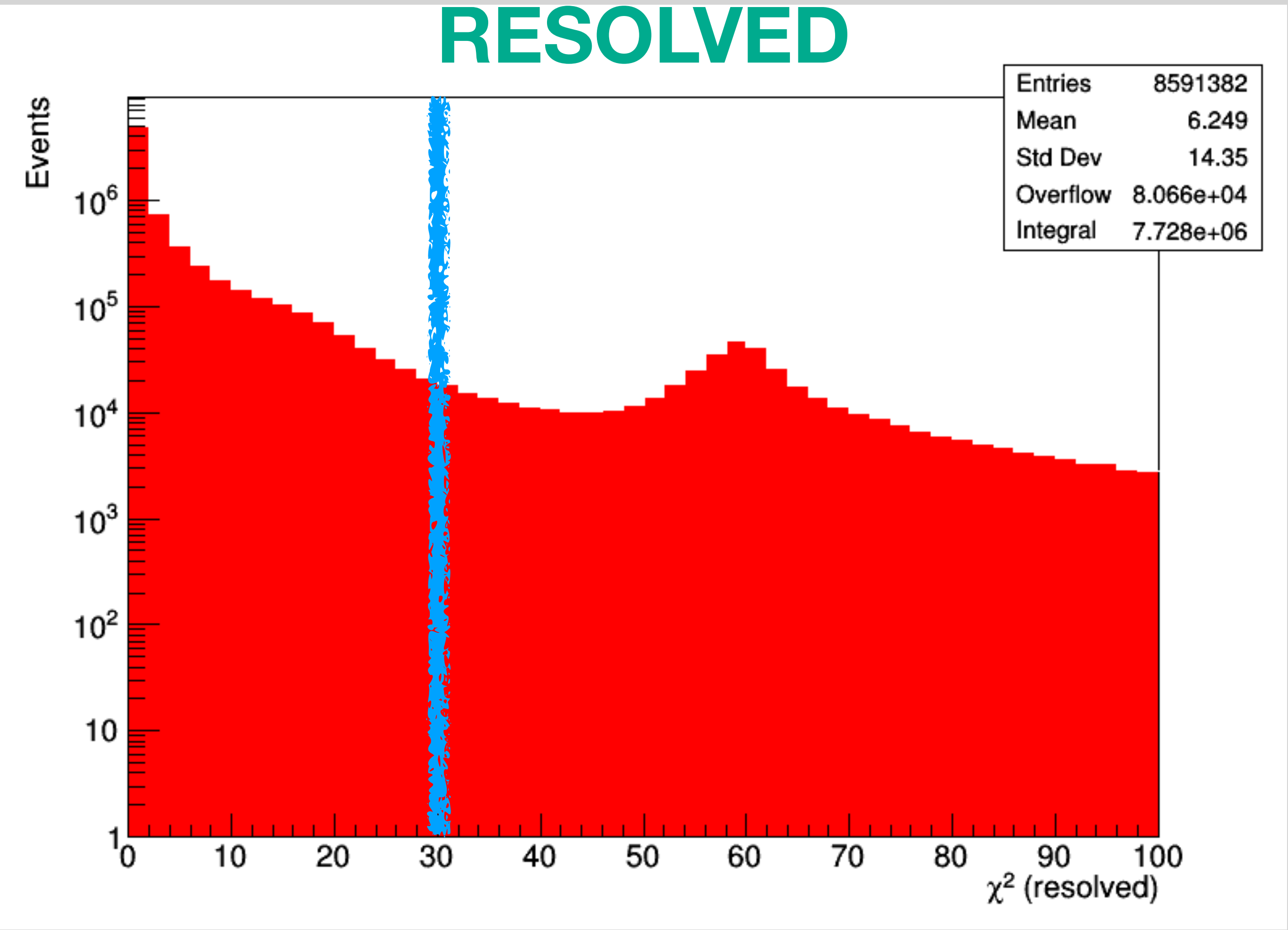

$\varepsilon_{\chi^2<30}$ = 93%

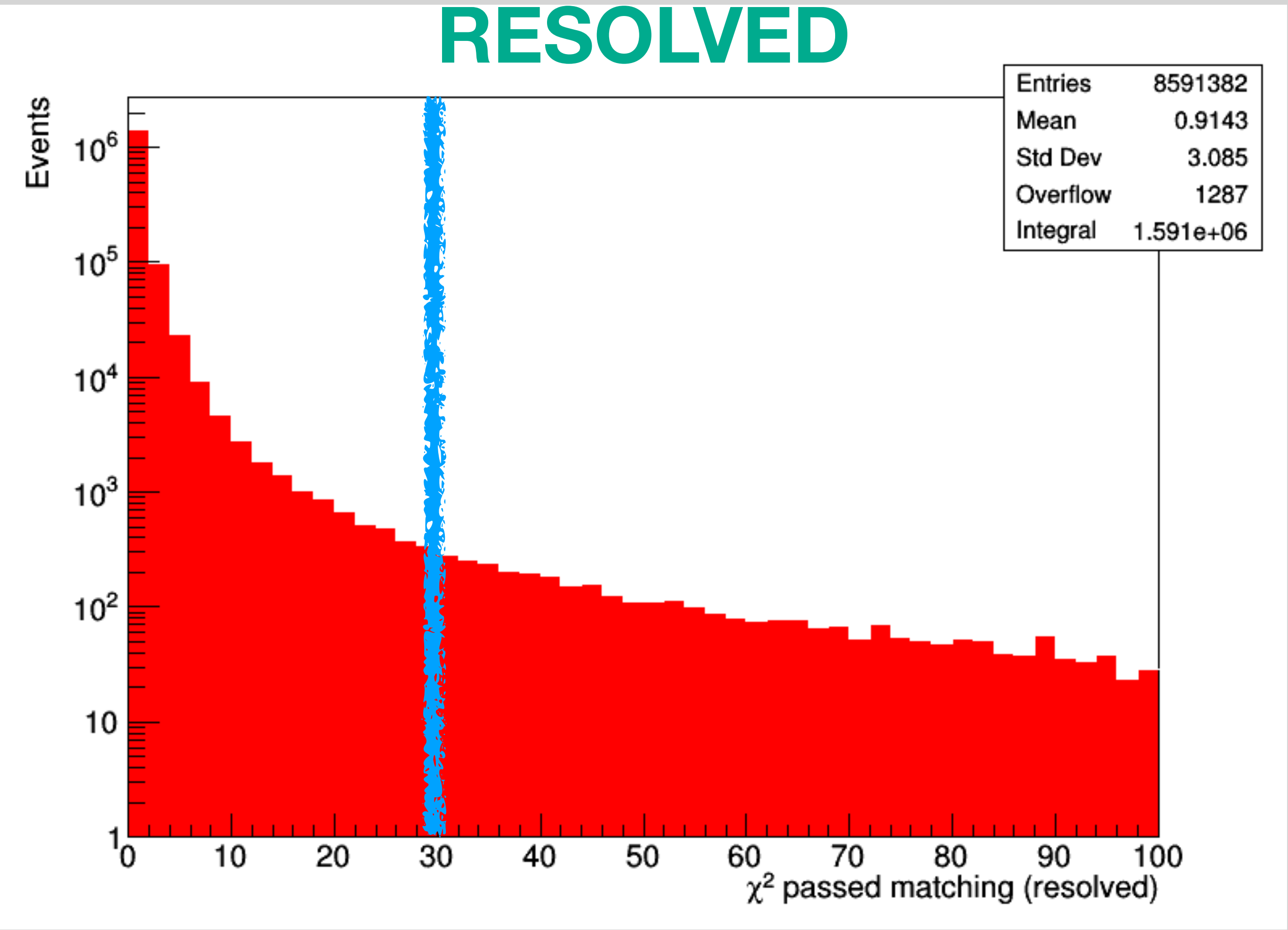

$\varepsilon_{\chi^2<30 \text{ \&\& Matchable}}$ = 22%

pass matching requirements

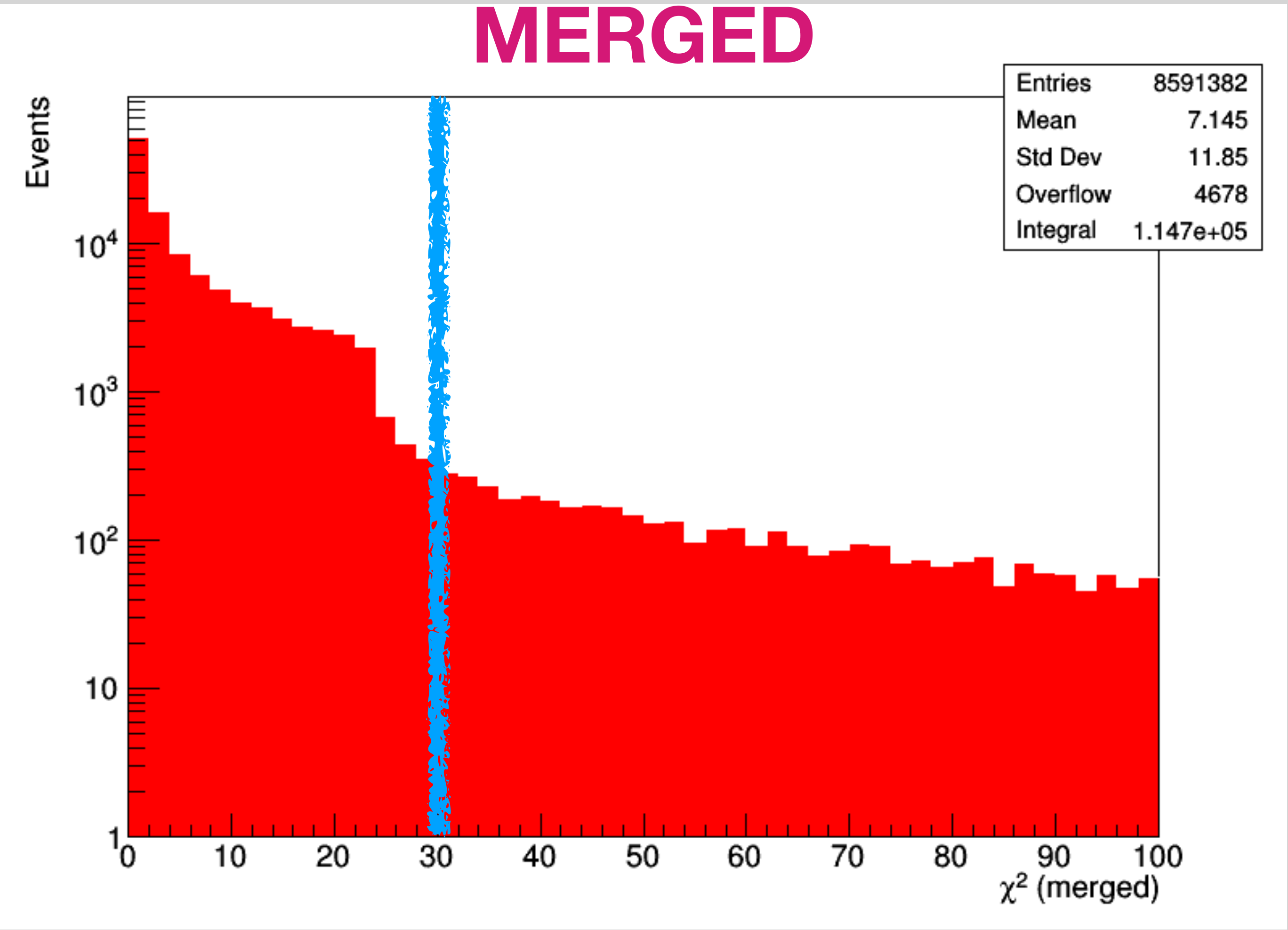

$\varepsilon_{\chi^2<30}$ = 93%

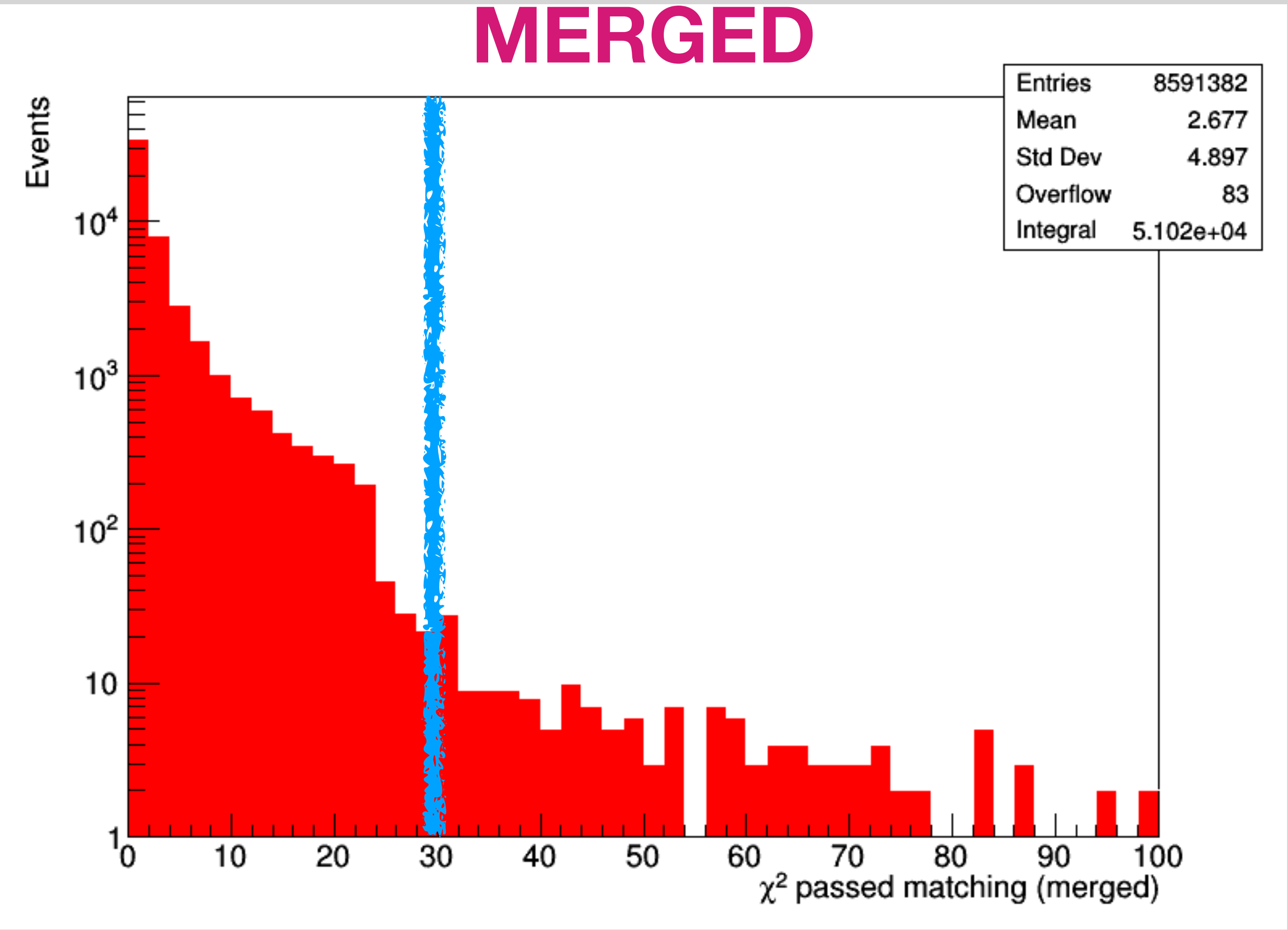

$\varepsilon_{\chi^2<30 \text{ \&\& Matchable}}$ = 46%

BACKUP: B-Jets in Merged Topology

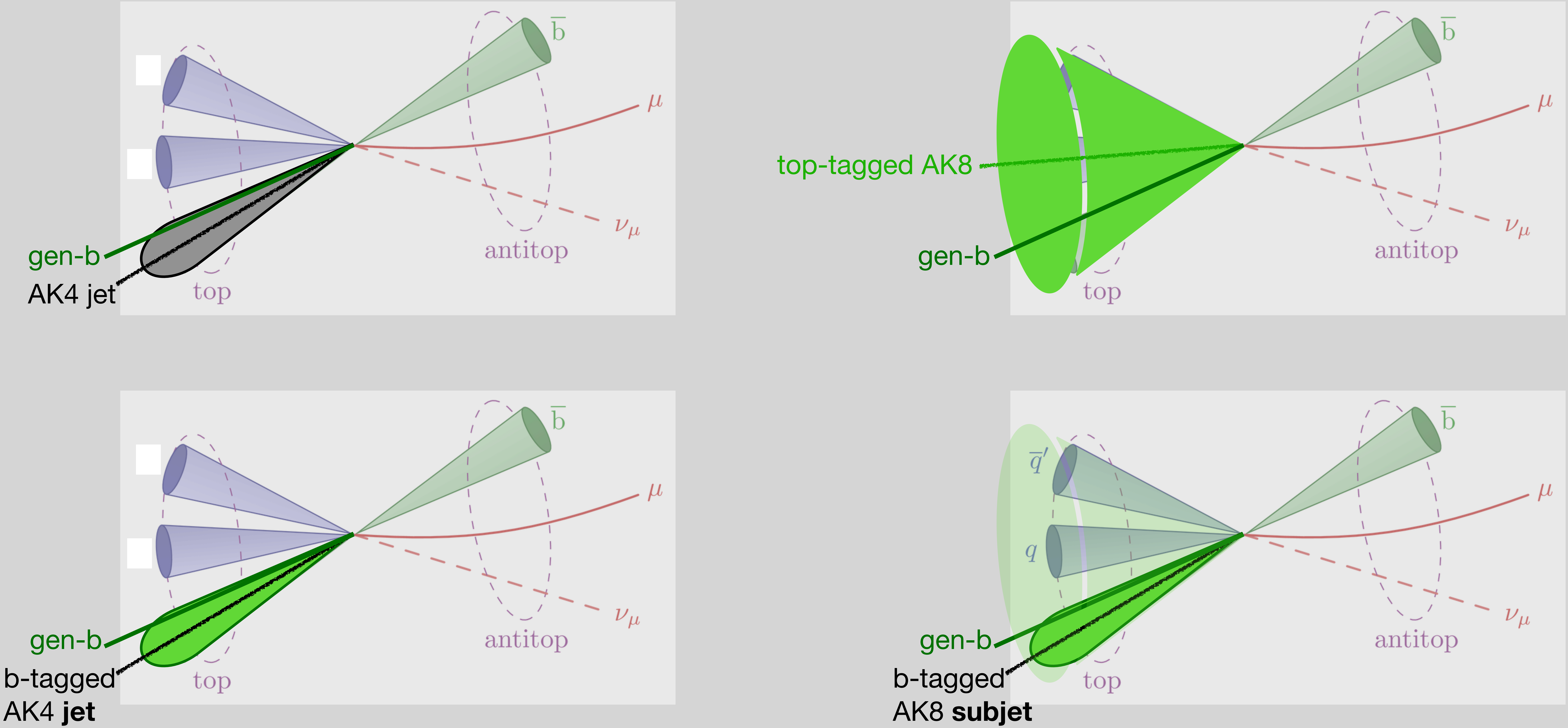

BACKUP: S.C. Framework[1]

- Parameterized production spin density matrix for the ttbar system in the following manner:

x-sec · Polarizations · Correlations

$$\mathscr{R}^I = f_I[A^I \mathbf{1} \otimes \mathbf{1} + \tilde{B}_i^{I+} \sigma^i \otimes \mathbf{1} + \tilde{B}_i^{I-} \mathbf{1} \otimes \sigma^i + \tilde{C}_{ij}^I \sigma^i \otimes \sigma^j]$$

- Angular distribution that encodes the spin structure of the ttbar system:

$$\frac{1}{\sigma}\frac{d\sigma}{d\Omega_+ d\Omega_-} = \frac{1}{(4\pi)^2}\left(1 + \mathbf{B}'_1 \cdot \hat{d}_t + \mathbf{B}'_2 \cdot \hat{d}_{\bar{t}} - \hat{d}_t \cdot C' \cdot \hat{d}_{\bar{t}}\right)$$

  - $d\Omega_{+/-}$ = differential solid angles of each decacy product from the top and antitop quark
  - $\hat{d}_t, \hat{d}_{\bar{t}}$ = directions of their decay products.

[1] https://doi.org/10.1007/JHEP12(2015)026

BACKUP: Bernreuther

- Polarization and correlation **structure functions** are decomposed in the following orthonormal basis constructed in the rest frame of the top quark:

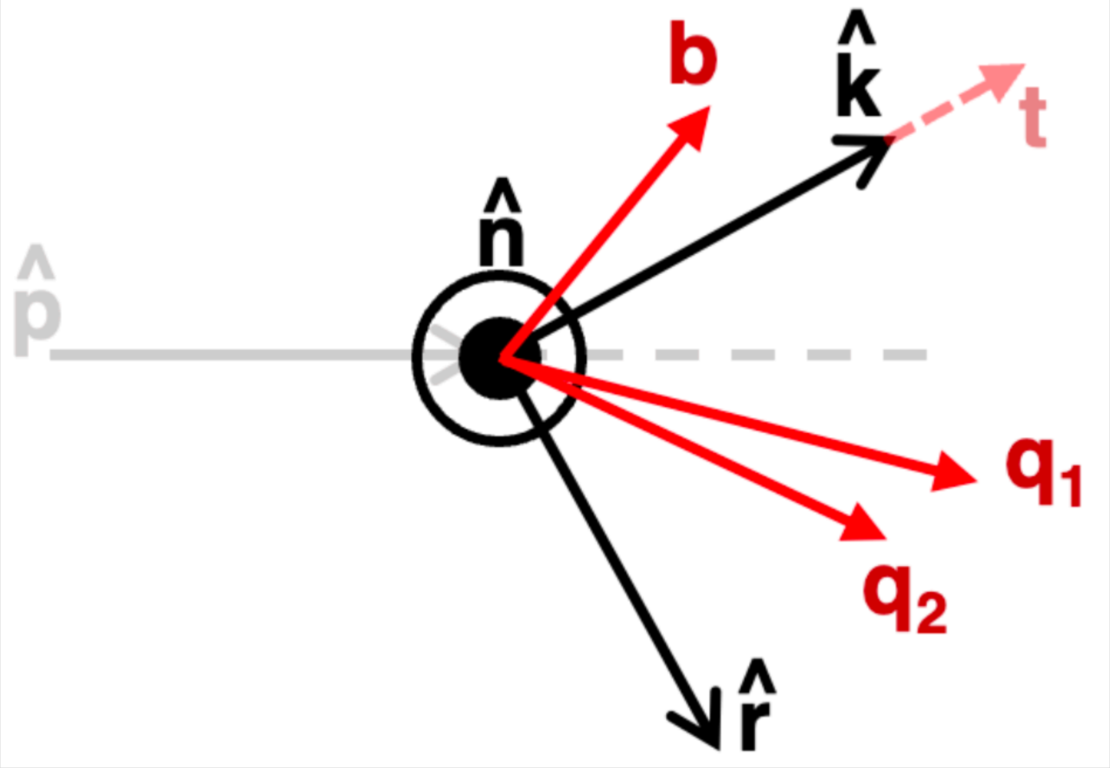

$$\{\hat{n}, \hat{r}, \hat{k}\}: \quad \hat{k} = t\hat{o}p_{+\frac{2}{3}} \quad \hat{r} = \frac{1}{r}(\hat{p} - y\hat{k}), \quad \hat{n} = \frac{1}{r}(\hat{p} \times \hat{k})$$

$$y = \hat{k} \cdot \hat{p}, \qquad r = \sqrt{1 - y^2}$$

- The structure functions are ultimately tied back to the expectation value of the top quark and antiquark spin operators with respect to a chosen reference axes $\hat{a}$ and $\hat{b}$:

$$\mathbf{B}_1(\hat{\mathbf{a}}) = P(\hat{\mathbf{a}})\kappa_{\hat{d}_t} \quad \mathbf{B}_2(\hat{\mathbf{b}}) = -\bar{P}(\hat{\mathbf{b}})\kappa_{\hat{d}_{\bar{t}}} \quad C(\hat{\mathbf{a}}, \hat{\mathbf{b}}) = \kappa_{\hat{d}_t}\kappa_{\hat{d}_{\bar{t}}}\frac{\sigma(\uparrow\uparrow) + \sigma(\downarrow\downarrow) - \sigma(\uparrow\downarrow) - \sigma(\downarrow\uparrow)}{\sigma(\uparrow\uparrow) + \sigma(\downarrow\downarrow) + \sigma(\uparrow\downarrow) + \sigma(\downarrow\uparrow)}$$

$$P(\hat{\mathbf{a}}) = \langle 2\mathbf{S}_t \cdot \hat{\mathbf{a}} \rangle \qquad \bar{P}(\hat{\mathbf{b}}) = \langle 2\mathbf{S}_{\bar{t}} \cdot \hat{\mathbf{b}} \rangle \qquad C = -9\langle \xi \rangle$$

BACKUP: Private EFT Samples

- The effects of these operators is investigated using privately produced MadGraph samples.
- Preliminary investigation: effect of c_{tu}^{1} on hadronic b quark kinematics.

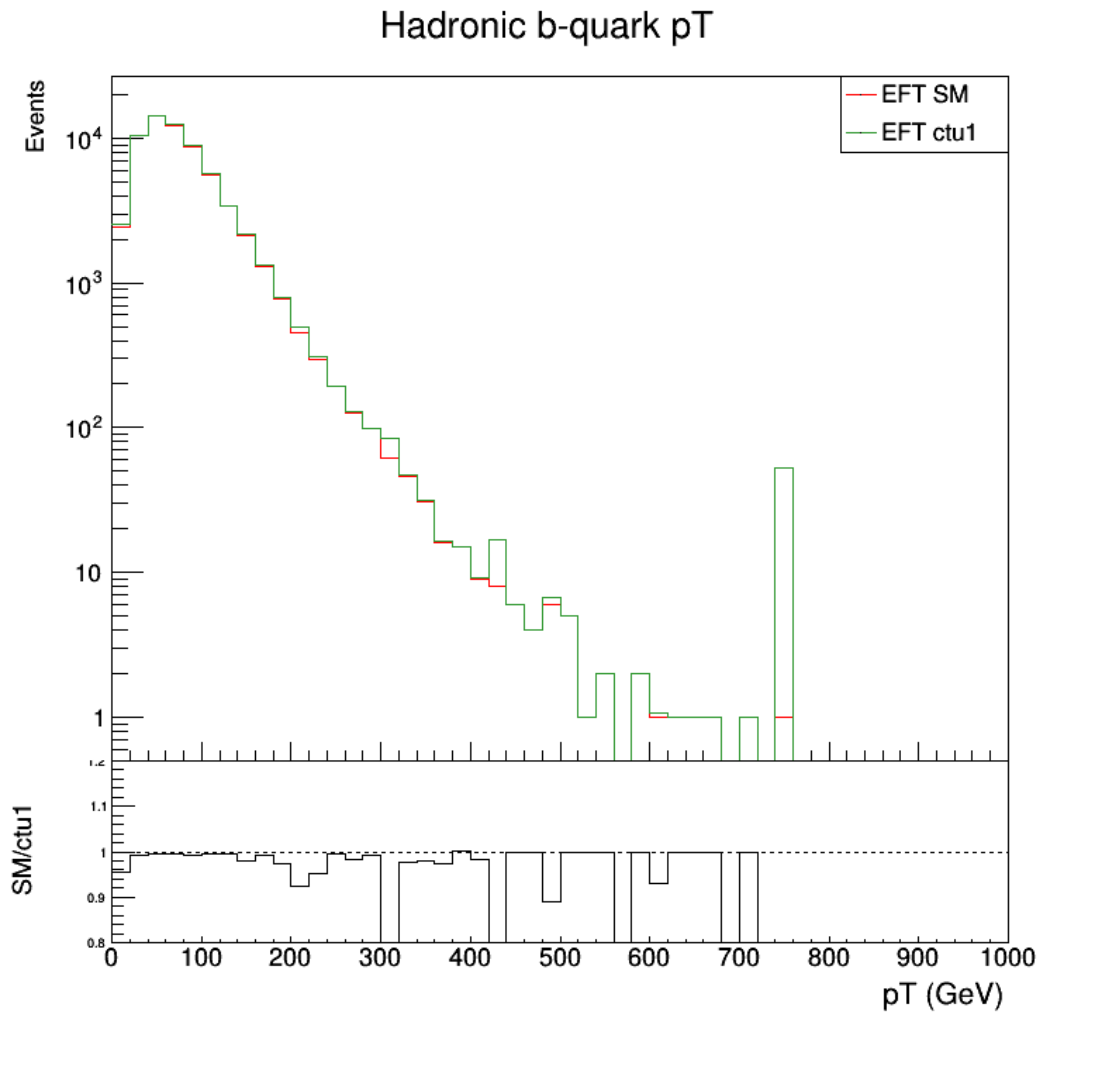

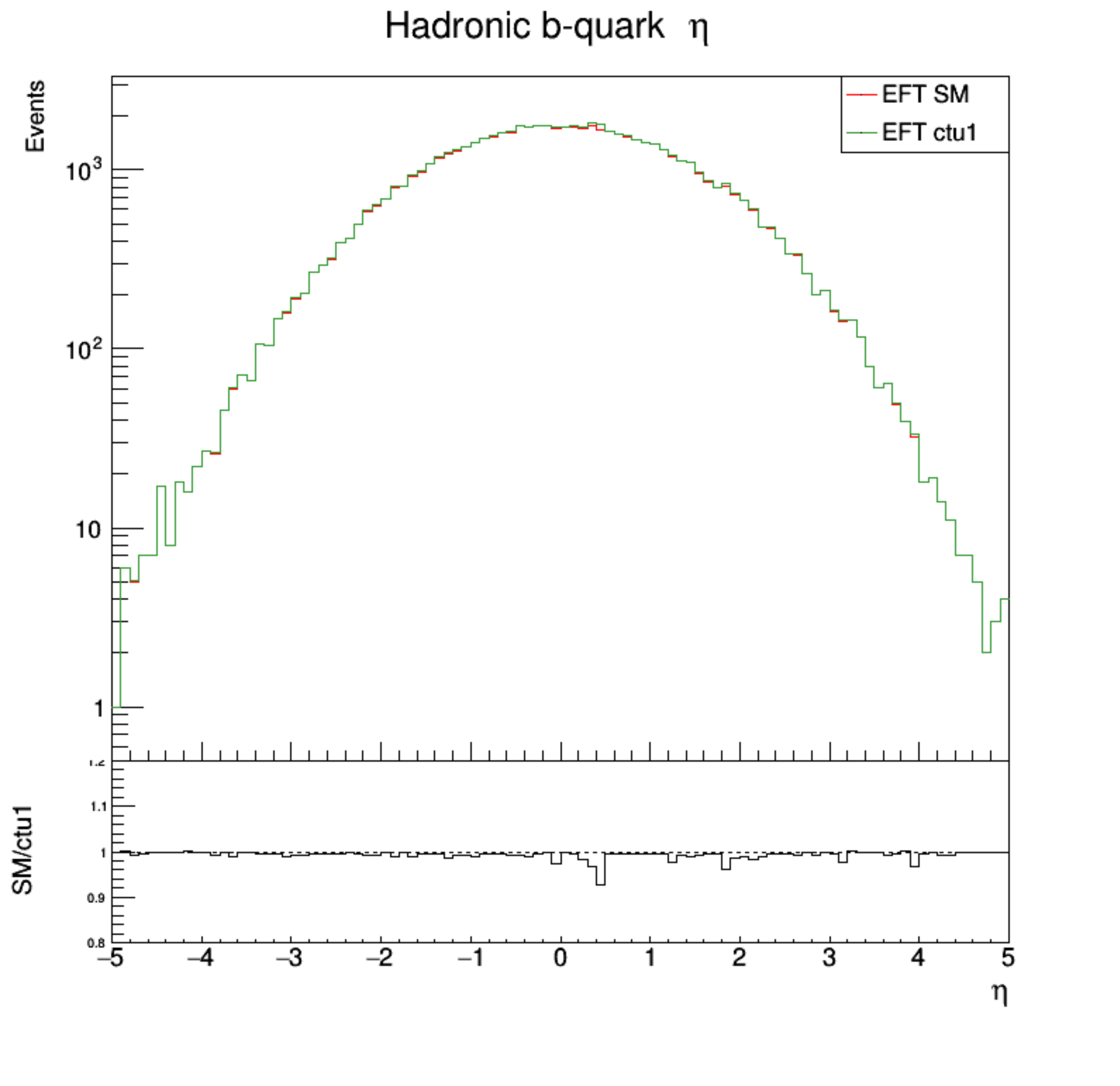

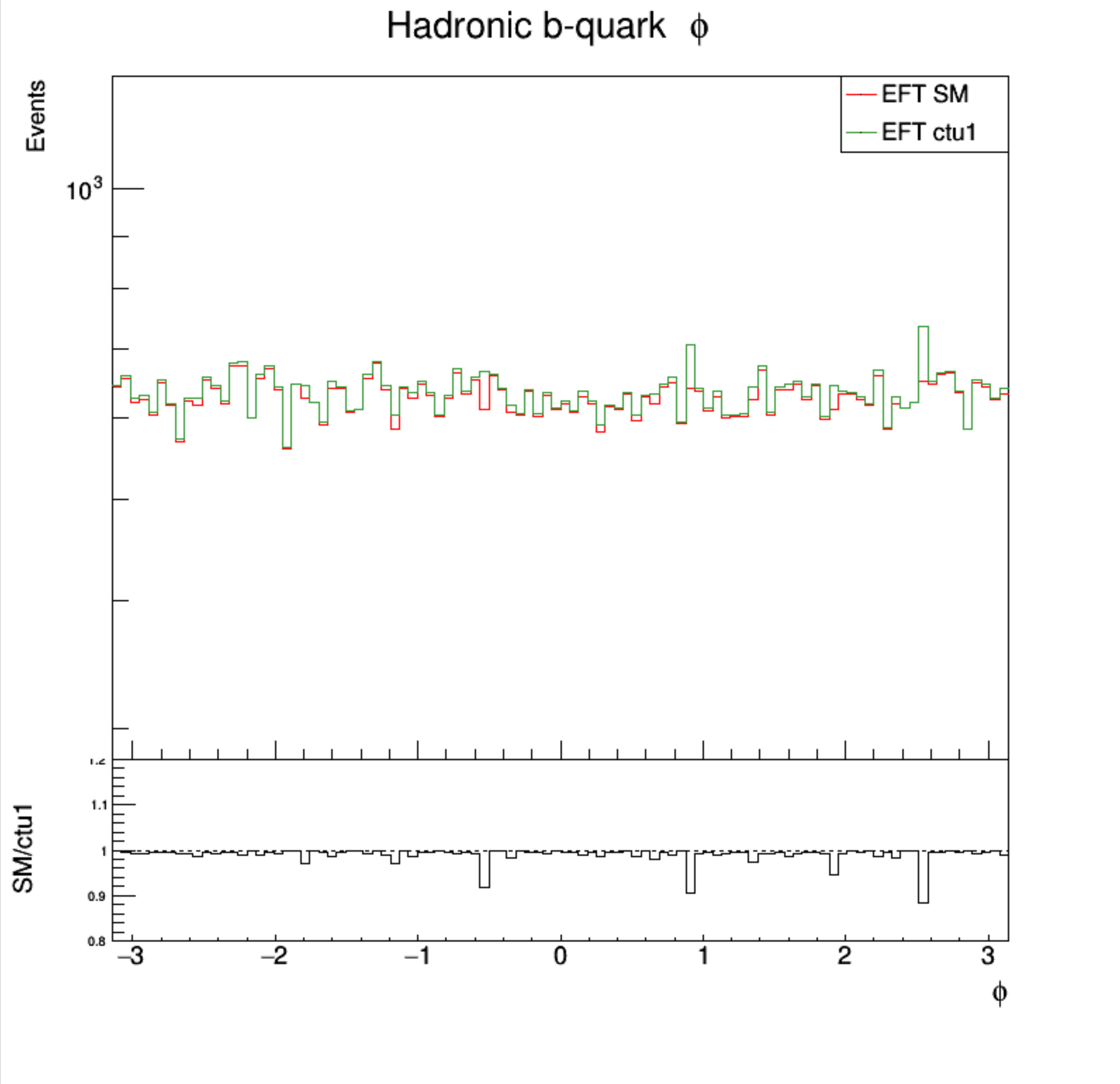

BACKUP: Bernreuther Xi

Bernreuther's angular distributions capture spin correlation information:

$$\frac{1}{\sigma}\frac{d\sigma}{d\xi} = \frac{1}{2}\Big(1 - C\xi\Big)\,\ln\!\Big(\frac{1}{|\xi|}\Big)$$

$$\xi = \cos\theta_+ \cos\theta_-$$

$$\cos\theta_+ = \hat{\ell}_+ \cdot \hat{\mathbf{a}}\,, \qquad \cos\theta_- = \hat{\ell}_- \cdot \hat{\mathbf{b}}$$

Using this angular distribution we can use <u>any</u> set of reference axes **â** and $\hat{\mathbf{b}}$ to project the lepton's direction onto.

For example, we can use each axes from the basis {**n̂**, **r̂**, $\hat{\mathbf{k}}$} and construct all combinations of the product ξ and we get:

$$\xi_{ij} = \begin{matrix} (\hat{l_+}\cdot\hat{n})(\hat{l_-}\cdot\hat{n}) & (\hat{l_+}\cdot\hat{n})(\hat{l_-}\cdot\hat{r}) & (\hat{l_+}\cdot\hat{n})(\hat{l_-}\cdot\hat{k}) \\ (\hat{l_+}\cdot\hat{r})(\hat{l_-}\cdot\hat{n}) & (\hat{l_+}\cdot\hat{r})(\hat{l_-}\cdot\hat{r}) & (\hat{l_+}\cdot\hat{r})(\hat{l_-}\cdot\hat{k}) \\ (\hat{l_+}\cdot\hat{k})(\hat{l_-}\cdot\hat{n}) & (\hat{l_+}\cdot\hat{k})(\hat{l_-}\cdot\hat{r}) & (\hat{l_+}\cdot\hat{k})(\hat{l_-}\cdot\hat{k}) \end{matrix}$$

These distributions of **these 9 variables capture all the spin-correlation information** contained in the decay particle's direction of flight.

BACKUP: Bernreuther vs Baumgart

Baumgart's distribution of decay angles:

$$\frac{d^4\sigma}{d\Omega\, d\bar{\Omega}} \propto 1 + \kappa\, \vec{P}\cdot\hat{\Omega} + \bar{\kappa}\, \vec{\bar{P}}\cdot\hat{\bar{\Omega}} + \kappa\bar{\kappa}\, \hat{\Omega}\cdot C\cdot\hat{\bar{\Omega}}$$

$$\frac{d^2\sigma}{d\cos\theta\, d\cos\bar{\theta}} \propto 1 + \kappa\, P^3\cos\theta + \bar{\kappa}\, \bar{P}^3\cos\bar{\theta} + \kappa\bar{\kappa}\, C^{33}\cos\theta\cos\bar{\theta}$$

$$\frac{d\sigma}{d(\cos\theta\cdot\cos\bar{\theta})} \propto (1 + \kappa\bar{\kappa}\, C^{33}\cos\theta\cdot\cos\bar{\theta})\, \log\left(\frac{1}{|\cos\theta\cdot\cos\bar{\theta}|}\right)$$

$$\frac{d\sigma}{d\cos\theta} \propto 1 + \kappa\, P^3\cos\theta$$

$$\frac{d\sigma}{d(\phi-\bar{\phi})} \propto 1 + \left(\frac{\pi}{4}\right)^2 \kappa\bar{\kappa}\left[\left(\frac{C^{11}+C^{22}}{2}\right)\cos(\phi-\bar{\phi}) + \left(\frac{C^{21}-C^{12}}{2}\right)\sin(\phi-\bar{\phi})\right]$$

$$\frac{d\sigma}{d(\phi+\bar{\phi})} \propto 1 + \left(\frac{\pi}{4}\right)^2 \kappa\bar{\kappa}\left[\left(\frac{C^{11}-C^{22}}{2}\right)\cos(\phi+\bar{\phi}) + \left(\frac{C^{21}+C^{12}}{2}\right)\sin(\phi+\bar{\phi})\right]$$

Bernreuther's angular distribution for dilepton decays:

$$\frac{1}{\sigma}\frac{d\sigma}{d\Omega_+ d\Omega_-} = \frac{1}{(4\pi)^2}\left(1 + \mathbf{B}_1'\cdot\hat{\ell}_+ + \mathbf{B}_2'\cdot\hat{\ell}_- - \hat{\ell}_+\cdot C'\cdot\hat{\ell}_-\right)$$

$$\frac{1}{\sigma}\frac{d\sigma}{d\cos\theta_+ d\cos\theta_-} = \frac{1}{4}\left(1 + B_1\cos\theta_+ + B_2\cos\theta_- - C\cos\theta_+\cos\theta_-\right)$$

$$\frac{1}{\sigma}\frac{d\sigma}{d\xi} = \frac{1}{2}\left(1 - C\xi\right)\ln\left(\frac{1}{|\xi|}\right) \qquad \xi = \cos\theta_+\cos\theta_-$$

$$\frac{1}{\sigma}\frac{d\sigma}{d\cos\theta_\pm} = \frac{1}{2}\left(1 + B_{1,2}\cos\theta_\pm\right)$$

No azimuthal analog in Bernreuther

BACKUP: Berneuther/Spin Analyser

$$\mathbf{B}_1(\hat{\mathbf{a}}) = P(\hat{\mathbf{a}})\kappa_{\hat{d}_t} \quad \mathbf{B}_2(\hat{\mathbf{b}}) = -\bar{P}(\hat{\mathbf{b}})\kappa_{\hat{d}_{\bar{t}}} \quad C(\hat{\mathbf{a}},\hat{\mathbf{b}}) = \kappa_{\hat{d}_t}\kappa_{\hat{d}_{\bar{t}}}\frac{\sigma(\uparrow\uparrow)+\sigma(\downarrow\downarrow)-\sigma(\uparrow\downarrow)-\sigma(\downarrow\uparrow)}{\sigma(\uparrow\uparrow)+\sigma(\downarrow\downarrow)+\sigma(\uparrow\downarrow)+\sigma(\downarrow\uparrow)}$$

- These analysing powers have been studied[1] analytically and their values for different choices in decay product can be seen below:

Table 1: Born results for spin analysing power of $\bar{d}$, b, u , least energetic light jet and thrust axis.

	$m_b = 0, \Gamma_W \to 0$	$m_b = 0, \Gamma_W$ kept	$m_b = 5$ GeV, $\Gamma_W \to 0$	$m_b = 5$ GeV, Γ_W kept
$\kappa^0_{\bar{d}}$	1	1	1	1
κ^0_b	−0.40622	−0.40867	−0.40553	−0.40800
κ^0_u	−0.31817	−0.31091	−0.31964	−0.31236
κ^0_j	0.50774	0.51088	0.50708	0.51021
κ^0_T	−0.31712	−0.31782	−0.31597	−0.31671

Table 2: QCD-corrected results for spin analysing powers.

	partons	jets, E-alg.	jets, D-alg.
$\kappa_{\bar{d}}$	0.9664(7)	0.9379(8)	0.9327(8)
$\delta^{QCD}_{\bar{d}}$ [%]	−3.36 ± 0.07	−6.21 ± 0.08	−6.73 ± 0.08
κ_b	−0.3925(6)	−0.3907(6)	−0.3910(6)
δ^{QCD}_b [%]	−3.80 ± 0.15	−4.24 ± 0.15	−4.18 ± 0.15
κ_u	−0.3167(6)	−0.3032(6)	−0.3054(6)
δ^{QCD}_u [%]	+1.39 ± 0.19	−2.93 ± 0.19	−2.22 ± 0.19
κ_j	–	0.4736(7)	0.4734(7)
δ^{QCD}_j [%]	–	−7.18 ± 0.13	−7.21 ± 0.13
κ_T	−0.3083(6)	–	–
δ^{QCD}_T [%]	−2.65 ± 0.19	–	–

- "In practice the most important spin analysers are, as far as non-leptonic top decays are concerned, the **b-quark jet** and the least energetic light (non-b-quark) jet. The QCD corrected results are $\kappa_b \approx -0.39$ and $\kappa_j \approx 0.47$. For the b-jet the difference between the parton level result and the jet result is small."

[1] https://arxiv.org/pdf/hep-ph/0205023.pdf

BACKUP: Optimizing Hadronic Spin Analyser

- Optimizing hadronic spin analyzer

$$q_{opt} \equiv p(d \to q_{soft})\hat{q}_{soft} + p(d \to q_{hard})\hat{q}_{hard}$$

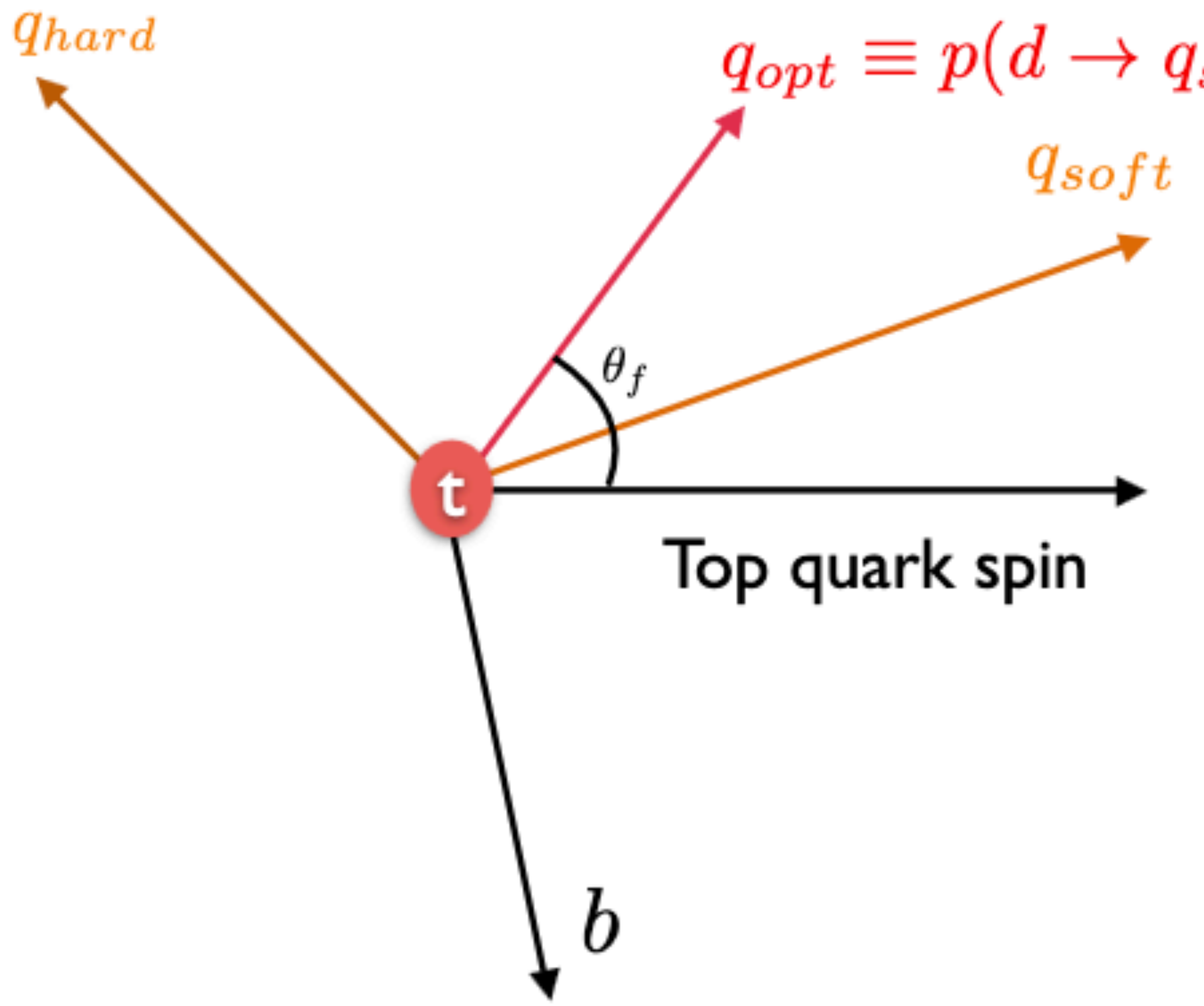

$$\frac{1}{\Gamma_f}\frac{d\Gamma_f}{d\cos\theta_f} = \frac{1}{2}(1 + \mathbf{0.64}\cos\theta_f)$$

[1] https://indico.cern.ch/event/1233341/contributions/5528229/attachments/2723738/4732895/Dorival_top2023.pdf

BACKUP: Operator Dependencies

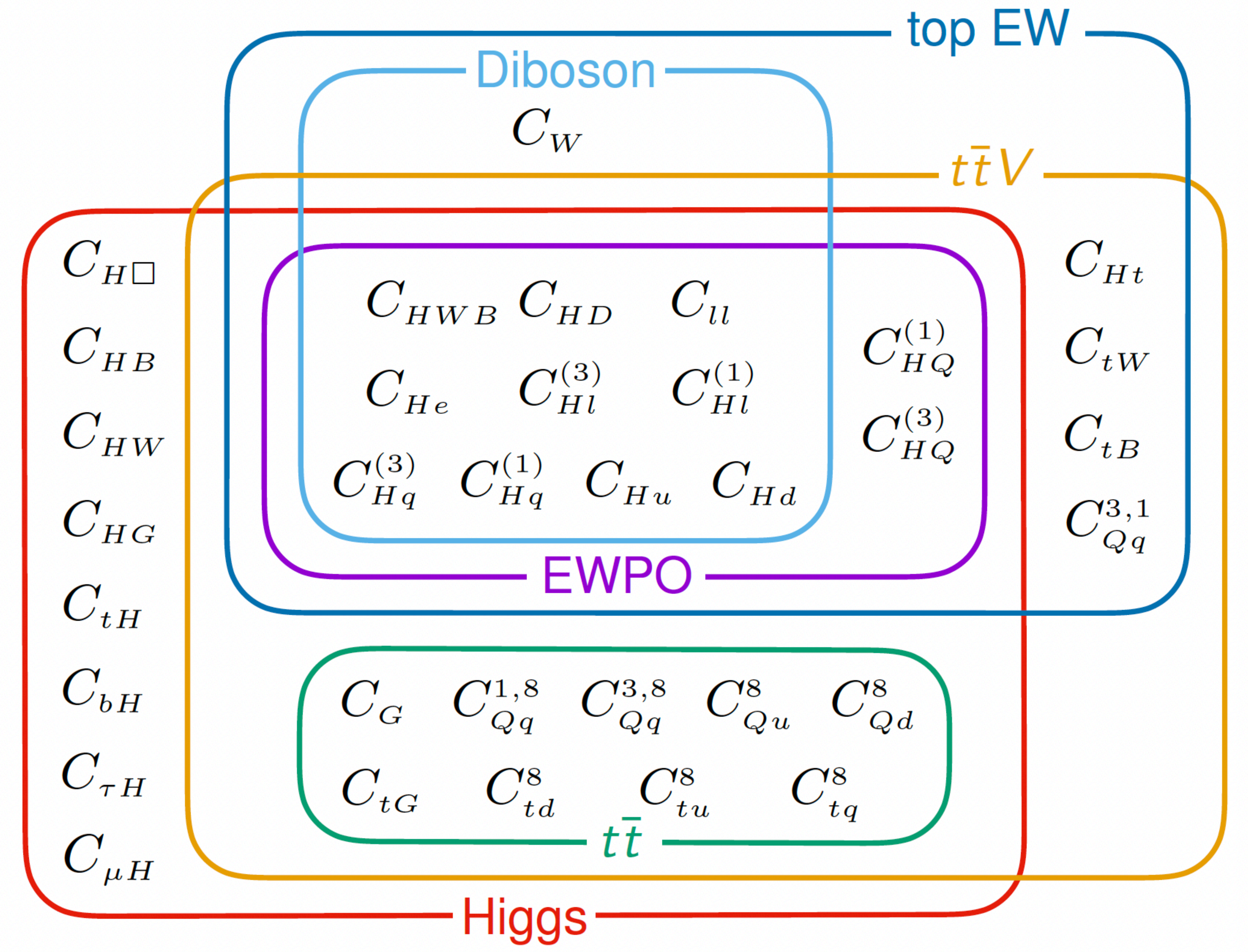

- This diagram demonstrates the overlapping dependeces that even a subset of WCs can have, thus motivating the use of a global approach to understanding any deviations to SM physics.

BACKUP: Operator Definitions

$$\mathcal{O}_{Qq}^{1,1}, \mathcal{O}_{Qq}^{3,1}, \mathcal{O}_{Qq}^{1,8}, \mathcal{O}_{Qq}^{3,8}, \mathcal{O}_{Qu}^{1}, \mathcal{O}_{Qu}^{8}, \mathcal{O}_{Qd}^{1}, \mathcal{O}_{Qd}^{8}, \quad \mathcal{O}_{tq}^{1}, \mathcal{O}_{tq}^{8}, \mathcal{O}_{tu}^{1}, \mathcal{O}_{tu}^{8}, \mathcal{O}_{td}^{1}, \mathcal{O}_{td}^{8}, \quad and \quad \mathcal{O}_{tG}$$

- Definitions in Warsaw basis:

$$c_{Qq}^{1,1} \equiv C_{qq}^{1(ii33)} + \frac{1}{6}C_{qq}^{1(i33i)} + \frac{1}{2}C_{qq}^{3(i33i)},$$
$$c_{Qq}^{3,1} \equiv C_{qq}^{3(ii33)} + \frac{1}{6}(C_{qq}^{1(i33i)} - C_{qq}^{3(i33i)}),$$
$$c_{Qq}^{1,8} \equiv C_{qq}^{1(i33i)} + 3C_{qq}^{3(i33i)},$$
$$c_{Qq}^{3,8} \equiv C_{qq}^{1(i33i)} - C_{qq}^{3(i33i)},$$

$$c_{tu}^{1} \equiv C_{uu}^{(ii33)} + \frac{1}{3}C_{uu}^{(i33i)},$$
$$c_{tu}^{8} \equiv 2C_{uu}^{(i33i)},$$
$$c_{td}^{1} \equiv C_{ud}^{1(33ii)},$$
$$c_{td}^{8} \equiv C_{ud}^{8(33ii)},$$

$$c_{tq}^{1} \equiv C_{qu}^{1(ii33)},$$
$$c_{Qu}^{1} \equiv C_{qu}^{1(33ii)},$$
$$c_{Qd}^{1} \equiv C_{qd}^{1(33ii)},$$
$$c_{tq}^{8} \equiv C_{qu}^{8(ii33)},$$
$$c_{Qu}^{8} \equiv C_{qu}^{8(33ii)},$$
$$c_{Qd}^{8} \equiv C_{qd}^{8(33ii)},$$

- Technically these are degrees of freedom in WC space

$$O_{qq}^{1(ijkl)} = (\bar{q}_i\gamma^\mu q_j)(\bar{q}_k\gamma_\mu q_l),$$
$$O_{qq}^{3(ijkl)} = (\bar{q}_i\gamma^\mu\tau^I q_j)(\bar{q}_k\gamma_\mu\tau^I q_l),$$
$$O_{qu}^{1(ijkl)} = (\bar{q}_i\gamma^\mu q_j)(\bar{u}_k\gamma_\mu u_l),$$
$$O_{qu}^{8(ijkl)} = (\bar{q}_i\gamma^\mu T^A q_j)(\bar{u}_k\gamma_\mu T^A u_l),$$
$$O_{qd}^{1(ijkl)} = (\bar{q}_i\gamma^\mu q_j)(\bar{d}_k\gamma_\mu d_l),$$
$$O_{qd}^{8(ijkl)} = (\bar{q}_i\gamma^\mu T^A q_j)(\bar{d}_k\gamma_\mu T^A d_l),$$
$$O_{uu}^{(ijkl)} = (\bar{u}_i\gamma^\mu u_j)(\bar{u}_k\gamma_\mu u_l),$$
$$O_{ud}^{1(ijkl)} = (\bar{u}_i\gamma^\mu u_j)(\bar{d}_k\gamma_\mu d_l),$$
$$O_{ud}^{8(ijkl)} = (\bar{u}_i\gamma^\mu T^A u_j)(\bar{d}_k\gamma_\mu T^A d_l),$$
$${}^\ddagger O_{quqd}^{1(ijkl)} = (\bar{q}_i u_j)\,\varepsilon\,(\bar{q}_k d_l),$$
$${}^\ddagger O_{quqd}^{8(ijkl)} = (\bar{q}_i T^A u_j)\,\varepsilon\,(\bar{q}_k T^A d_l),$$

[1] https://doi.org/10.48550/arXiv.1802.07237

BACKUP: Kinematic Independence

R. Schöfbeck parton-level (linear) correlations:
No strong feature (linear) correlation amongst the p_T-related, **C**harge **A**symmetry, and **S**pin **C**orrelation variables.

We can see the the three sets of variables have a near zero correlation value amongst them which makes them **kinematically independent of each other**.

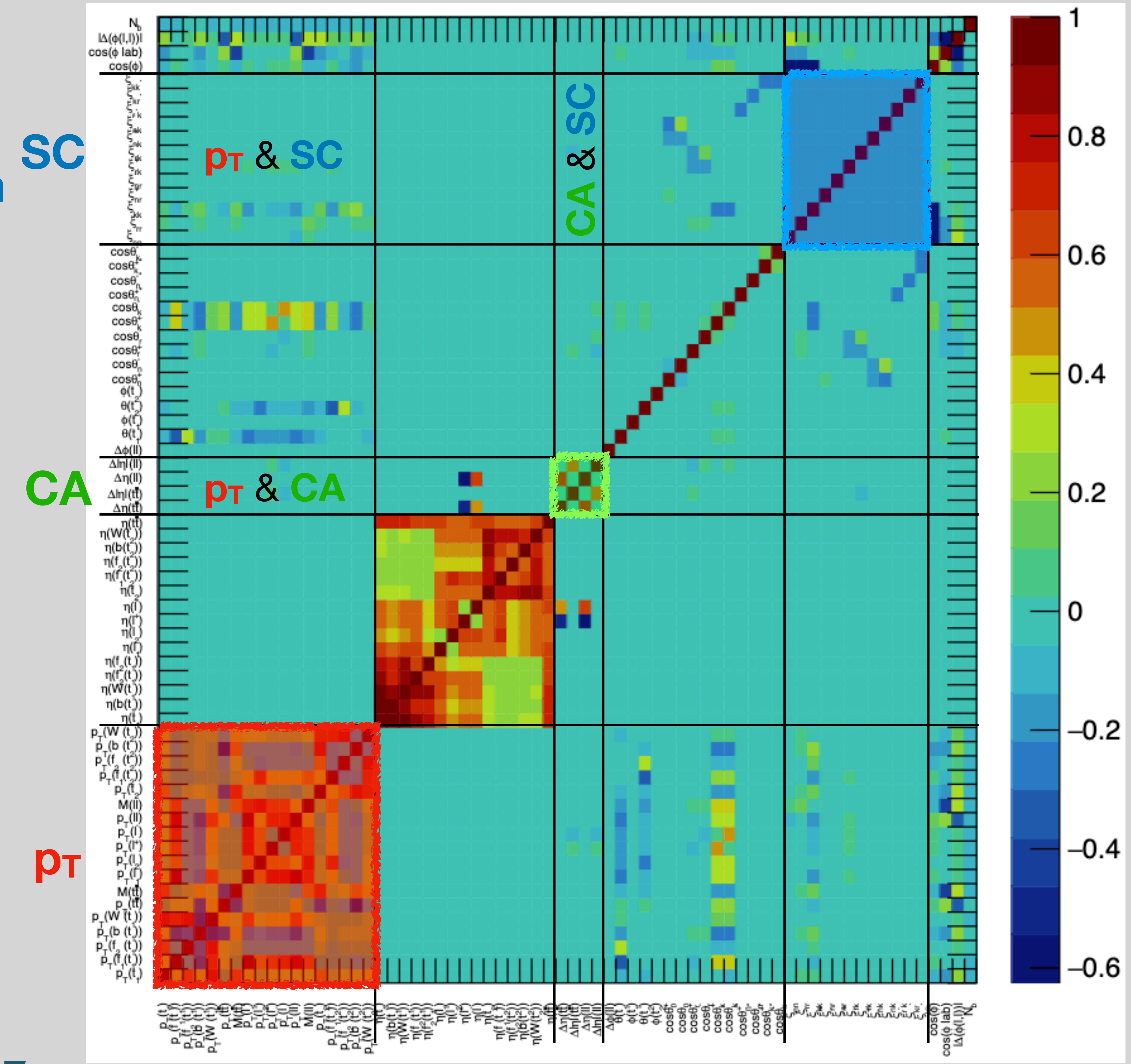

BACKUP: SM EFT Global Fits

- The LHC has allowed for the most precise measurements of top quark properties in history, making top quark data a powerful ingredient to incorporate in an appropriate global fit.
- EFT global fits[1] show combining data from different sectors improves the constraints of WC's.

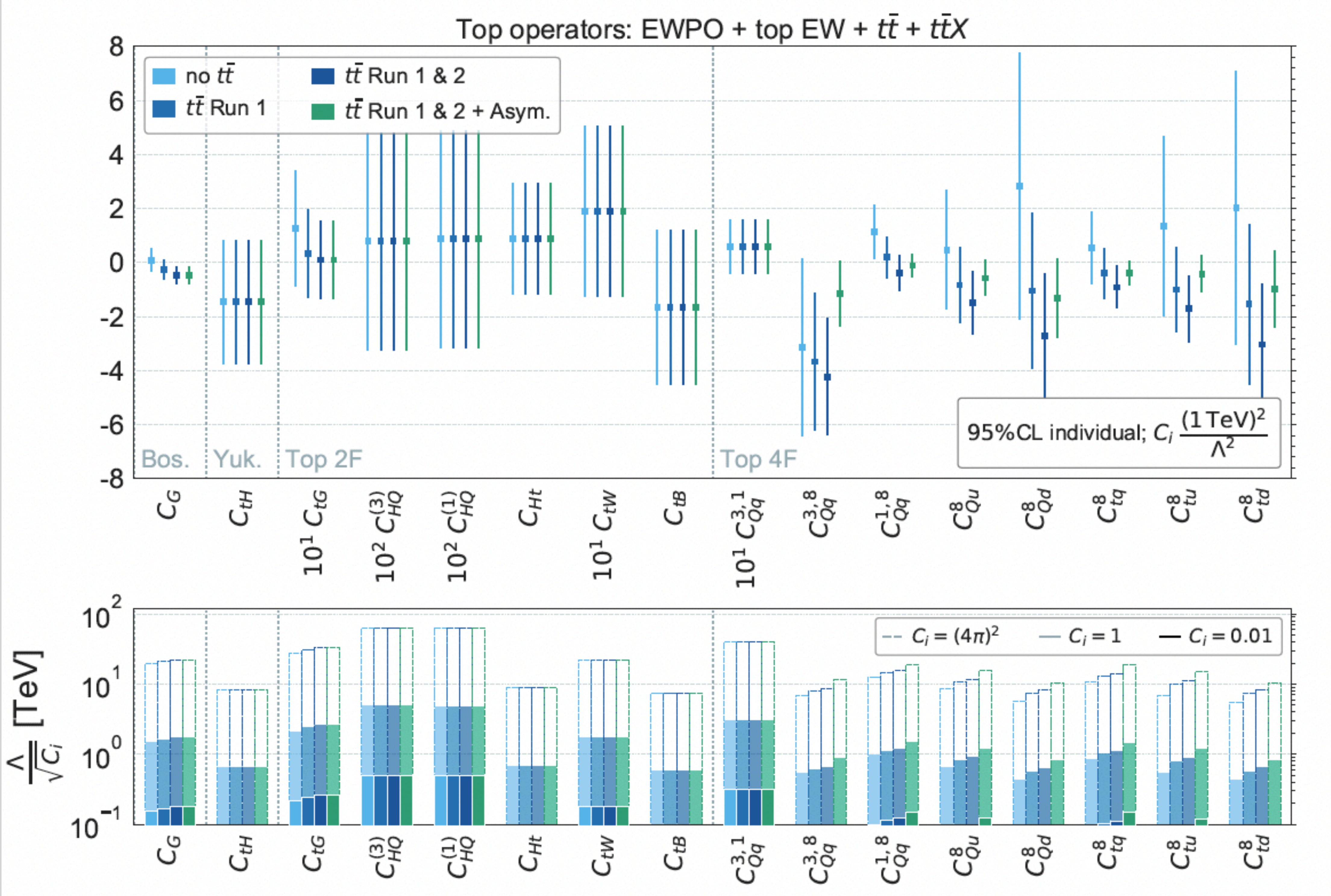

Individual WC constraints

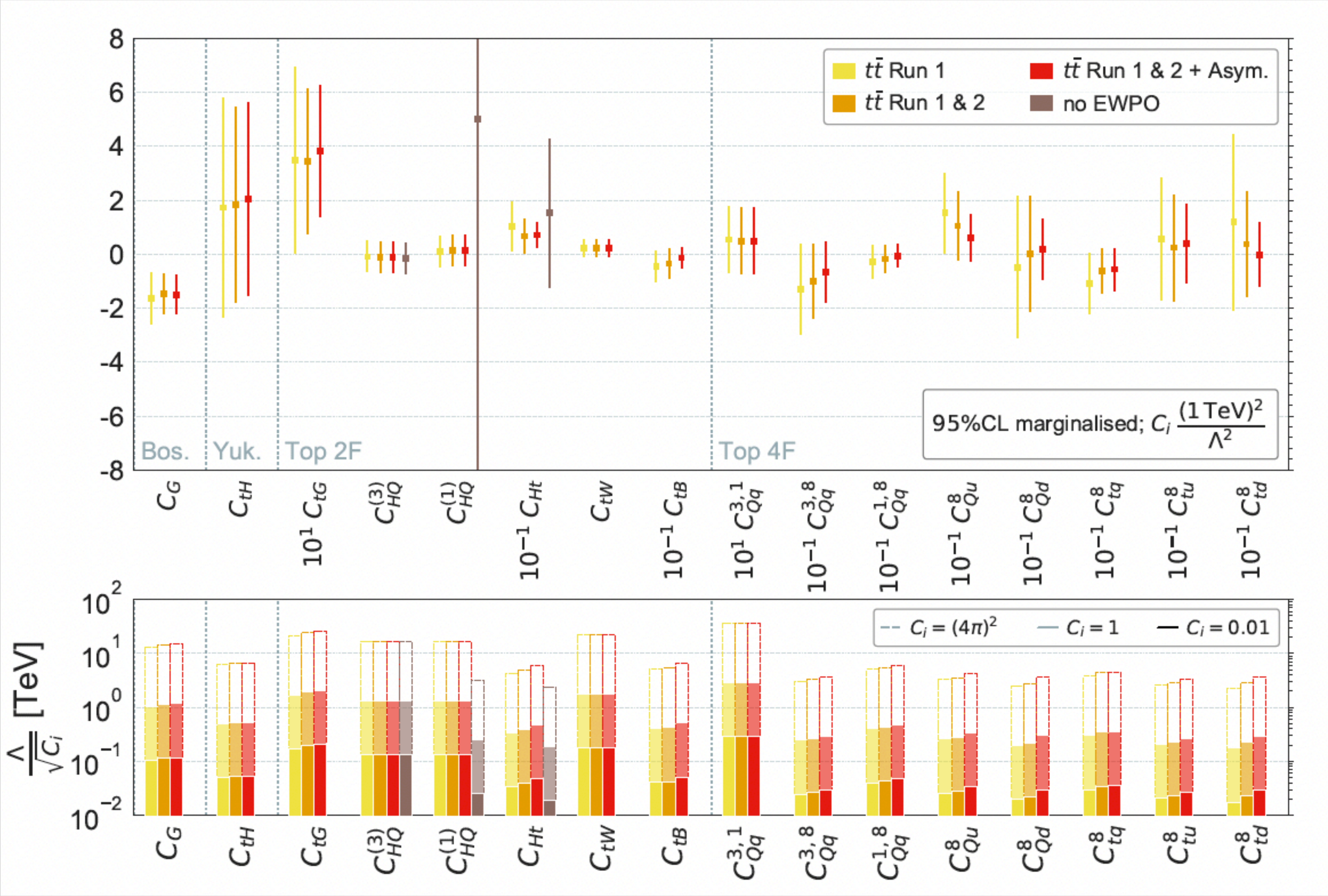

Marginalised WC constraints

[1] https://doi.org/10.1007/JHEP04(2021)279